SYNTHESIS AND REACTIVITY STUDIES OF ORGANOTIN(IV) COMPLEXES OF 2-[(*E*)-2-(3-FORMYL-4-HYDROXY)-1-DIAZENYL]BENZOIC ACID AND RELATED SYSTEMS: ASSESSMENT OF BONDING, STRUCTURE AND BIOLOGICAL APPLICATIONS

A THESIS SUBMITTED IN PARTIAL FULFILMENT OF THE REQUIREMENTS FOR THE DEGREE OF DOCTOR OF PHILOSOPHY

BY

KEISHAM SURJIT SINGH

DEPARTMENT OF CHEMISTRY
SCHOOL OF PHYSICAL SCIENCES
NORTH-EASTERN HILL UNIVERSITY
SHILLONG-793022

2006

General comments on presentation:

Cover: include a space between: Department" and "of":
This is a printing mistake. However, inside page of the thesis is correct.

The titles of Chapters 3 – 5 have a spelling error; see also pp ii-iii :
Corrected as suggested.

The alignment of the text on p. 101 is awry. "*et. al.*" must be presented in the correct form, i.e., "*et al.*":
Corrected as suggested.

"*cf*" must be presented in the correct form, i.e., "*cf.*"
Corrected as suggested.

The crystallographic study shows... {p. 5}:
Corrected as suggested.

"report is" should be "report is of" {p. 11:
Corrected as suggested.

"solid state" should be "solid-state" {p. 11} and elsewhere in the thesis: Corrected as suggested (p. 11, 46, 90, 125, 151).
"...of a few triorganotin(IV)" on p. 12 – triorganotin(IV) what? :
Corrected as suggested.
"the activity" should be "their activity" {p. 14}:
Not found in p. 14, but found in p. 13 and corrected.

"specific comments" should be "specific comment" {41}:
Corrected as suggested.
"in situ" should be "*in situ*":
not changed since both the conventions are used.

Specific comments/queries:

CHAPTER 2

T 2.2: Why are *R*int, *R*(*F*) and *wR*(*F*2) given to four decimal places for L3? Three for the residual electron density is also incorrect. See also Table 3.7; here, 2theta values need to be given to one decimal place. See also T 5.2 {p. 131}:

Errors were corrected for L^3 for *R*int, *R*(*F*), *wR*(*F*2) and also for the residual electron density and, now recorded to three decimal places {p. 27}. 2 theta values given in Table 3.7 / 5.2 are as per chemistry journal specifications and hence not changed.

p. 29: The carboxylate acid molecule [*sic.*] can not be a zwitterion – be more precise and in naming the compound as this is ambiguous – specify the compound as L3 and then discuss the zwitterionic nature of the N/OH group.:

The carboxylic acid molecule i.e. L^2HH' is zwitterion as evident from the electron density peak associated with the expected phenolic H atom and was found to be closer to the imine N-atom. The reviewer has mistaken L^2HH' with L^3HH' (see p.29).

p. 32: "Two dimensional network" is an incorrect description – a network is 3D – 2D layer or 2D array is correct.

Two dimensional network and 2D array reflect the same presentation and any of the presentations can be used and, hence not changed.

p. 33: there is no four-fold axis in the monoclinic unit cell

Query cited is not found in the text.

p. 38: the treatment of the H atoms in the refinements as given is inconsistent with the data listed in Table 2.4 to 2.6 that shows that some H atoms had been refined.

H-atoms were placed in the positions indicated by a difference electron density map and their positions were allowed to refine together with individual isotropic displacement parameters and hence the data is consistent with the data listed in Tables 2.4 to 2.6. Reviewer over looked to see the experimental details.

CHAPTER 3

How can the geometric parameters for **1** be equivalent to those of **4** if they are different structures? {p. 57} A reference to the source of the van der Waals radii should be given {p. 57}

The complexes **1** and **4** are tributyltin(IV) compounds of the same series where the ligands are different. This is reflected in the crystallographic parameters (refer to Table 3.7), for example, In compound **1**, the crystal system is triclinic and the space group is $P\bar{1}$ while in compound **4**, the crystal system is monoclinic and the space group is $P2_1/n$, and all other unit cell parameters are also different, as expected. However, the geometric parameters are of the order of same magnitude except for some which are clearly discussed in the text (see p.63). A reference to the source of van der Waals radii is excluded as this is very common and hence the reference is excluded.

Why is the inclusion of NMR and Mössbauer data "convenience of discussion"? {p 64}
The compound $Ph_3SnL^1H.OH_2$ was reported earlier by our group (T.S. Basu Baul, S.M. Pyke, K.K. Sarma, E.R.T.Tiekink, Main Gr. Met. Chem., **19** (1996) 807, this reference is also cited in this chapter i.e. ref. No. 33). The previous paper reports only ^1H & ^{13}C and X-ray structure of the complex. This compound was used as one of the starting materials for obtaining other derivatives, e.g. complexes **2-5**. Since all the triphenyltin complexes (**2-5**) of present investigation were investigated by ^{119}Sn NMR, ESI-MS and Mossbauer spectroscopy and hence the starting triphenyltin compound i.e. $Ph_3SnL^1H.OH_2$ (**1**) was also investigated by the ^{119}Sn NMR, ESI-MS and Mossbauer spectroscopic techniques in order to compare and discuss the spectral results more authoritatively. Hence, $Ph_3SnL^1H.OH_2$ (**1**) included.

"isostructural" is used in the wrong context here {p. 65} – the author means same coordination number/geometry {see also p. 77}. It is more precise to mention that the structures of **2** and **3** are isomorphous {p. 71}
Isostructural is correct which means same coordination/ geometry, and hence not changed.

It is not possible to locate H atoms in X-ray crystallography. There can be evidence but as there are no electrons in a bound H atom, only between its nucleus and the atom it is bound to, the position of an H atom can only be inferred. The candidate needs to modify the discussion on p. 73 accordingly.
Agreed with the reviewer's comment concerning location of H-atom. While solving the structures, H-atoms were placed in the positions indicated by a difference electron density map and their positions were allowed to refine together with individual isotropic thermal parameters. This is a standard practice to

locate H-atoms and the results were also published by us i.e. T.S. Basu Baul, K.S. Singh et al., J. Organomet. Chem., **690** (2005) 4232 (Thesis ref. No. 20) and hence the text is not modified.

It is not acceptable to have the numbering scheme in 3.3.3 and beyond. Structure **1** has already been assigned and so structure **1** on page 78 should be **6**, *etc.*
For convenience of discussion, the chapters are divided into sections and sub-sections. So there is no need to change the compound numbers in the text.

It should be mentioned that the structures of **4** and **5**, in 3.3.3, are isomorphous {p. 80}
Isostructural is correct which means same coordination/ geometry, and hence not changed.

Throughout the thesis mention is made of "graph set motif" – this must be accompanied by a citation to the literature.
Graph set motif reference is already provided in the text which is Ref. No. 69.

Lorentz should not be italicized on p. 91; see also p. 94 and later in the thesis
Lorentz is italicized in the thesis. Both normal and italics style are correct. We have adopted the chemistry journal style but not the crystallography journal and hence not changed.

The description of the experimental sections in Chapter 3 must be condensed into one cohesive summary. It appears that the candidate has "cut & paste" from the publications. This is not entirely acceptable. The entire chapter must be selfconsistent and read as such. Aspects of the discussion (numbering scheme) and experimental must be consolidated.

For convenience of discussion of the section i.e. 3.4.5 (X-ray crystallography), has been divided further into sub-sections. i.e.3.4.5.1 (tributyltin), 3.4.5.2 (triphenyltin) and 3.4.5.3 (tribenzyltin). It deals with three different set of samples (i.e. R = Bu, Ph, Bz). Furthermore, the structural refinements were obtained using different programmes. So the mention of the separate experimental details for three different types is necessary in order to have authoritative information and hence not condensed.

CHAPTER 4

Why can not the 13C NMR be recorded for the L7-L10 ligands? What is the meaning of "...complexed ligands, which were generated in situ, are..." {p. 102}

It is clearly mentioned in the text, that the free ligands L^7HH'-$L^{10}HH'$ could not be synthesized owing to the solubility problem of one of the starting materials in water and common organic solvents. (Please refer to section 2.3 synthesis of ligands, p.22). Therefore, ^1H & ^{13}C NMR could not be recorded. However, the ligand frame work could be generated during the reaction of R_3SnL^6H (R = Bu and Ph) with appropriate substituted aniline (complexed ligands) (Refer to Section 2.2, p.22).

The meaning of the sentence beginning "Δ and ρ values..." is unclear and needs attention {p. 106}

We feel that the discussion is clear and is also mentioned in a similar way in the publication i.e. T.S.Basu Baul, K.S.Singh, A. Lycka, A. Linden, X. Song, A. Zapata & G. Eng, Appl.Organometal.chem., 20 (2006) 788-797 and hence, not changed.

The word "atomic" occurring between "anisotropic" and "displacement" is unnecessary {p. 115}

Corrected in the thesis, as suggested.

The statement in the box on p. 109 should be included in 4.5.5 without the box. In fact this statement appears a little melodramatic – the most useful criterion for judging a structure is the value of *wR*(*F*2) which should be less than 0.200.

The purpose of using the box is to highlight the justification. So it can be seen at a glance and the same justification has also appeared in the publication cited above. Hence, not changed.

CHAPTER 5

Some comments concerning Chapter 5 are to be found above

Corrected as suggested.

The word "but" {p. 151} referring to the benzene solvent molecule is inappropriate.

Corrected as suggested.

CHAPTER 6

It would be useful to indicate the significance of the various values, *e.g.*, are high values desirable?

The low values of the toxicity data are desirable and are clearly mentioned in the text and in the tables 6.1-6.4. The significance of these values are also justified in the text.

SYNTHESIS AND REACTIVITY STUDIES OF ORGANOTIN(IV) COMPLEXES OF 2-[(*E*)-2-(3-FORMYL-4-HYDROXY)-1-DIAZENYL]BENZOIC ACID AND RELATED SYSTEMS: ASSESSMENT OF BONDING, STRUCTURE AND BIOLOGICAL APPLICATIONS

A THESIS SUBMITTED IN PARTIAL FULFILMENT OF THE REQUIREMENTS FOR THE DEGREE OF DOCTOR OF PHILOSOPHY

BY

KEISHAM SURJIT SINGH

DEPARTMENT OF CHEMISTRY

SCHOOL OF PHYSICAL SCIENCES

NORTH-EASTERN HILL UNIVERSITY

SHILLONG-793022

2006

Synthesis and Reactivity studies of Organotin(IV) Complexes of 2-[(E)-2-(3-formyl-4-hydroxy) -1- diazenyl]benzoic acid and Related Systems: Assessment of Bonding, Structure and Biological Applications

A Thesis submitted in partial fulfilment of the requirements for the degree of doctor of philosophy

By

Keisham Surjit Singh

DEPARTMENT OF CHEMISTRY
SCHOOL OF PHYSICAL SCIENCES
NORTH-EASTERN HILL UNIVERSITY
SHILLONG-793022
2006

Dedicated to my Parents

DEPARTMENT OF CHEMISTRY

NORTH-EASTERN HILL UNIVERSITY, NEHU PERMANENT CAMPUS, UMSHING
SHILLONG 793 022 (INDIA)

CERTIFICATE

This is to certify that the research work presented in the thesis entitled "Synthesis and Reactivity Studies of Organotin(IV) Complexes of 2-[(*E*)-2-(3-formyl-4-hydroxy)-1-diazenyl]benzoic acid and Related Systems: Assessment of Bonding, Structure and Biological Applications" is carried out by Mr. Keisham Surjit Singh under my supervision in the Department of Chemistry, School of Physical Sciences, North-Eastern Hill University, Shillong. The work embodied in the thesis does not form the basis for the award of any previous degree, diploma, fellowship or any other similar title and that it represents entirely an independent work on the part of the candidate.

Dr. T. S. Basu Baul

Supervisor
Department of Chemistry
North-Eastern Hill University
Shillong 793 022

Prof.R.H.Duncan Lyngdoh

Head
Department of Chemistry
North-Eastern Hill University
Shillong 793 022

Date: 13.07.06

Place: Shillong

Tushar S. Basu Baul

Tel: +91 364 2722626; **Fax**: 91 364 2550486 (work)
Email: basubaul@nehu.ac.in

DECLARATION

I hereby, declare that the thesis entitled "Synthesis and Reactivity studies of Organotin (IV) Complexes of 2-[(*E*)-2-(3-formyl-4-hydroxy)-1-diazenyl]benzoic acid and Related Systems: Assessment of Bonding, Structure and Biological Applications" is the result of the work carried out by me under the supervision of Dr. T. S. Basu Baul, Department of Chemistry, School of Physical Sciences, North-Eastern Hill University, Shillong for the award of Doctor of Philosophy in Chemistry. The contents of the thesis did not form the basis of the award of any previous degree to me or to anybody else. The work presented in the thesis is original and the outcome of some useful results has been published in the international journals.

To the best of my knowledge the thesis has not been submitted for any degree to this university or any other university.

13/07/06

Keisham Surjit Singh

Department of Chemistry
North Eastern Hill University
Shillong.

ACKNOWLEDGEMENTS

I would like to express my deep sense of gratitude to my thesis supervisor Dr. T. S. Basu Baul, Department of Chemistry, North-Eastern Hill University, Shillong who has introduced me in this exciting field of organometallic chemistry and given me an insight into the organotin chemistry. I am greatly indebted for his invaluable advice, guidance, constant inspiration, boundless enthusiasm and his dedication towards this research work.

I am highly thankful to Prof. R. H. Duncan Lyngdoh, Head, Department of Chemistry, North-Eastern Hill University, Shillong, for providing me all the facilities available in our department. I take this opportunity to thank Prof. M. K. Mahanti, Dean, School of Physical Sciences, Prof. R. K. Poddar and Prof. K. Ismail, former Head of Department of Chemistry and other faculty members of the department for their valuable suggestions.

I owe a special thank to all our collaborators, Dr. A. Linden, Institute of Organic Chemistry, University of Zurich, Switzerland, Prof. R. Butcher, Department of Chemistry, Howard University, USA, Dr. A. Lycka, Resaearch Institute for Organic Syntheses, Czech Republic, Prof. M. Holcapek, University of Pardubice, Department of Analytical Chemistry, Czech Republic, Prof. G. Eng, Department of Chemistry and Physics, University of the District of Columbia, USA and Dr. Dick de Vos, The Netherlands for their invaluable help through out the Ph. D. programme.

for providing spectral and x-ray data.

I am thankful to Sophisticated Instruments Facility, I. I. Sc., Bangalore and North-Eastern Hill University, Shillong, for providing spectral data. I am also thankful to Mr. P. S. Dkhar for providing IR spectra. I extend my thanks to all the non teaching staff for their cooperation.

It is my great pleasure to convey my heartfelt thanks to all my Lab mates Mr. Pradip Das, Mr. Wandondor Rynjah, Mr. Cheerfulman Masharing, Miss. Archana Mizar and Miss Smita Basu for their cooperation and pleasant association with me during my course of research in Shillong which will remain stay in my heart. My sincere thanks go to my brother Dr. Keisham Sarjit Singh and my friend Mr. K. Pachunga for their valuable help. I would also like to thank all the research scholars for the helpful discussion during my stay in Shillong.

It remains incomplete if I don't acknowledge Inter University Consortium, Department of Atomic Energy, Govt. of India for providing me the financial assistance.

Finally my honest and humble regards goes to my parents, Mr. Keisham Chaoba Singh and Mrs. Keisham Binodini Devi and to my brothers and sisters and, all my family members for their constant support and encouragements in all sphere of my life.

Above all, I thank God, for giving me strength, good health and his mercy bestows showered upon me.

Keisham Surjit Singh

CONTENTS

CHAPTER 3

TRIORGANOTIN(IV) COMPLEXES OF 2-[(*E*)-(3-FORMYL-4-HYDROXYPHENYL)-DIAZENYL]- AND 2-{(*E*)-4-HYDROXY-3-[(*E*)-4-(ARYL)IMINOMETYHY]PHENYL-DIAZENYL}- BENZOIC ACIDS: SYNTHESES, CHARECTERIZATION AND STRUCTURES

CHAPTER 4

TRIORGANOTIN(IV) COMPLEXES OF 4-[(*E*)-(3-FORMYL-4-HYDROXYPHENYL)-DIAZENYL]- AND 4-{(*E*)-4-HYDROXY-3-[(*E*)-4-(ARYL)IMINOMETHYL]PHENYL-DIAZENYL}-BENZOIC ACIDS: SYNTHESES, CHARECTERIZATION AND STRUCTURES

CHAPTER 5

DIORGANOTIN(IV) COMPLEXES OF 2-[(*E*)-(3-FORMYL-4-HYDROXYPHENYL)-DIAZENYL]- AND 2-{(*E*)-4-HYDROXY-3-[(*E*)-4-(ARYL)IMINOMETHYL]PHENYL DIAZENYL}- BENZOIC ACIDS: SYNTHESES, CHARECTERIZATION AND STRUCTURES

CHAPTER 6

BIOLOGICAL APPLICATIONS OF ORGANOTIN(IV) COMPLEXES OF 2-[(*E*)-(3-FORMYL-4-HYDROXYPHENYL)-DIAZENYL]- AND 2-{(*E*)-4-HYDROXY-3-[(*E*)-4-(ARYL)IMINOMETHYL]PHENYLDIAZENYL}BENZOIC ACIDS

List of Publications

Abbreviation

Å	Angstrom (X-ray)
asym	asymmetric
br	broad (NMR)
Bz	benzyl
COSY	Correlation spectroscopy (NMR)
J	coupling constant (NMR)
d	doublet (NMR)
dd	doublet of doublet (NMR)
d_{calcd}	density calculated (X-ray)
ESI-MS	Electrospray ionization mass spectrometry
GOF	Goodness of fit (X-ray)
gs	gradient selected (NMR)
HMBC	Heteronuclear multiple bond connectivity (NMR)
HMQC	Heteronuclear multiple quantum correlation(NMR)
HSQC	Hetronuclear single quantum correlation (NMR)
Hz	Hertz (NMR)
ID	inhibition dose
IS (δ)	Isomer shift (Mössbauer)
LC	Lethal concentration
Γ	line widths (Mössbauer)
Me	methyl
μ	absorption coefficient (X-ray)
m	multiplet (NMR)
M.p.	melting point
^{n}Bu	n-butyl
Ph	phenyl
QS (Δ)	quadrupole splitting (Mössbauer)
QSAR	Quantitative structure-activity relationship
sym	symmetric
^{t}Bu	t-butyl
t	triplet (NMR)
V	volume (X-ray)
Z	formula unit per unit cell (X-ray)

PREFACE

The thesis entitled "Synthesis and reactivity studies of organotin(IV) complexes of 2-[(*E*)-2-(3-formyl-4-hydroxy)-1-diazenyl]benzoic acid and related systems: Assessment of bonding, structure and biological applications" has aimed to explore the chemistry of organotin(IV) carboxylates with some arylazo and arylazo-imino ligands.

The sequence of the chapters reflects the preparation of arylazo- and arylazo-imino ligands and subsequent reactions with organotin precursors and their characterization with the help of analytical and spectroscopic data. The solid state structures of some representative complexes were determined using single crystal X-ray crystallography. The work has been divided in six chapters.

Chapter 1

This is a general introductory chapter which highlights a brief account of the chemistry and structural possibilities of organotin(IV) azo-carboxylates. This is followed by biological applications of organotin(IV) compounds.

Chapter 2

This chapter describes the preparation of various ligands, *viz.*, 2-[(*E*)-(3-formyl-4-hydroxyphenyl)-1-diazenyl]benzoic acid, 2-{(*E*)-4-hydroxy-3-[(*E*)-4-(aryl)iminomethyl] phenyldiazenyl}benzoic acid and 4-[(*E*)-(3-formyl-4-hydroxyphenyl)-1-diazenyl] benzoic acid. The ligands were fully characterized by elemental analysis, IR and ^{1}H-, ^{13}C-NMR including 2D NMR techniques. In some cases, the structures of the ligands were accomplished by single crystal X-ray crystallography.

Chapter 3

This chapter describes the synthesis and characterization of various triorganotin(IV) complexes derived from *o*-carboxylate ligands i.e. 2-[(*E*)-(3-formyl-4-hydroxyphenyl)-1-diazenyl]benzoic acid and 2-{(*E*)-4-hydroxy-3-[(*E*)-4-(aryl)iminomethyl]phenyldiazenyl}benzoic acid. The triorganotin(IV) groups studied are tri-n-butyl-, triphenyl- and tribenzyl. Among these, tribenzyltin(IV) compounds deserve specific comments. The reaction of Bz_3SnCl with sodium 2-[(*E*)-2-(3-formyl-4-hydroxyphenyl)-1-diazenyl]benzoate proceeded via debenzylation and oxidative decarbonylation. This reaction afforded a cyclic dinuclear dibenzyltin(IV) complex, $[Bz_2\{O_2CC_6H_4\{N(H)\text{-}N{=}(C_6H_3\text{-}4(=O)\text{-}5\text{-}O)\}\text{-}o\}Sn]_2$ (see Chapter 5 for details). However, the

desired product of composition $Bz_3SnLH.OH_2$ was obtained by reacting equimolar amounts of Bz_3SnOH with 2-[(*E*)-2-(3-formyl-4-hydroxyphenyl)-1-diazenyl]benzoic aicd in anhydrous toluene. Further, the reactions of Bz_3SnCl with sodium 2-{(*E*)-4-hydroxy-3-[(*E*)-4-(aryl)iminomethyl]phenyldiazenyl}benzoates, were attempted under identical reaction conditions in the expectation of obtaining the corresponding $Bz_3Sn(IV)$ derivatives. Instead, the work-up of the reaction mixture yielded crystals of the same cyclic dibenzyltin(IV) dimer, i.e. $[Bz_2\{O_2CC_6H_4\{N(H)\text{-}N{=}(C_6H_3\text{-}4(=O)\text{-}5\text{-}O)\}\text{-}o\}Sn]_2$. In these reactions, cleavage of the H-C=N-Ar part from the ligand molecule and simultaneous debenzylation was noticed. Attempted reactions of 2-{(*E*)-4-hydroxy-3-[(*E*)-4-(aryl)iminomethyl]phenyldiazenyl}benzoic acid with Bz_3SnOH in anhydrous toluene afforded the desired products $Bz_3SnLH.OH_2$ in moderate to good yields. The geometry of the complexes were determined using ^{119}Sn NMR spectroscopic techniques in solution. The solid state structures were confirmed by single crystal X-ray crystallography in combination with ^{119}Sn Mössbauer spectroscopy.

Chapter 4

This chapter deals with synthesis of various triorganotin(IV) complexes derived from *p*-carboxylate ligands i.e. 4-[(*E*)-(3-formyl-4-hydroxyphenyl)-1-diazenyl]benzoic acid and 4-{(*E*)-4-hydroxy-3-[(*E*)-4-(aryl)iminomethyl]phenyldiazenyl}benzoic acid. This chapter discusses the synthesis, spectroscopic characterization and crystallography study of tri-n-butyltin(IV)- and triphenyl(IV) complexes.

Chapter 5

The chemistry of diorganotin(IV) complexes of the ligands 2-[(*E*)-(3-formyl-4-hydroxyphenyl)-diazenyl] benzoic acid and 2-{(*E*)-4-hydroxy-3-[(*E*)-4-(aryl) iminomethyl] phenyldiazenyl} benzoic acid are described. The di-n-butyltin(IV) complexes of the type $\{[^nBu_2Sn(LH)]_2O\}_2$ and a dibenzyltin(IV) complex $[(PhCH_2)_2\{O_2CC_6H_4\{N(H)\text{-}N{=}(C_6H_3\text{-}4(=O)\text{-}5\text{-}O)\}\text{-}o\}Sn]_2$ were fully characterized by elemental analysis, IR, NMR (^1H, ^{13}C, ^{119}Sn), ^{119}Sn Mössbauer spectroscopy. The decomposition of the compounds was studied using ESI-MS spectroscopic analysis. X-ray diffraction analyses results are also presented in this chapter.

Chapter 6

The concluding chapter deals with the biological applications of organotin(IV) complexes of various arylazo- and arylazo-imino ligands described above. The first part of the

chapter discusses the toxicity study of tri-n-butyltin(IV) complexes of these ligands which were screened against second instars stage of *Aedes aegypti* and *Anopheles stephensi* mosquito larvae.

The following section deals with the embryo toxicity study of a ligand 2-[(*E*)-(3-formyl-4-hydroxyphenyl)-diazenyl] benzoic acid and its tri-n-butyltin(IV) complex on two sea urchin species, *viz.*, *Paracentrotus lividus* and *Sphaerechinus granularis*.

The last part of this chapter describes *in vitro* cytotoxicity study of a di-n-butyltin(IV) complex of 2-{(*E*)-4-hydroxy-3-[(*E*)-4-(methyl phenyl)iminomethyl]phenyldiazenyl}benzoic acid i.e. $\{[^{n}Bu_2Sn(L^2H)]_2O\}_2$. The cytotoxic activity was tested across a panel of human cell lines *viz.*, WIDR (colon cancer), M19 MEL (melanoma), A498 (renal cancer), IGROV (ovarian cancer) and H226 (non-small cell lung cancer), MCF7 (breast cancer), EVSA-T (breast cancer). The results were compared with the standard drugs which are used clinically.

CHAPTER 1

A BRIEF REVIEW OF ORGANOTIN(IV) COMPLEXES OF AZO-CARBOXYLIC ACIDS

1.1 Introduction

The use of tin compounds in a large variety of applications is well known and organotin(IV) carboxylates are well represented in this context, having uses in industry and agriculture [1-3]. In addition, an area of current interest involves the screening of organotin(IV) compounds for potential anti-tumour activity and focuses upon results obtained in the past decade or so, as well as upon other therapeutic applications of tin compounds [4]. A number of early reviews recording advances in the screening for antitumour potential of organotins are available [5-10]. In the recent reviews, published in 1991 and 1994, the structural chemistry of organotin carboxylates was surveyed [11,12]. This survey revealed that there exists a rich structural diversity for these compounds where very different structures are found even though the chemical formulae may be quite similar. In view of these, a number of structures are being reported till today highlighting the interest in this particular class of compound.

1.2 Organotin(IV) complexes of azo carboxylic acid

The organotin(IV) carboxylates derived from azo ligands (Fig. 1.1) have been reported by Majee and Banerjee [13]. This type of ligands is well suited for the preparation of a variety of interesting organotin complexes because the ligands i.e. arylazobenzoic acids with a wide variety of nuclear substituents can be easily prepared by diazotization of the amino benzoic acid followed by coupling with suitable aryl moiety and have a very favourable steric arrangement for the complexation. In this context, a series of triorganotin(IV) derivatives of arylazobenzoic acids were prepared and investigated spectroscopically [13,14] which offered interesting structural possibilities. Their UV spectra recorded in non-polar solvents exhibited a large bathochromic shifts and such shifts were predicted for N→Sn co-ordination (Fig. 1.2). These interaction was found to be absent in co-ordinating solvents as the weak N→Sn bond is replaced by a donor solvent molecule (S) as shown in Fig. 1.3.

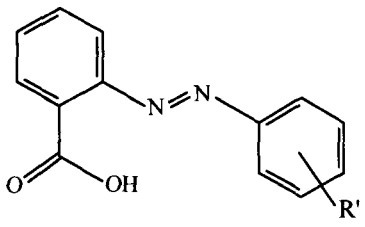

Fig. 1.1

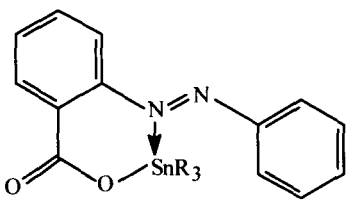

Fig. 1.2

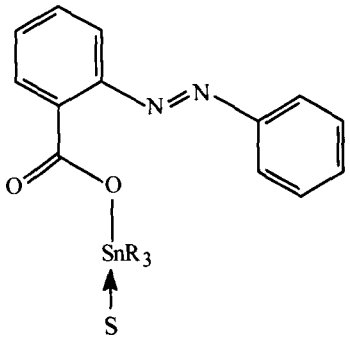

Fig. 1.3

Further, when the aryl group contains a donor group in the *ortho*- position of the coupling moiety, the arylazobenzoato moiety was postulated to function as a terdentate ligand (Fig. 1.4). In view of this, structures of triphenyltin(IV)/ tricyclohexyltin(IV) complexes of *o*-(2-hydroxy-5-methylphenylazo)benzoic acid (Fig.1.5) and triphenyltin(IV) complexes of *o*-(2-hydroxy-naphthylazo)benzoic acid (Fig. 1.6) have been studied by ^{119}Sn Mössbauer spectroscopy. In addition, triphenyltin(IV) complexes of *o*-(4-dimethylaminophenylazo)benzoic and *o*-(4-hydroxynaphthylazo)benzoic were also investigated (Figs. 1.7 and 1.8).

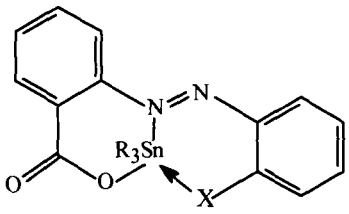

(X = -OH or $-NH_2$)

Fig. 1.4

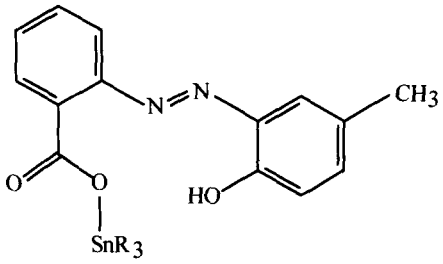

(R = phenyl- or cyclohexyl-)

Fig. 1.5

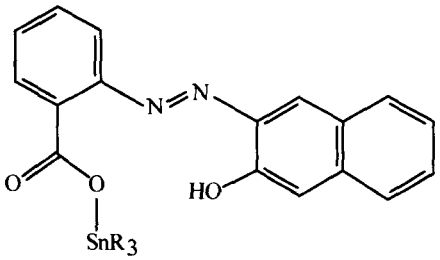

(R = phenyl-)

Fig. 1.6

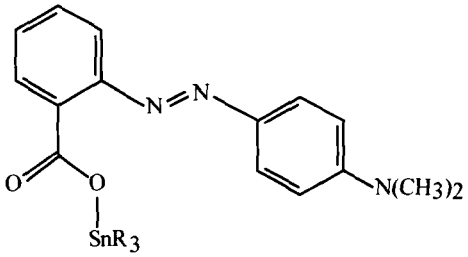

(R = phenyl-)

Fig. 1.7

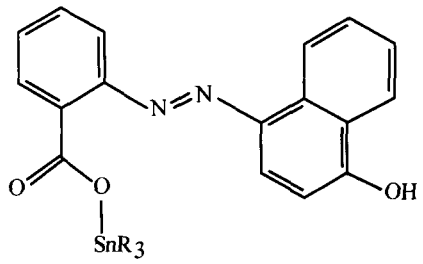

(R = phenyl-)

Fig. 1.8

A few years after, the crystal structure of the triphenyltin(IV) *o*-(2-hydroxy-5-methylphenylazo)benzoate was determined in the hope that the complex would constitute the first example of a six-coordinated triorganotin(IV) compound. Crystals of the triphenyltin(IV) *o*-(2-hydroxy-5-methylphenylazo) benzoate (see Fig.1.5; R = Ph) comprise discrete molecular units, in which the carboxylato group functions as an anisobidentate chelating ligand [Sn-O(I): 2.070(5), Sn...O(2): 2.463(7) Å], thus rendering the tin atom five co-ordinated (Fig. 1.9). The unit-cell projection of the compound reveals that there is no intermolecular carboxylato-bridging. The geometry at the tin atom is intermediate between tetrahedral and *cis*-trigonal bipyramidal, in which the carboxylato ligand spans equatorial and axial sites. The two C–O bond distances of the carbonyl group are as expected unequal [C-O(1): 1.296(8); C-O(2): 1.224(8) Å]. The structure of the triphenyltin(IV) *o*-(2-hydroxy-5-methylphenylazo)benzoate complex as shown in Fig. 1.9 is, therefore, the first characterized example of a truly monomeric triorganotin carboxylate. It is interesting to note that, in spite of the bulky phenyl groups attached to tin and the very large steric demands of the arylazobenzoato group which prevent intermolecular bridging, the carboxyl group prefers to function as a chelating ligand giving the five- coordinated structure rather than as a unidentate ligand.

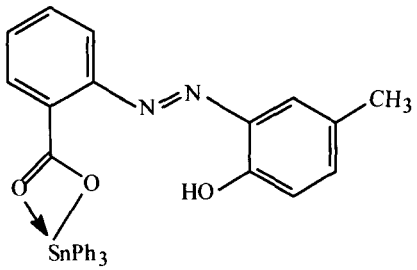

Fig. 1.9

Recently, a series of triorganotin(IV) complexes of formulation R_3SnO_2CR' where R = Me, Et, ^nBu, Ph and cHex and $R'CO_2$ residue of *o*-(2-hydroxy-5-methylphenylazo)benzoic acid, has been investigated in detail [16]. Among these, the structure of triphenyltin(IV) compound was investigated earlier by Harrison *et al.*[15]. The triphenyltin(IV) compound was again synthesized and upon recrystallization from acetone/methanol (1/9) solution afforded an acetone solvated product. The structure of triphenyltin(IV) *o*-(2-hydroxy-5-methylphenylazo)benzoate acetone solvate (2/1) [17] resembles closely that of the unsolvated form as shown in Fig. 1.9 [15]. The Sn atom exists in a distorted tetrahedral geometry with Sn-O(1) being 2.079(5) Å (cf.2.070(5) Å in the unsolvated form). The Sn...O(2) separation is 2.656(5) Å and is responsible for the expansion of the C-Sn-C angle to 116.9(3)°. There are no close interaction between the solvent acetone molecule and the compound. The same coordination geometry has been reflected in tricyclohexyltin(IV) compound as shown in Fig. 1.9 for triphenyltin(IV) analogue, and with the range of angles subtended at tin being 96.7(2)-120.1(2)°. The Sn...O(2) separation is 2.759(4) Å [16]. On the other hand, trialkyltin(IV) compounds (R = Me, Et, ^nBu) are polymers [16] and comprise distorted *trans*-R_3SnO_2 trigonal bipyramidal geometries (Fig. 1.10). The carboxylate ligand is bidentate bridging; however, the Sn-O bonds are not equivalent. The disparity in the Sn-O bond distances, [O(1)-Sn-O(2)], increases in the order Me (0.323 Å) < Et (0.350 Å) < ^nBu (0.415 Å). The intramolecular Sn...O(2) separations are 3.175(4), 3.18(1), and 3.245(3) Å for Me, Et, ^nBu, respectively.

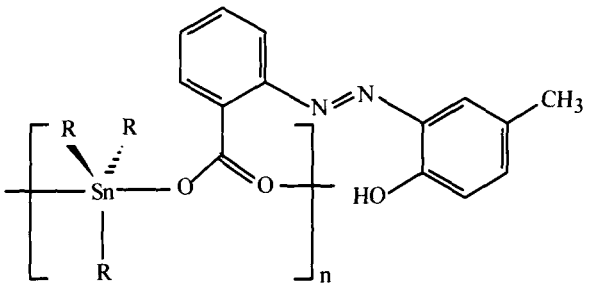

(R = methyl-, ethyl- or *n*-butyl-)

Fig. 1.10

The different behaviour, among various triorganotin(IV) compounds, has been ascribed to the steric demands of the tin-bound substituents. A fair correlation was found between the difference in ^{117}Sn chemical shift between the solution and solid states and, the carbonyl oxygen-tin distance of the triorganotin(IV) compounds, only when the data of triphenyltin(IV) compound, are

omitted. This indicated that the mesomeric effect of the phenyl group does not express its influence to the same extent in the solid and solution states, unlike the inductive effects. The crystal structures of the complexes were correlated with other spectroscopic data. By contrast, a good correlation including triphenyltin(IV) compound was found between the ^{119}Sn Mössbauer quadrupole splitting and the difference in ^{117}Sn chemical shift between the solution and solid states.

Trimethyltin(IV)- [18] and triethyltin(IV)- [19] complexes of *p*-(2-hydroxy-5-methylphenylazo)benzoic acid were also investigated crystallographically. Both the structures are polymeric owing to the presence of bidentate bridging carboxylate ligands. The intramolecular separation of 2.139(3) Å is shorter than the intermolecular Sn...O(2) distance of 2.497(3) Å in Me_3Sn compound. In Et_3Sn compound, the carboxylate ligands form disparate Sn-O(1) and Sn...O(2) distances of 2.149(4) Å and 2.586(4) Å, respectively. The structures of Me_3Sn and Et_3Sn resemble closely that found for the *ortho*- analogue as shown in Fig. 1.10 [16] and structures conform to a common motif, i.e. trans-C_3SnO_2.

The influence of molecular geometry in halodiorganotin(IV) complexes of the *o*-(2-hydroxy-5-methylphenylazo)benzoic acid was also studied [20]. The crystal and molecular structures of three compounds were presented in which the carboxylate residue has been kept constant and the R_2Sn moiety has been altered such that R = Me, ^{t}Bu and Ph. The crystallographic study shows that two distinct motifs are adopted owing to different modes of coordination of the carboxylate ligands. The chlorodimethyltin(IV) complex is dimeric with the two tin atoms being bridged by two $^-O_2CR'$ anions each of which coordinates a tin atom via one of the carboxylate oxygen atom and the second tin atom via the phenoxide oxygen atom and the complex exists in a zwitterionic form. The tin atom geometry is trigonal bipyramidal, *trans*-O_2SnC_2Cl (Fig. 1.11). By contrast to the dimeric structure for chlorodimethyltin(IV) complex, the structures of chlorodi-t-butyltin(IV) and chlorodiphenyltin(IV) complexes are monomeric with the tin atoms in *cis*-O_2SnC_2Cl trigonal bipyramidal geometries (Fig. 1.12). The $^-O_2CR'$ anion coordinates the tin atom via the caboxylate oxygen atoms only.

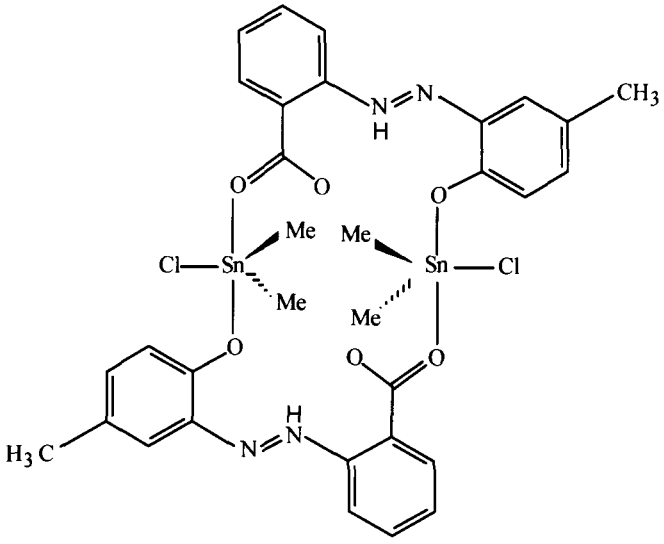

(R = methyl-)

Fig. 1.11

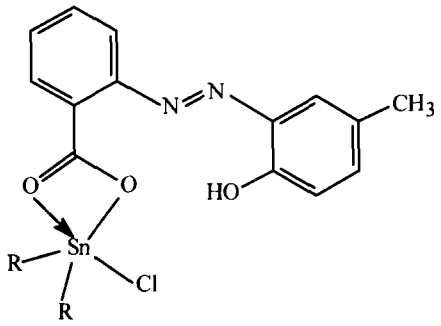

(R = *t*-butyl- or phenyl-)

Fig. 1.12

The crystal and molecular structures of two more compounds of the general formula $R_2Sn(O_2CR')_2$ are also reported where R = ^{t}Bu and Ph [21] (Fig. 1.13). For the R = ^{t}Bu compound, the tin atom exists in a skew-trapezoidal bipyramidal geometry in which the trapezoidal plane is defined by two asymmetrically chelating carboxylate ligands and the organic residues lie over the weaker Sn...O interactions. A similar coordination geometry is found in the R = Ph compound which was isolated as a di-chloroform solvate. The chloroform molecules exert an influence on the molecular geometry in that a conformational change in the carboxylate ligand is induced in order to facilitate the formation of intermolecular hydrogen bonds.

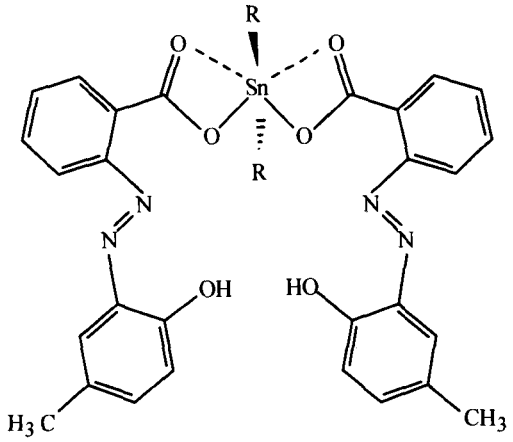

(R = *t*-butyl- or phenyl-)

Fig. 1.13

Systematic variations in the Sn-ligand parameters in these and related compounds are correlated with the varying Lewis acidity at the tin centres. The replacement of one carboxylate ligand in [^{t}Bu$_2$Sn(O$_2$CR')$_2$] by a chloride, i.e. yielding [^{t}Bu$_2$Sn(O$_2$CR')Cl] [20], results in a significant contraction of the Sn-O(2) distance to 2.402(3) Å while maintaining the primary Sn-O(1) interaction constant at 2.105(3) Å. The comparable distances for the [Ph$_2$Sn(O$_2$CR')Cl] structure are 2.365(3) Å and 2.090(3) Å, respectively [20]. These results are correlated with the enhanced Lewis acidity of the tin centre in the respective R$_2$SnCl moieties. For the R = Ph, substituting a carboxylate ligand in [Ph$_2$Sn(O$_2$CR')$_2$] with a phenyl group leading to [Ph$_3$Sn(O$_2$CR')] [17] results in Sn-O(1) and Sn-O(2) of 2.079(5) Å and 2.656(5) Å, respectively, a result consistent with the reduced Lewis acidity of the tin atom in Ph$_3$Sn compared with Ph$_2$Sn. The Lewis acidity of the tin center was found to decreases in the order Ph$_3$Sn < Ph$_2$Sn < Ph$_2$SnCl and ^{t}Bu$_2$Sn< ^{t}Bu$_2$SnCl for the phenyltin and tert-butyltin compounds, respectively.

More recently, a comprehensive study of organotin(IV) complexes was carried out involving 5-(arylazo)salicylic acid from the point of view of structural motifs and biological applications. A series of triphenyltin(IV) complexes of 5-(arylazo)salicylic acid has provided X-ray quality crystals in which the ligand aryl residue has been varied (aryl = phenyl- [22], 2-methylphenyl- [22], 3-methylphenyl- [22], 4-methylphenyl- [23], 4-methoxyphenyl- [22] and 4-chlorophenyl- [24]), and Ph$_3$Sn was held constant. The solid state structures of these triphenyltin(IV) complexes were evaluated using ^{119}Sn Mössbauer and X-ray crystallography. The triphenyltin(IV) complexes adopt a monomeric distorted tetrahedral configuration defined by a C$_3$O donor set where the carboxylate ligand coordinating in a monodentate mode (Fig. 1.14). The relatively small variations observed for the geometric parameters across the series of

triphenyltin(IV) complexes indicated that the variable substitution in the aryl residue has little influence on the tin geometry.

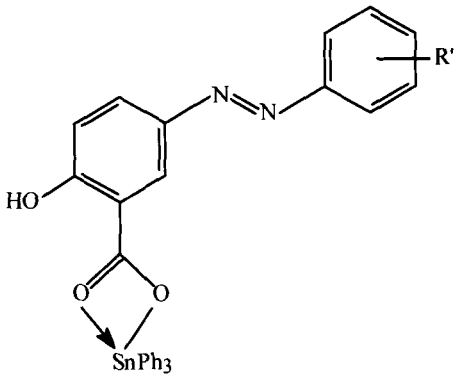

(R' = H, 2-methyl-, 3-methyl-, 4-methyl-, 4-methoxy- or 4-chloro-)

Fig. 1.14

Further, one of the tetrahedral triphenyltin(IV) complexes was subjected to the reactivity study towards 2,2'-bipyridine to ascertain the ability of 2,2'-bipyridine to coordinate to the Sn-complex and the resultant changes in the molecular architecture. The crystal structure of the product revealed that the 2,2'-bipyridine moiety does not coordinate to the Sn atom, but forms a cyclic tetrameric adduct of formula $[Ph_3SnO_2CR'(H_2O)]_2.bipy_2$ ($^-O_2CR'$= 5-(2-methylphenylazo)salicylate) through hydrogen bonding between the water ligand of $Ph_3SnO_2CR'(H_2O)$ and the 2,2'-bipyridine N atoms (Fig. 1.15) [23].

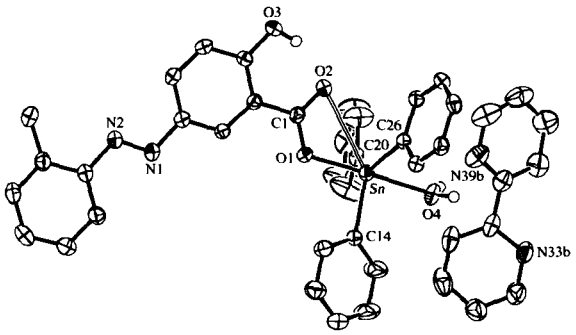

(a)

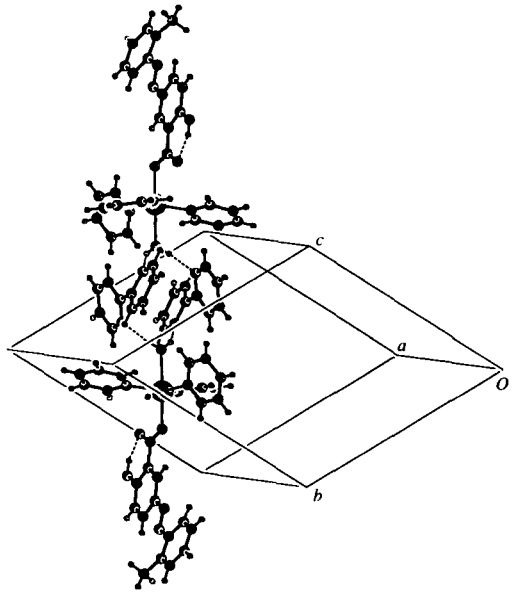

(b)

Fig.1.15 (a) The molecular structure of $Ph_3SnO_2CR'(H_2O)$.bipy (b) The hydrogen-bonded tetrameric motif in the molecular structure of $Ph_3SnO_2CR'(H_2O)$.bipy, consisting of two $Ph_3SnO_2CR'(H_2O)$.bipy and two bipy molecules.

The trialkyltin(IV) complexes, *viz.*, Me_3 [24], $^nBu_3$ [22,24] were investigated by ^{119}Sn Mössbauer and ^{119}Sn NMR spectroscopy. ^{119}Sn Mössbauer spectroscopy shows that these complexes are polymeric and feature a *trans*-trigonal bipyramidal geometry with a planar SnR_3 unit and two apical carboxylate oxygen atoms derived from bidentate bridging carboxylate ligands. These trialkyltin complexes dissociate in solution to a tetrahedral species as indicated by ^{119}Sn NMR data.

In addition, a series of di-n-butyltin complexes involving 5-(arylazo)salicylic acid have been studied in great detail in view of possible biological applications. A systematic investigation of the structures of the di-n-butyltin complexes of 5-(arylazo)salicylic acid was carried out. The carboxylate residue was varied by virtue of changes to the aryl group (aryl = phenyl- [25], 2-methylphenyl- [26], 3-methylphenyl- [25], 4-methylphenyl- [25], 4-bromophenyl- [25] and 4-chlorophenyl- [27]), and the $^nBu_2$ was held constant. In general, the crystallographic results indicated that the complexes adopt a skew-trapezoidal bipyramidal arrangement around the tin atom (Fig. 1.16).

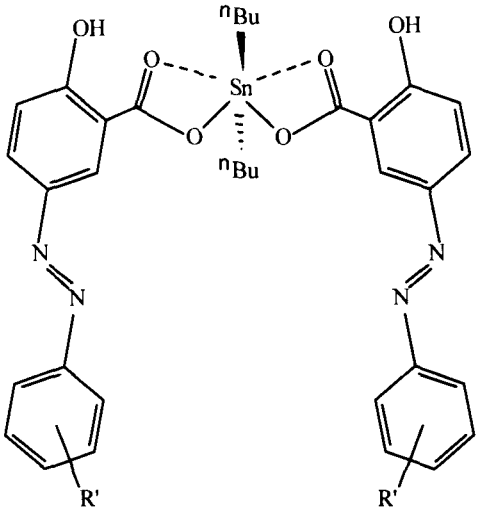

(R' = H, 2-methyl-, 3-methyl-, 4-methyl-, 4-bromo- or 4-chloro-)

Fig. 1.16

In addition, there are weak bridging intermolecular Sn...O contacts in di-*n*-butyltin(IV) complexes when carboxylate residue is phenyl-, 2-methylphenyl- or 3-methylphenyl- but not in substituents at 4-position (e.g. 4-methylphenyl-, 4-bromophenyl- and 4-chlorophenyl-), where one of the hydroxyl oxygen atoms from a neighbouring molecule coordinates weakly with the Sn atom, thereby completing a seventh coordination site in the extended Sn coordination sphere (Fig. 1.17).

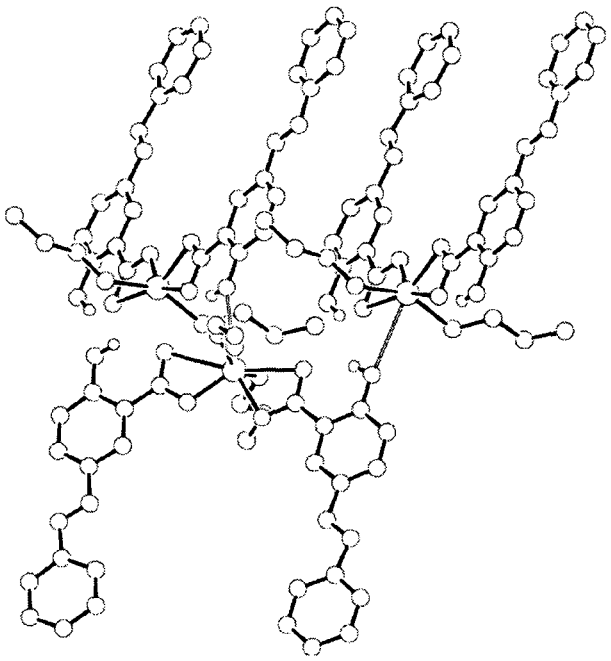

Fig.1.17 Three segments of the chain structure formed by the weak Sn···O interaction (open bonds) in di-n-butyltin(IV) complexes when carboxylate residue is phenyl.

The Sn...O distance is 3.080(2) and 3.439(2) Å in di-n-butyltin(IV) complexes when carboxylate residue is phenyl-, 2-methylphenyl- or 3-methylphenyl-. The values are significantly shorter than the sum of the van der Walls radii of the Sn and O atoms. This interaction links the molecules into polymeric chains or head-to-head dimeric units as shown in Fig 1.18.

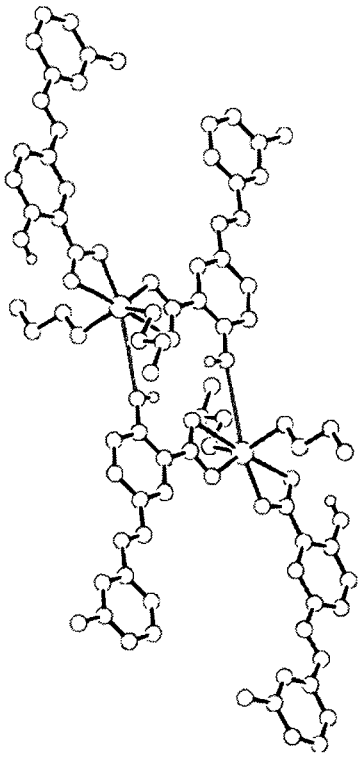

Fig.1.18 The dimeric unit formed by the weak Sn···O interaction in di-n-butyltin(IV) complexes when carboxylate residue is 3-methylphenyl.

The crystal structures of these complexes were correlated with ^{117}Sn CP MAS NMR and ^{119}Sn Mössbauer data, while their solution behaviour was evaluated using ^{119}Sn NMR in non coordinating solvents.

Another interesting report is of diorganotin(IV) complexes containing mixed arylazobenzoates of composition $[R_2Sn(O_2CR')(O_2CR'')]$ where R = ^{n}Bu or Me and $^-O_2CR'$ and $^-O_2CR''$ are two different 5-(arylazo)salicylates. A full characterization of the structures of the complexes in the solid-state was accomplished by single crystal X-ray crystallography [28]. The complexes were found to adopt the usual dicarboxylato structural type with a skew-trapezoidal bipyramidal arrangement around the tin atom as shown in Fig. 1.16.

A sterically congested organotin(IV) complex was obtained by the reaction of sodium 4-(4'-dimethylaminophenylazo)benzoate and {[2-(dimethylaminomethyl)phenyl](diphenyl)}tin chloride [29]. The crystal structure of the complex revealed that the tin atom exists in a slightly

distorted trans-trigonal bipyramidal geometry defined by three *ipso*-carbon atoms of the phenyl groups in equatorial positions, with the intramolecularly bound nitrogen atom for the $CH_2N(CH_3)_2$ group and the oxygen atom of the carboxylate groups in apical positions (Fig. 1.19).

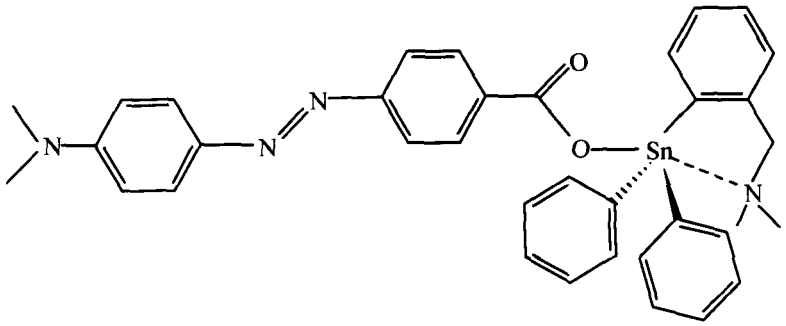

Fig.1.19

As a part of a wider study designed to ascertain the reason(s) for the structural variation found in these systems, the reactivity of a few triorganotin(IV)halide/hydroxide was studied with a new ligand system e.g. 5-(2'-carboxyphenylazo)salicylaldehyde. The molecular structure of $[Ph_3Sn(O_2CR')(OH_2)]$ (Fig. 1.20) [30] reveals that the carboxylate group coordinate to the tin atom via one of the oxygen atoms only (Sn-O = 2.161(5) Å. The tin atom is also coordinated by a water molecule (Sn-O =2.527(5) Å) and exists in a trigonal bipyramidal geometry with the three phenyl groups in equatorial positions; the O-Sn-O axial angle is 176.3(2)°. The lattice is stabilized by H-bonding contacts as well as charge-transfer interactions. A brief report of a polymeric trimethyltin(IV) compound $[Me_3Sn(O_2CR')]_n$ is also there in the literature [31]. The tin atom in this compound is fivefold-coordinated, existing in a distorted trigonal bipyramidal geometry (Fig. 1.21). The trigonal plane is defined by the three methyl groups and the axial positions by symmetry related oxygen atoms; Sn-O(1) = 2.174(6) Å, Sn-O(2)' = 2.448(7) Å and the tin atom lies 0.1246(7) Å out of the plane in the direction of the more strongly bound O(1) atom.

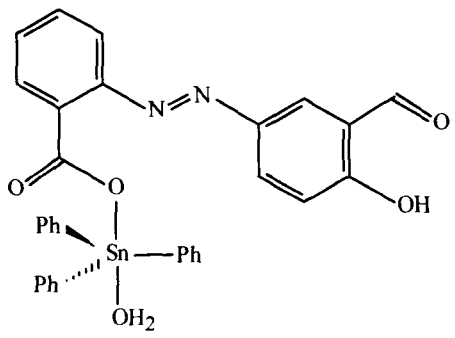

Fig.1.20

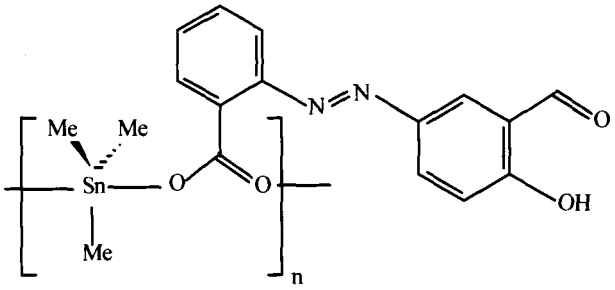

Fig.1.21

Further work in this area involving 5-(2'-carboxyphenylazo)salicylaldehyde (systematic name: 2-[(*E*)-2-(3-formyl-4-hydroxyphenyl)-1-diazenyl] benzoic acid) and related systems constitute the subject matter of the thesis and are described in the forth coming chapters.

1.3 Biological activity of organotin(IV) azocarboxylates

Triorganotin(IV) *o*-(arylazo)benzoates [32] (Fig.1.22) were screened *in vitro* for their biological activity against several microorganisms. These complexes were found to exhibit considerable activity against *Staphylococcus aureus, Bacillus Cereus, Sarcina lutea, Bacillus pumilus, Micrococcus flovus,* and *Bacillus subtitis.*

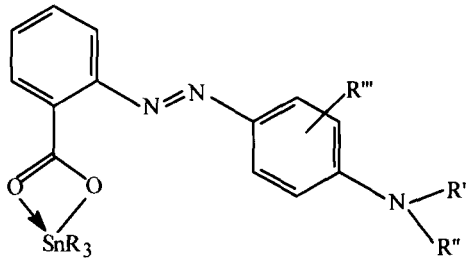

Fig. 1.22

The activity were correlated on the nature of aryl R', R'', R'''-substituents. The significant inhibition of bacterial growth by triorganotin *o*-(arylazo)benzoates compared to corresponding *o*-(arylazo)benzoic acid was explained and mechanism was proposed for arresting bacterial growth. The enzymatic proteins in their relatively rigid planar peptide structure possess carbonyl group capable of forming metal-oxygen bond with the stannyl groups of organotin carboxylate and this bond formation is further augmented by the nearby β- azoic nitrogen and stannyl carboxylate carbonyl oxygens which form bifurcated hydrogen bonds with the peptide N-H groups (N-H....N

= 2.97 Å, N-H....O = 3.29 Å), thus, enhancing the electron density on the peptide oxygen. A stereocomputer simulated molecular model of the mode of attachment of peptide unit (Gly-Gly) with crystallographic structure of triphenyltin(IV) *o*-[2-bromo-4-(dimethyl amino)phenylazo]benzoate is shown in Fig.1.23.

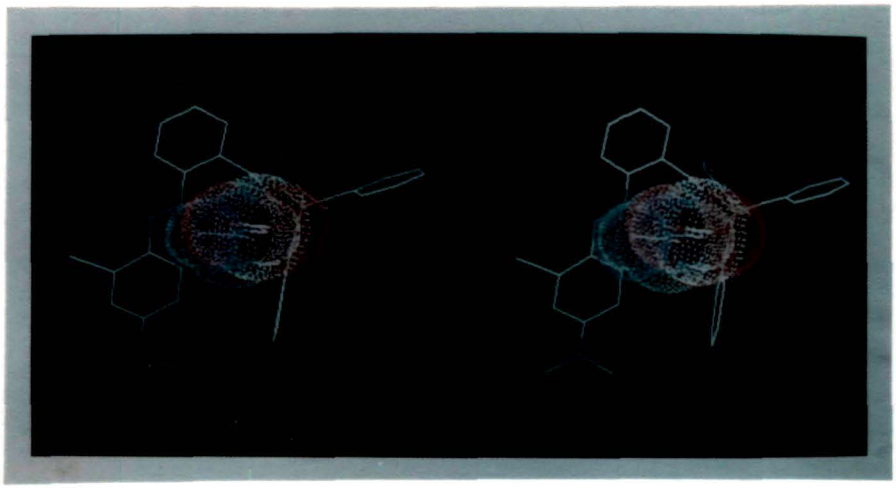

Fig. 1.23

Organotin(IV) complexes of 5-(arylazo)salicylic acid have been studied in great detail for evaluating their biological properties. A series of organotin(IV) complexes of formulations $^{n}Bu_2Sn(O_2CR')_2$, Ph_3SnO_2CR' and $^{n}Bu_3SnO_2CR'$ ($^{-}O_2CR'$ = substituted 5-(arylazo)salicylate) were subjected to toxicities studies against second larval instar of *Aedes aegypti* mosquito larvae [27]. The results indicate that all the triorganotin(IV) compounds have activities of an order of magnitude higher than for the diorganotin(IV) derivative. The LC_{50} values (concentration at which the test compounds killed 50% of the tested organisms) for the triorganotin(IV) compounds ranged from 0.53 to 3.50 mg l^{-1}. Also, the data indicated that the tri-n-butyltin(IV) compounds were more effective than the phenyl derivatives. Although the triorganotin(IV) compounds, are not as effective as organophosphorus insecticides [33] in their larvicial effects, their advantages lie in their biodegradability and lack of known resistance by this species of mosquitoes.

In addition, a representative di-n-butyltin(IV) compound of formulation $^{n}Bu_2Sn(O_2CR')_2$ ($^{-}O_2CR'$ = substituted 5-(arylazo)salicylate), was tested across a panel of human cell lines *viz.*, WIDR (colon cancer), M19 MEL (melanoma), A498 (renal cancer), IGROV (ovarian cancer) and

H226 (non-small cell lung cancer), MCF7 (breast cancer), EVSA-T (breast cancer) to establish the activity [25]. The data clearly show that the di-n-butyltin(IV) compound is more active *in vitro* than cisplatin and etoposide against all seven human cancer cell lines.

The toxicity studies of tri-n-butyltin(IV) complexes of formulation $^{n}Bu_3SnO_2CR'$(O_2CR' = substituted 5-(arylazo)salicylate) and the parent 5-(arylazo)salicylic acid were evaluated by using sea urchin early developmental stages as recommended model organisms for toxicity tests [34]. The present report also throw light on the effects of new organotin compounds towards two species of sea urchin, *Paracentrotus lividus* and *Sphaerechinus granularis*, in order to compare variation in the impact incidence of contaminant exposure among different species. Biological activity tests of the tri-n-butyltin(IV) complexes demonstrated that the (i) embryos exposed to the tri-n-butyltin(IV) complexes at 10^{-5} and 10^{-7} M solutions presented blocks and strong developmental anomalies. (ii) embryos treated with free 5-(arylazo)salicylic acid at 10^{-5} M concentration stopped to develop at the blastula stage. At 10^{-7} M, they developed regularly as the control. (iii) embryos treated with tri-n-butyltin(IV) chloride (positive control) did not develop any more. (iv) sensitivity of *S. granularis* embryos was like that of *P. lividus*. The developmental anomalies can be seen in Figs. 1.24 and 1.25.

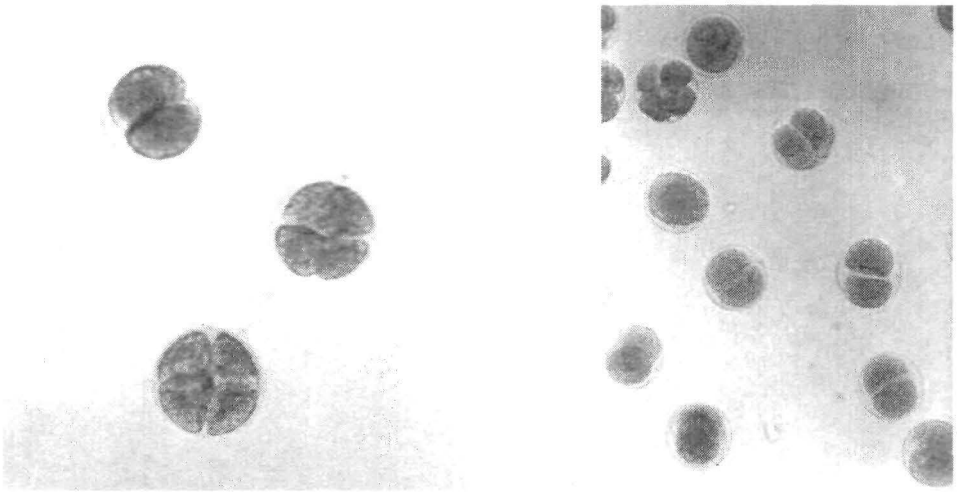

(a) (b)

Fig.1.24 Sea urchin control embryos and treated embryos with tri-n-butyltin(IV) compounds. Anomalous embryos exposed to tri-n-butyltin(IV) compounds solutions did not show any significant difference under optical microscopy: *P. lividus* (a) and *S. granularis* (b) anomalous embryos, after incubation in 10^{-5} M solution of the compound for 48 h. The blastomeres are of different sizes and are blocked at the two to four- cell stages.

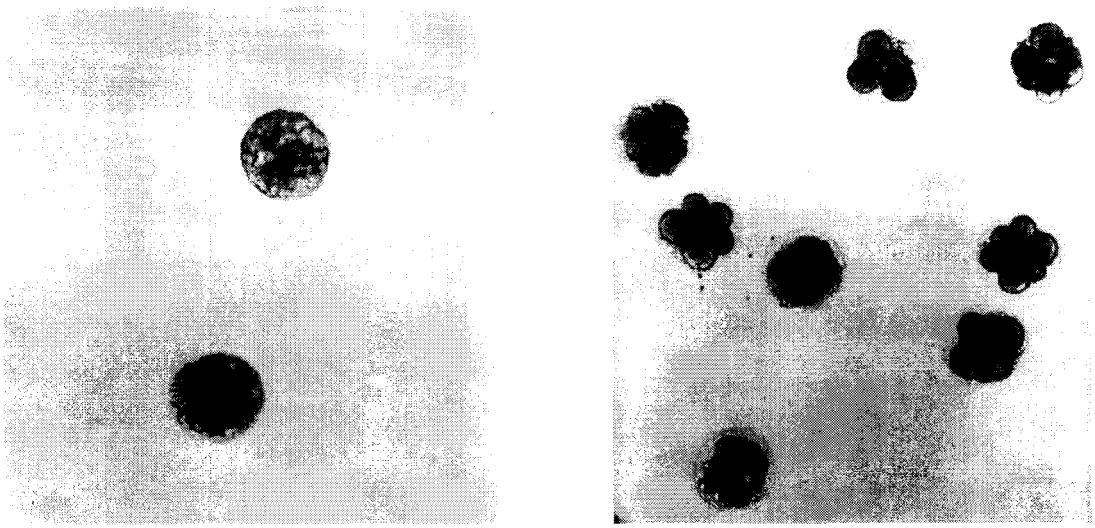

(a) (b)

Fig.1.25 Sea urchin control embryos and treated embryos with tri-n-butyltin(IV) compounds. Anomalous embryos exposed to tri-n-butyltin(IV) compounds solutions did not show any significant difference under optical microscopy: *P. lividus* (a) and *S. granularis* (b) anomalous embryos, after incubation in 10^{-7} M solution of the compound for 48 h and arrested anomalous embryos.

In conclusion, the tri-n-butyltin(IV) compounds induced high embryonic mortality in *P. lividus* and *S. granularis;* and were as toxic as tri-n-butyltin(IV) chloride independently of the presence of the ligands.

From the foregoing description of the structural chemistry of organotin(IV) azocarboxylates, it is clear that there exists a rich diversity in Sn atom geometry and coordination modes of the azocarboxylates themselves. Such complexes are likely to find wide application in biology, medicine etc.

References

[1] A.G. Davies, P.J. Smith, in: G. Wilkinson, F.G.A. Stone, E.W. Abel (Eds.), Comprehensive Organometallic Chemistry, Vol. 2, Pergamon Press, Oxford, 1982, Ch. 11.

[2] C.J. Evans, S. Karpel, Organotin Compounds in Modern Technology, J. Organomet. Chem. Library, Vol. 16, Elsevier, Amsterdam, 1985.

[3] I. Omae, Organotin Chemistry, J. Organomet. Chem. Library, Vol. 21, Elsevier, Amsterdam, 1989.

[4] M. Gielen, E.R.T. Tiekink, in: M. Gielen, E.R.T. Tiekink (Eds.), Metallotherapeutic Drug and Metal-Based Diagnostic Agents: ^{50}Sn Tin Compounds and Their Therapeutic Potential, Wiley, 2005, pp. 421-439.

[5] F. Huber, R. Barbieri, in: N.F. Cardarelli (Eds.), Tin as a Vital Nutrient: Implications in Cancer Prophylaxis and other Physiological Processess, CRC Press, Boca Ration, 1986, pp. 175-187.

[6] A.J. Crowe, Drugs of the Future **12** (1987) 255.

[7] L.R. Sherman, F. Huber, Appl. Organomet. Chem. **2**, (1988) 65.

[8] A.K. Saxena, F. Huber, Coord. Chem. Rev. **95** (1989) 109.

[9] A.J. Crowe, in: M. Gielen (Eds.), Tin Compounds and their Potential as Pharmaceutical Agents, NATO ASI Series, Vol. H37, Springer-Verlag, Berlin, 1990, pp. 69-114.

[10] J.M. Tsangaris, D.R. Williams, Appl. Organomet. Chem. **6** (1992) 3.

[11] E.R.T. Tiekink, Appl. Organomet. Chem. **5** (1991) 1.

[12] E.R.T. Tiekink, Trends Organomet. Chem. **1** (1994) 71.

[13] B. Majee, S. Banerjee, J. Organometal. Chem. **139**, 39 (1977).

[14] B. Majee, S. Banerjee, J. Organometal. Chem. **140**, 151 (1977).

[15] P.G. Harrison, K. Lambert, T.J. King, B. Majee, J. Chem. Soc., Dalton Trans. 363 (1983).

[16]R. Willem, I. Verbruggen, M. Gielen, M. Biesemans, B. Mahieu, T.S. Basu Baul, E.R.T.Tiekink, Organometallics **17** (1998) 5758.

[17] T.S. Basu Baul, E.R.T. Tiekink, Z. Kristallogr. **211** (1996) 489.

[18] T.S. Basu Baul, E.R.T. Tiekink, Acta Crystallogr. C **52** (1996) 1428.

[19] T.S. Basu Baul, E.R.T. Tiekink, Z. Kristallogr. NCS **212** (1997) 365.

[20] T.S. Basu Baul, E.R.T. Tiekink, Z. Kristallogr. **213** (1998) 62.

[21] T.S. Basu Baul, E.R.T. Tiekink, Z. Kristallogr. **214** (1999) 566.

[22] T.S. Basu Baul, S. Dhar, S.M. Pyke, E.R.T. Tiekink, E. Rivarola, R. Butcher, F.E. Smith, J. Organomet. Chem. **633** (2001) 7.

[23] T.S. Basu Baul, W. Rynjah, E. Rivarola, A. Linden, J. Organomet. Chem. **690** (2005) 613.

[24] T.S. Basu Baul, S. Dhar, N. Kharbani, S.M. Pyke, R. Butcher, F.E. Smith, Main Group Met. Chem. **22** (1999) 413.

[25] T.S. Basu Baul, W. Rynjah, R. Willem, M. Biesemans, I. Verbruggen, M. Holčapek, D. de Vos, A. Linden, J. Organomet. Chem. **689** (2004) 4691.

[26] T.S. Basu Baul, S. Dhar, E.R.T. Tiekink, Main Group met. Chem. **24** (2001) 293.

[27] T.S. Basu Baul, S. Dhar, E. Rivarola, F.E. Smith, R. Butcher, X. Song, M. McCain, G. Eng, Appl. Organomet. Chem. **17** (2003) 261.

[28] T.S. Basu Baul, W. Rynjah, E. Rivarola, C. Pettinari, A. Linden, J. Organomet. Chem. **690** (2005) 1413.

[29] A. Ruzicka, A. Lycka, R. Jambor, P. Novak, I. Cisarova, M. Holcapek, M. Erben, J. Holecek, Appl. Organomet. Chem. **17** (2003) 168.

[30] T.S. Basu Baul, S.M. Pyke, K.K. Sarma, E.R.T. Tiekink, Main Group met. Chem. **19** (1996) 807.

[31] T.S. Basu Baul, E.R.T. Tiekink, Z. Kristallogr. NCS **212** (1997) 363.

[32] B.B. Maji, S. Pain, G. Biswas, K.L.Ghatak, S.N.Ganguly, A. Banerjee, Indian Acad.Sci.(Chem. Sci.) **105**, 183 (1993)

[33] S.C. Rawlins, J.O.H. Wan, J. Am. Mosq. Control Assoc. **11** (1995) 59.

[34] T.S. Basu Baul, W. Rynjah, K.S. singh, C. Pellerito, P. D'Agati, L. Pellerito, Appl. Organomet. Chem. **19** (2005) 1189.

CHAPTER 2

SYNTHESIS AND STRUCTURAL CHARECTERIZATION OF LIGANDS

2.1 Introduction

The development of organotin(IV) carboxylate chemistry is highly dependent on a facile synthetic access to the ligands. The ligands used herein are of two types where the carboxylic acid group placed (i) in *ortho*- position e.g. 2-[(*E*)-2-(3-formyl-4-hydroxyphenyl)-1-diazenyl]- and 2-{(*E*)-4-hydroxy-3-[(*E*)-4-(aryl)iminomethyl]phenyldiazenyl}- benzoic acids and (ii) in *para*- position e.g. 4-[(*E*)-2-(3-formyl-4-hydroxyphenyl)-1-diazenyl]- and 4-{(*E*)-4-hydroxy-3-[(*E*)-4-(aryl)iminomethyl]phenyldiazenyl}- benzoic acids. The ligands, 2-[(*E*)-2-(3-formyl-4-hydroxyphenyl)-1-diazenyl]- and 4-[(*E*)-2-(3-formyl-4-hydroxyphenyl)-1-diazenyl]-benzoic acids were prepared by usual diazo-coupling reactions which contain an azo group. The aromatic monoamines react with 2-[(*E*)-2-(3-formyl-4-hydroxyphenyl)-1-diazenyl]benzoic acid to form products, such as 2-{(*E*)-4-hydroxy-3-[(*E*)-4-(aryl)iminomethyl]phenyldiazenyl} benzoic acid, which contain both azo and Schiff base (i.e. imino) linkages. A similar azo-Schiff base organic compound, namely *N*-*p*-methoxybenzylidene-*p*-phenylazoaniline, is a mesogen and exhibits a nematic liquid-crystal phase; its X-ray structure has also been determined recently [1]. In addition, structures of two similar molecules containing *meta* azo and imine substituents, also exhibiting liquid crystalline properties, have recently been determined [2,3]. The potential usefulness of such polyaromatic systems has prompted us to investigate the reactivity towards organotin(IV) moiety. However, this family of ligands await characterization as mesogens and the determination of other essential features such as thermotropic, lyotropic and macroscopic (e.g. optical) properties. It should be mentioned here that the condensation products of aromatic monoamines with 4-[(*E*)-2-(3-formyl-4-hydroxyphenyl)-1-diazenyl]benzoic acid is not possible owing to the insolubility of the later in common organic solvents and water. The ligand frameworks (L^7HH'-$L^{10}HH'$) were generated *in situ* during the reactions of R_3SnL^6H (R = ^{n}Bu or Ph) with the appropriate *p*-substituted anilines (refer to Chapter 4).

The ligands used in the present study are described in section 2.2.

2.2 Ligands used in present study ($L^{1\text{-}10}HH'$)

The ligands and their systematic names are given in Table 2.1.

Table 2.1: Ligands, their names and abbreviation

Ligand	Name	Abbreviation[a]
(a) Ligands containing an *ortho*-carboxylic acid group		
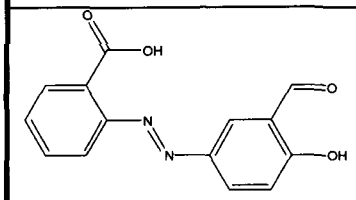	2-[(*E*)-2-(3-formyl-4-hydroxy-phenyl)-1-diazenyl] benzoic acid	**L^1HH'**
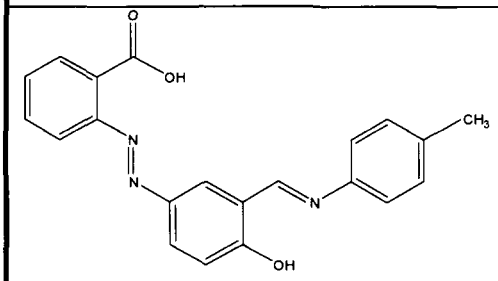	2-{(*E*)-4-hydroxy-3-[(*E*)-4-methyl-phenyliminomethyl]phenyldiazenyl}-benzoic acid	**L^2HH'**
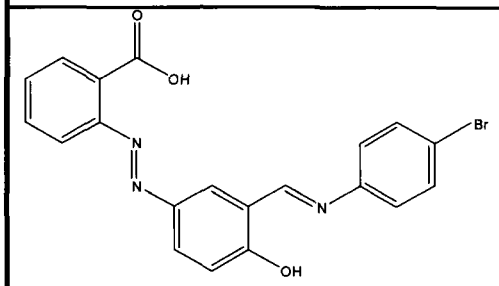	2-{(*E*)-4-hydroxy-3-[(*E*)-4-bromo-phenyliminomethyl]phenyldiazenyl}-benzoic acid	**L^3HH'**
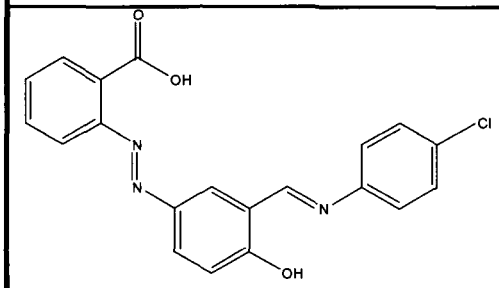	2-{(*E*)-4-hydroxy-3-[(*E*)-4-chloro-phenyliminomethyl]phenyldiazenyl}-benzoic acid	**L^4HH'**

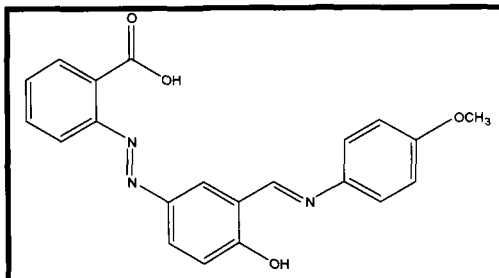	2-{(*E*)-4-hydroxy-3-[(*E*)-4-methoxy-phenyliminomethyl]phenyldiazenyl}-benzoic acid	**L^5HH'**
(b) Ligands containing a *para*-carboxylic acid group[b]		
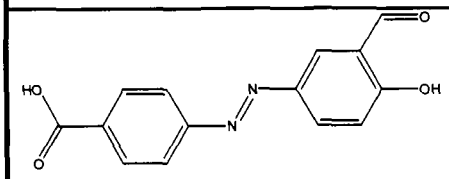	2-[(*E*)-2-(3-formyl-4-hydroxy-phenyl)-1-diazenyl]benzoic acid	**L^6HH'**
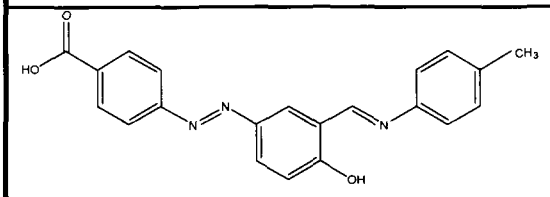	4-{(*E*)-4-hydroxy-3-[(*E*)-4-methyl-phenyliminomethyl]phenyldiazenyl}-benzoic acid	**L^7HH'**
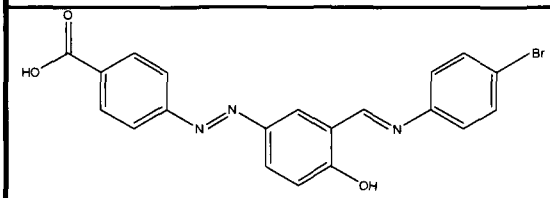	4-{(*E*)-4-hydroxy-3-[(*E*)-4-bromo-phenyliminomethyl]phenyldiazenyl}-benzoic acid	**L^8HH'**
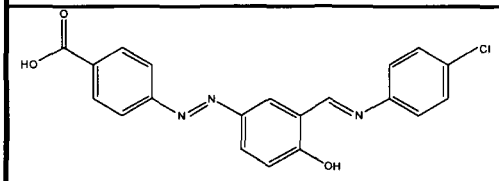	4-{(*E*)-4-hydroxy-3-[(*E*)-4-chloro-phenyliminomethyl]phenyldiazenyl}-benzoic acid	**L^9HH'**
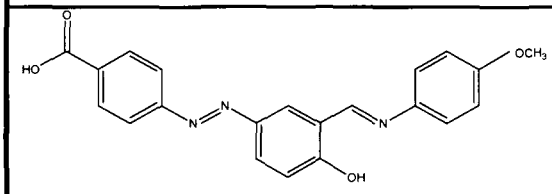	4-{(*E*)-4-hydroxy-3-[(*E*)-4-methoxy-phenyliminomethyl]phenyldiazenyl}-benzoic acid	**$L^{10}HH'$**

[a]H and H' represent hydroxy and carboxylic acid H atoms, respectively.

[b]The ligands, L^7HH'-$L^{10}HH'$ were generated *in situ* (refer to Chapter 4).

2.3 Synthesis of ligands

The 2-[(*E*)-2-(3-formyl-4-hydroxyphenyl)-1-diazenyl]benzoic acid (L^1HH') was prepared by the diazo-coupling reaction between the anthranilic acid and salicylaldehyde in alkaline medium under cold conditions by the method described in our earlier report [4]. The 2-{(*E*)-4-hydroxy-3-[(*E*)-4-(aryl)iminomethyl]phenyldiazenyl}benzoic acids ($L^{2\text{-}5}HH'$) were prepared by condensation of L^1HH' with appropriate *p*-substituted anilines in anhydrous toluene-ethanol mixture. The 4-[(*E*)-2-(3-formyl-4-hydroxyphenyl)-1-diazenyl]benzoic acid (L^6HH') was prepared by the diazo-coupling reaction between the *p*-aminobenzoic acid and salicylaldehyde in an alkaline medium under cold conditions. On the other hand, the 4-{(*E*)-4-hydroxy-3-[(*E*)-4-(aryl)iminomethyl]phenyldiazenyl}benzoic acids ($L^{7\text{-}10}HH'$) could not be prepared by the condensation of L^6HH' with appropriate the substituted anilines owing to the insolubility of the pre-ligand in common organic solvents and water. However, the deprotonated $L^{7\text{-}10}HH'$ frameworks were generated during the reactions of R_3SnL^6H (R = ^{n}Bu or Ph) with the appropriate *p*-substituted anilines (refer to Chapter 4). The ligand frameworks are shown in Table 2.1, along with their abbreviations. The details of their synthesis and characterization data are presented in section 2.6 while their spectroscopic data are summarized below.

2.4 Spectroscopic characterization

The IR spectra of the ligands (L^1HH'-$L^{10}HH'$) are very complex due to the presence of a large number of vibrational modes due to ring stretch, deformation, in-plane and out-of-plane ring and CH deformations. However, these modes are of little value in the understanding of the structure of the ligands. Valuable information can, however, be obtained from the frequencies of carboxylate stretch, Ar-OH (C-O vibration involving hydroxyl group of salicylaldehyde moiety), the N=N and C=N stretches. Unfortunately, even these modes could not be identified with certainty in all the cases because of the presence of the complex nature of the vibrations in the region where these modes are expected.

The diagnostically important infrared absorption frequencies for the carboxylate antisymmetric [ν_{asym}(OCO)] stretching vibration for the L^1HH' have been detected at 1733 cm^{-1}, around the 1725 cm^{-1} region for $L^{2\text{-}5}HH'$ and 1679 cm^{-1} for L^6HH'. The assignment of the

symmetric [ν_{sym}(OCO)] stretching vibration band could not be made owing to the complex pattern of the spectra.

The ^{1}H- and ^{13}C- NMR signals of L^{1}HH' [4] and L^{6}HH' were assigned by the use of correlated spectroscopy (COSY), heteronuclear single-quantum correlation (HMQC) and heteronuclear multiple-bond connectivities (HMBC) experiments using gradient coherence selection and also by examining the spin-spin splitting pattern of the signals. The conclusions drawn from the L^{1}HH' assignments were then subsequently extrapolated to the other ligands (L$^{2-5}$HH') owing to their data similarity. The ^{1}H-NMR integration values were completely consistent with the formulation of the products. The number of ^{13}C signals corresponds with the proposed formulations of the products. The basic ligand frame-work is shown in Figs. 2.1- 2.3 along with the abbreviations and numbering schemes for spectroscopic analyses. The detailed spectral features are shown below:

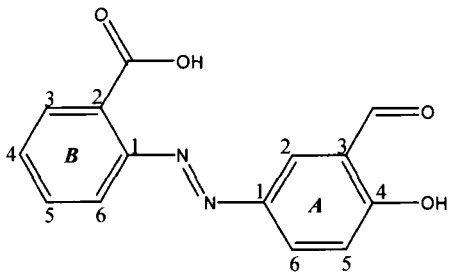

Fig. 2.1 Generic structure of the ligand, L^{1}HH'

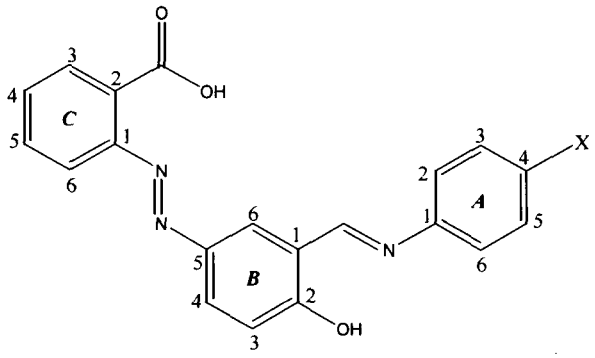

[Abbreviations: L^{2}HH': X = 4-CH_3; L^{3}HH': 4-Br, L^{4}HH': 4-Cl, L^{5}HH': 4-OCH_3]

Fig. 2.2 Generic structure of the ligand, L^{2}HH'- L^{5}HH'

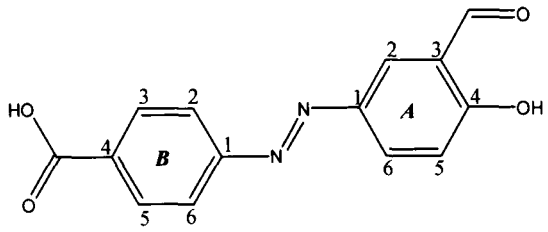

Fig. 2.3 Generic structure of the ligand, L^6HH'

2.4.1 2-[(E)-2-(3-formyl-4-hydroxyphenyl)-1-diazenyl]benzoic acid (L^1HH') [4]

IR (cm^{-1}): 1733 $\nu(OCO)_{asym.}$ ^{1}H-NMR (Pyridine-d_5/ 600 MHz); δ_H: 7.15 [d, 8.8 Hz, 1H, (A) H5], 7.52 [dt, 1.5, 7.7 Hz, 1H, (B) H5], 7.58 [dt, 1.5, 7.7 Hz, 1H, (B) H4], 7.80 [dd, 1.5, 7.7 Hz, 1H, (B) H6], 8.21 [dd, 1.5, 7.7 Hz, 1H, (B) H3], 8.29 [dd, 2.6, 8.8 Hz, 1 H, (A) H6], 8.67 [d, 2.6 Hz, 1H, (A) H2], 10.64 [s, 1 H, (A) H3] and 11.51 [bs, 2 H, (B) H7 and (A) H4] ppm. ^{13}C-NMR (Pyridine-d_5/150 MHz); δ_C: 118.1 [(B) C6], 118.5 [(A) C5], 127.0 [(A) C2], 128.5 [(A) C3], 129.7 [(A) C6], 129.9 [(B) C5], 130.0 [(B) C3] 131.4 [(B) C4], 132.1 [(B) C1], 145.9 [(A) C4], 150.9 [(B) C2], 164.7 [(A) C1], 169.9 [(B) C7] and 191.9 [(A) C7] ppm.

2.4.2 2-{(E)-4-hydroxy-3-[(E)-4-methylphenyliminomethyl]phenyldiazenyl}benzoic acid (L^2HH')

IR (cm^{-1}): 1725 $\nu(OCO)_{asym.}$ ^{1}H-NMR (DMSO-d_6 / 500.13 MHz); δ_H: 2.38 [s, 3H, CH_3], 7.18 [d , 1H, (B) H3], 7.32 [part of AA'BB' system, 2H, (A) H3 & H5], 7.43 [part of AA'BB' system, 2H, (A) H2 & H6], 7.60 [m, 1H, (C) H4], 7.61 [m, 1H, (C) H6], 7.69 [m, 1H, (C) H5], 7.84 [m, 1H, (C) H3], 7.98 [dd, 1H, (B) H4], 8.29 [d, 1H, (B) H6], 9.16 [s, 1H, C(H)=N], 12.91 [brs, 1H, CO_2H], 14.16 [brs, 1H, OH] ppm. ^{13}C-NMR (DMSO-d_6/ 125.76 MHz); δ_C: 20.7 [CH_3], 118.3 [(B) C3], 118.33 [(C) C6], 119.2 [(B) C1], 121.4 [(A) C2 & C6], 126.5 [(B) C4], 129.2[(B) C6], 129.3 [(C) C3], 129.9 [(C) C4], 130.1 [(A) C3 & C5], 130.2 [(C) C2], 131.7 [(C) C5], 137.1 [(A) C4], 144.5 [(A) C1], 144.9 [(B) C5], 150.9 [(C) C1], 161.7 [C(H)=N], 164.5 [(B) C2], 168.5 [CO_2H] ppm.

2.4.3 2-{(E)-4-hydroxy-3-[(E)-4-bromophenyliminomethyl]phenyldiazenyl}benzoic acid (L^3HH')

IR (cm^{-1}): 1723 $\nu(OCO)_{asym.}$ ^{1}H-NMR (DMSO-d_6 / 500.13 MHz); δ_H : 7.21 [d, 1H, (B) H3], 7.48 [part of AA'MM' system , 2H, (A) H2 & H6], 7.60 [m , 1H, (C) H6], 7.61 [m, 1H, (C) H4], 7.70 [m, 1H, (C) H5], 7.71 [part of AA'MM' system, 2H, (A) H3 & H5], 7.84 [m, 1H, (C)

H3], 7.99 [dd, 1H, (B) H4], 8.31 [d, 1H, (B) H6], 9.16 [s, 1H, C(H)=N], 12.99 [brs, 1H, CO_2H], 13.57 [brs, 1H, OH] ppm. ^{13}C-NMR (DMSO-d_6 / 125.76 MHz); δ_C: 118.2 [(B) C3], 118.4 [(C) C6], 119.4 [(B) C1], 120.4 [(A) C4], 123.7 [(A) C2 & C6], 126.9 [(B) C4], 128.8 [(B) C6], 129.3 [(C) C3], 129.9 [(C) C4], 130.2 [(C) C2], 131.7 [(C) C5], 132.5 [(A) C3 & C5], 145.1 [(B) C5], 147.0 [(A) C1], 150.9 [(C) C1], 163.1 [C(H)=N], 163.8 [(B) C2], 168.5 [CO_2H] ppm.

2.4.4 2-{(E)-4-hydroxy-3-[(E)-4-chlorophenyliminomethyl]phenyldiazenyl}benzoic acid (L^{4}HH')

IR (cm^{-1}): 1725 $\nu(OCO)_{asym}$. ^{1}H-NMR (DMSO-d_6 / 500.13 MHz); δ_H: 7.21 [d, 1H, (B) H3], 7.53 [part of AA'BB' system, 2H, (A) H3 & H5], 7.57 [part of AA'BB' system, 2H, (A) H2 & H6], 7.60 [m, 1H, (C) H6], 7.61 [m, 1H, (C) H4], 7.69 [m, 1H, (C) H5], 7.83 [m, 1H, (C) H3], 7.99 [dd, 1H, (B) H4], 8.31 [d, 1H, (B) H6], 9.16 [s, 1H, C(H)=N], 12.97 [brs, 1H, CO_2H], 13.59 [brs, 1H, OH] ppm. ^{13}C-NMR (DMSO-d_6 / 125.76 MHz); δ_C: 118.1 [(B) C3], 118.4 [(C) C6], 119.4 [(B) C1], 123.4 [(A) C2 & C6], 126.9 [(B) C4], 128.7 [(B) C6], 129.3 [(C) C3], 129.5 [(A) C3 & C5], 129.9 [(C) C4], 130.2 [(C) C2], 131.6 [(A) C4], 131.7 [(C) C5], 145.1 [(B) C5], 146.6 [(A) C1], 150.9 [(C) C1], 163.1 [C(H)=N], 163.8 [(B) C2], 168.5 [CO_2H)] ppm.

2.4.5 2-{(E)-4-hydroxy-3-[(E)-4-methoxyphenyliminomethyl]phenyldiazenyl}benzoic acid (L^{5}HH')

IR (cm^{-1}): 1723 $\nu(OCO)_{asym}$. ^{1}H-NMR (DMSO-d_6 / 500.13 MHz); δ_H: 3.84 [s, 3H, OCH_3], 7.08 [part of AA'MM' system, 2H, (A) H3 & H5], 7.17 [d , 1H, (B) H3], 7.53 [part of AA'MM' system, 2H, (A) H2 & H6], 7.60 [m, 1H, (C) H4], 7.61 [m, 1H, (C) H6], 7.70 [m, 1H, (C) H5], 7.83 [m, 1H, (C) H3], 7.96 [dd, 1H, (B) H4], 8.26 [d, 1H, (B) H6], 9.16 [s, 1H, C(H)=N], 12.90 [brs, 1H, CO_2H], 14.24 [brs, 1H, OH] ppm. ^{13}C-NMR (DMSO-d_6/ 125.76 MHz); δ_C: 55.5 [OCH_3], 114.8 [(A) C3 & C5], 118.2 [(B) C3], 118.3 [(C) C6], 119.3 [(B) C1], 122.9 [(A) C2 & C6], 126.3 [(B) C4], 128.9 [(B) C6], 129.3 [(C) C3], 129.8 [(C) C4], 130.2 [(C) C2], 131.7 [(C) C5], 139.8 [(A) C1], 144.9 [(B) C5], 150.9 [(C) C1], 158.9 [(A) C4], 160.4 [C(H)=N], 164.3 [(B) C2], 168.5 [CO_2H] ppm.

2.4.6 4-[(E)-2-(3-formyl-4-hydroxyphenyl)-1-diazenyl]benzoic acid (L^{6}HH')

IR (cm^{-1}) 1679 $\nu(OCO)_{asym.}$ ^{1}H-NMR (DMSO-d_6 /500.13 MHz); δ_H: 7.24 [d,1H, (A) H5], 7.95 [m (part of AA'BB' system), 2H, (B) H2 & H6], 8.14 [dd, 1H, (A) H6], 8.16 [m (part of AA'BB' system), 2H, (B) H3 & H5], 8.25 [d, 1H, (A) H2], 10.38 [s, 1H, C(H)=O], ppm. Signals

for the phenol and carboxylic acid were exchanged due to the presence of water in the solvent. ^{13}C-NMR (DMSO-d_6 /125.76 MHz); δ_C: 118.7 [(A) C5], 122.4 [(B) C2 & C6], 122.8 [(A) C3], 124.5 [(A) C2], 129.9 [(A) C6], 130.7 [(B) C3 & C5], 132.5 [(B) C4], 144.8 [(A) C1], 154.3 [(B) C1], 164.2 [(A) C4], 166.8 [CO_2H)], 190.5 [C(H)=O], ppm.

2.5 X-ray crystallography

Crystals of the ligands suitable for an X-ray crystal-structure determination were obtained from toluene (L^2HH' and L^3HH') and chloroform/ DMSO mixture (L^4HH') by slow evaporation of the solvent at room temperature. The crystal structures of three of the ligands (**L^2HH'- L^4HH')** have been determined. The data collection and refinement parameters are given in Table 2.2, while selected geometric parameters are collected in Table 2.3.

Table 2.2: Crystallographic data and structure refinement parameters for the ligands (L^2HH'-L^4HH')

	$L^2HH'.0.5H_2O$	$L^3HH'.0.5C_7H_8$	$L^4HH'.0.5H_2O$
Empirical formula	$C_{21}H_{17}N_3O_3.0.5H_2O$	$C_{20}H_{14}BrN_3O_3.0.5C_7H_8$	$C_{20}H_{14}ClN_3O_3.0.5H_2O$
Formula weight	368.39	470.32	388.80
Crystal size (mm)	0.10 × 0.2 × 0.20	0.20 × 0.13 × 0.08	0.50 × 0.35 × 0.28
Crystal shape	Prism	Tablet	Prism
Temperature (K)	160(1)	160(1)	293(2)
Crystal system	Monoclinic	Triclinic	Monoclinic
Space group	*C2/c*	$P\bar{1}$	*C2/c*
a (Å)	13.0688(4)	8.2708(1)	13.2451(19)
b (Å)	21.8141(6)	10.7547(3)	21.668(4)
c (Å)	12.5941(4)	12.3929(3)	12.664(2)
α (°)	90	88.1844(17)	90
β (°)	92.487(2)	85.3535(16)	91.69(2)
γ (°)	90	69.6152(13)	90
V (Å^3)	3587.0(2)	1029.91(5)	3632.8(10)
Z	4	2	8
D_x (g cm^{-3})	1.364	1.516	1.422
μ (mm^{-1})	0.0948	2.033	2.12
Transmission factors (min, max)	-	0.671, 0.795	0.415, 0.522
Reflections measured	39399	23736	3534
Independent reflections (R_{int})	4113 (0.079)	4718 (0.0467)	3382 (0.037)
Reflections with $I > 2\sigma(I)$	2633	3707	1707
Number of parameters	263	304	254
$R(F)$ ($I > 2\sigma(I)$ reflns)	0.050	0.0368	0.076
$wR(F^2)$ (all data)	0.136	0.0977	0.216
GOF(F^2)	1.02	1.034	1.06
max, min $\Delta\rho$ (e/Å^3)	0.29, -0.19	0.392, -0.541	0.20, -0.25

Table 2.3: Selected bond lengths (Å) and angles (°) for $L^2HH'.0.5H_2O$, $L^3HH'.0.5C_7H_8$ and $L^4HH'.0.5H_2O$

	$L^2HH'.0.5H_2O$	$L^3HH'.0.5C_7H_8$	$L^4HH'.0.5H_2O$
C(18) -C(21)/ [C(18) –Br][a]/ [C(18) –Cl][b]	1.504(2)	1.902(2)	1.730(5)
O(1) -C(1)/ [O(2) -C(1)][b]	1.329(2)	1.329(3)	1.311(6)
O(2) -C(1)/ [O(1) -C(1)][b]	1.211(2)	1.206(3)	1.207(6)
O(3) -C(11)	1.303(2)	1.333(2)	1.333(6)
N(1) -N(2)	1.270(2)	1.262(2)	1.269(5)
N(2)-N(1)-C(3)/ [N(2)-N(1)-C(7)][b]	115.0(1)	114.8(2)	114.2(4)
N(1)-N(2)-C(8)	115.6(1)	115.5(2)	114.3(4)
C(14)-N(3)-C(15)	125.2(1)	121.7(2)	123.0(4)
O(2)-C(1)-O(1)	119.6(2)	120.1(2)	118.6(5)
O(2)-C(1)-C(2)/ [O(1)-C(1)-C(2)][b]	122.3(2)	121.8(2)	122.1(5)
O(1)-C(1)-C(2)/ [O(2)-C(1)-C(2)][b]	118.2(1)	118.1(2)	119.2(5)
N(1) -C(3)/ [N(1) -C(7)][b]	1.424(2)	1.429(3)	1.426(6)
N(2) -C(8)	1.403(2)	1.408(3)	1.411(6)
N(3) -C(14)	1.295(2)	1.286(3)	1.287(6)
N(3) -C(15)	1.415(2)	1.416(3)	1.407(6)
C(4)-C(3)-N(1)/ [C(6)-C(7)-N(1)][b]	122.2(1)	122.6(2)	122.6(4)
C(2)-C(3)-N(1)/ [C(2)-C(7)-N(1)][b]	117.5(1)	117.4(2)	117.1(4)
C(9)-C(8)-N(2)/ [C(13)-C(8)-N(2)][b]	115.6(1)	115.1(2)	114.9(4)
N(3)-C(14)-C(10)/ [N(3)-C(14)-C(12)][b]	120.5(1)	120.2(2)	120.3(5)
C(16)-C(15)-N(3)/ [C(20)-C(15)-N(3)][b]	123.6(1)	123.4(2)	125.5(4)
C(20)-C(15)-N(3)/ [C(16)-C(15)-N(3)][b]	117.0(1)	117.0(2)	116.3(4)

Geometric parameters in square brackets with superscript "a" and "b" refer to the $L^3HH'.0.5C_7H_8$ (Fig. 2.6) and $L^4HH'.0.5H_2O$ (Fig. 2.8), respectively.

The structures of the ligands (L^2HH'- L^4HH') are discussed in sequel:

2.5.1 Crystal structure of 2-{(E)-4-hydroxy-3-[(E)-4-methylphenyliminomethyl] phenyldiazenyl}benzoic acid hemihydrate ($L^2HH'.0.5H_2O$)

In the crystal structure of $L^2HH'.0.5H_2O$, the asymmetric unit contains one molecule of the carboxylic acid in a general position plus a water molecule that sits on a C_2-axis, thereby giving a L^2HH':water ratio of 2:1. The three ring system of L^2HH' has an extended conformation with both external rings slightly twisted with respect to the central aromatic ring (Fig. 2.4) [5].

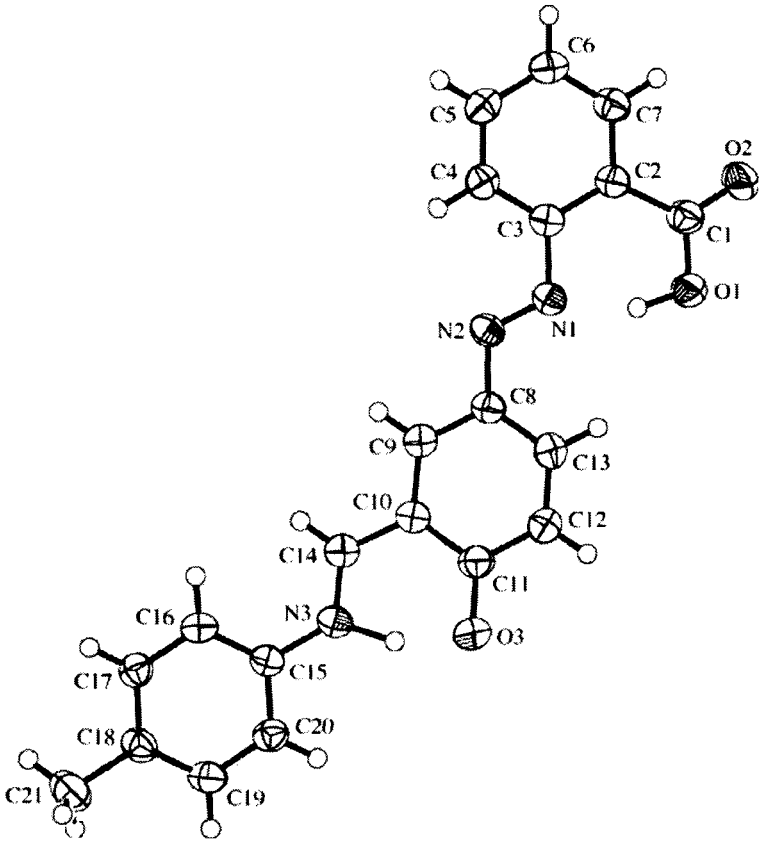

Fig. 2.4 View of the molecule of $L^2HH'.0.5H_2O$ showing the atom-labelling scheme (50% probability ellipsoids).

The carboxylic acid group is coplanar with its parent phenyl ring [O(1)-C(1)-C(2)-C(7) = 174.8(1)°]. The carboxylic acid molecule appears to be a zwitterion. The electron density peak associated with the expected phenolic H-atom was found to be closer to the imine N-atom (Table 2.4), although a plotted difference *Fourier* map of the region suggested that the electron density due to this H-atom is quite smeared out. Plots of difference *Fourier* maps with the H-atom

position idealized firstly on the O-atom and then on the N-atom showed that neither idealized position fitted the observed electron density optimally, although a better match was obtained when the N-atom was considered to be protonated.

Table 2.4: Hydrogen bonding geometry (Å, °) for $L^2HH'.0.5H_2O$

D-H···A	D-H	H···A	D···A	D-H···A
O(1)-H(1)···N(1)	1.00(3)	1.63(3)	2.582(2)	156(2)
N(3)-H(3)···O(3)	1.17(3)	1.42(3)	2.533(2)	156(2)
O(22)-H(22)···O(2^i)	0.99(2)	1.89(3)	2.866(2)	169(2)

Primed atoms refer to the molecule in the symmetry related position: $2-x, y, \frac{1}{2}-z$

The carboxylic acid hydroxy group in L^2HH' forms an intramolecular hydrogen bond with the nearest adjacent azo N-atom, while the protonated imine N-H atom forms an intramolecular hydrogen bond with the adjacent deprotonated phenolic hydroxy O-atom. Both of these interactions form six-membered loops with a graph set motif [6] of S(6). In addition, one H-atom of the water molecule forms an intermolecular hydrogen bond with the carbonyl O-atom of the carboxylic acid group of one L^2HH' molecule. The C_2-symmetry of the water molecule means that the second H-atom of the water molecule forms an identical intermolecular hydrogen bond with a second carboxylic group of another L^2HH' molecule. The net result is the formation of a discrete hydrogen-bonded unit consisting of one water molecule and two molecules of the ligand molecules (Fig. 2.5).

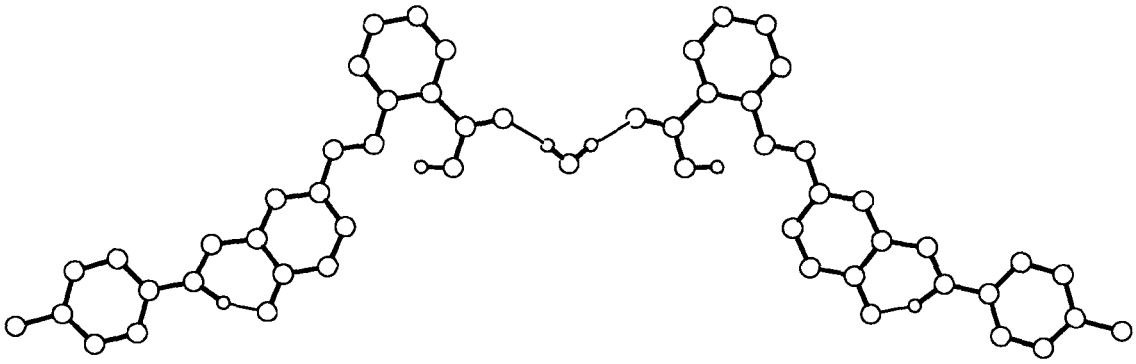

Fig. 2.5 Hydrogen-bonded unit consisting of one water molecule and two molecules of the L^2HH'

2.5.2 Crystal structure of 2-{(E)-4-hydroxy-3-[(E)-4-bromophenyliminomethyl] phenyldiazenyl}benzoic acid toluene hemisolvate ($L^3HH'.0.5C_7H_8$)

The asymmetric unit in $L^3HH'.0.5C_7H_8$ [7] contains one molecule of the carboxylic acid plus half of a toluene molecule that is disordered about a centre of inversion. The three-ring system of L^3HH' has an extended and reasonably flat conformation (Fig. 2.6).

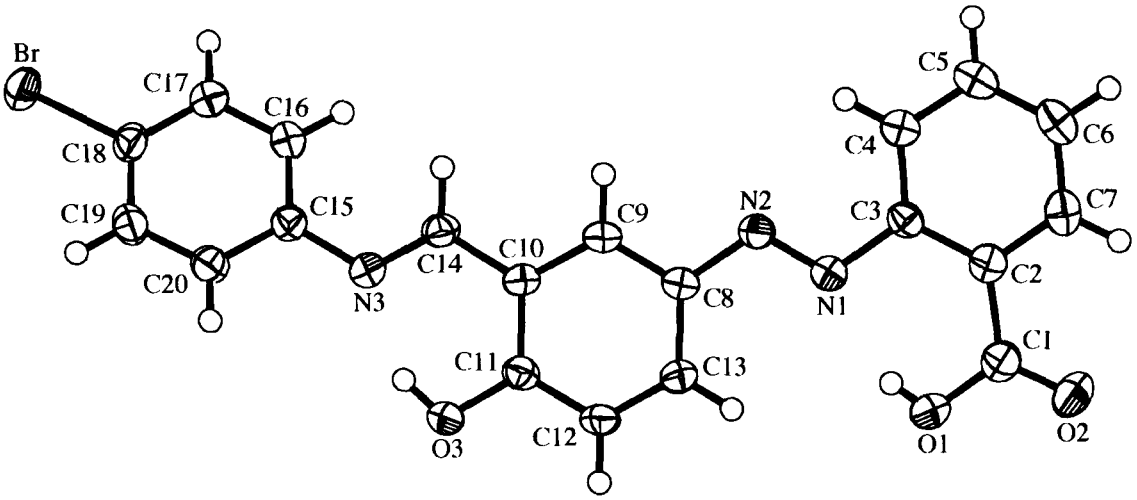

Fig. 2.6 View of the molecule of $L^3HH'.0.5C_7H_8$ showing the atom-labelling scheme (50% probability ellipsoids)

The angles between the plane of the central ring and those of the benzoic acid and 4-bromophenyl rings are 6.01(11)° and 27.78(11)°, respectively. The carboxylic acid group is coplanar with its parent phenyl ring [O(1)-C(1)-C(2)-C(7) = 179.60(19)°]. The molecular conformation and dimensions are very similar to those of the 4-methylphenyl (L^2HH') analogue (Table 2.3), with the exception that the L^2HH' crystallized in a zwitterionic form where the phenolic H atom had migrated to the imine N atom. In L^3HH', this H atom is clearly located on the phenolic O atom. The carboxylic acid H atom forms an intramolecular hydrogen bond with the nearest N atom of the adjacent diazo group, while the phenolic H atom forms an intramolecular hydrogen bond with the adjacent imine N atom. Both of these interactions close six-membered hydrogen-bonded rings.

The molecules pack in a way that facilitates several C-H...O and C-H...Br interactions (Table 2.5). These interactions link the solvent and substrate molecules together into two

dimensional networks, which lie parallel to the (101) plane (Fig. 2.7). The C-H...O angles are consistent with the most probable value of 160° for two-centre interactions [8].

Table 2.5: Hydrogen bonding geometry (Å, °) for $L^3HH'.0.5C_7H_8$

D-H···A	D-H	H···A	D···A	D-H···A
O(1)-H(1)···N(1)	0.73(3)	1.92(3)	2.593(2)	154(4)
O(3)-H(3)···N(3)	0.87(3)	1.76(3)	2.554(2)	151(3)
C(6)-H(6)···Br(2^{i})	0.95	2.92	3.630(2)	133
C(12)-H(12)···O(3^{ii})	0.95	2.53	3.388(3)	151
C(17)-H(17)···O(1^{iii})	0.95	2.49	3.419(3)	166
C(26)-H(26)···O(2^{iv})	0.95	2.50	3.374(6)	153

Primed atoms refer to the molecule in the symmetry related position:
(i) 1+x,1+y,z-1; (ii) 2-x,-y,-z; (iii) x-1,y,1+z;
(iv) 2-x,1-y,-z

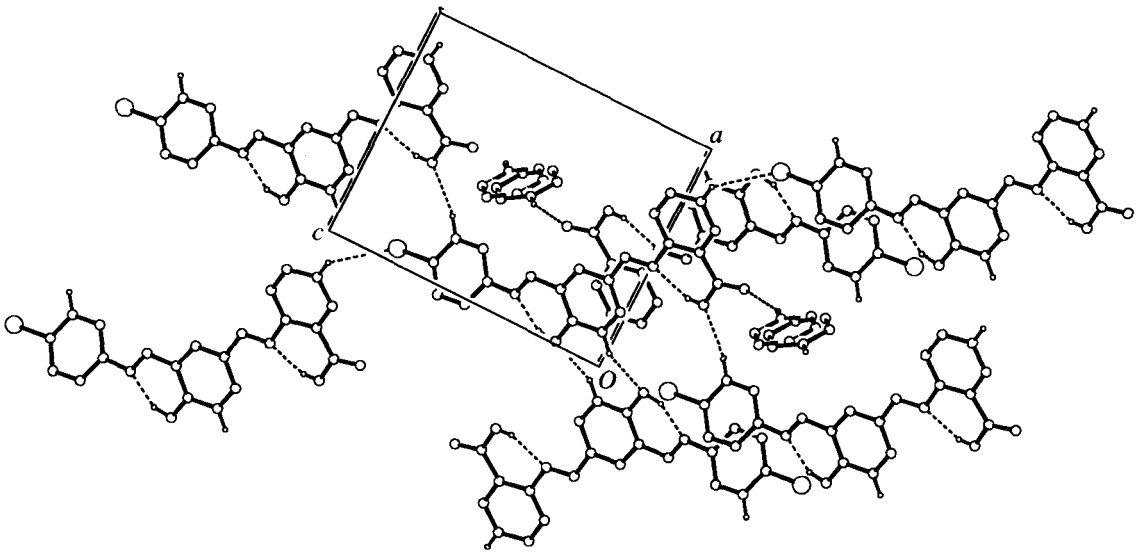

Fig. 2.7 The molecular packing of $L^3HH'.0.5C_7H_8$ showing the solvent and substrate molecules forming two dimensional networks

2.5.3 *Crystal structure of 2-{(E)-4-hydroxy-3-[(E)-4-chlorophenyliminomethyl] phenyldiazenyl}benzoic acid hemihydrate* ($L^4HH'.0.5H_2O$)

The crystal structure of L^4HH' [9] is similar to that of the L^2HH' and crystallizes as $L^4HH'.0.5H_2O$ (Fig. 2.8). Interstitial water molecules (one for each two of the L^4HH'molecules) are located on four fold axes that pass through the unit cell. The three-ring system assumes an

extended conformation, with both outer rings slightly twisted with respect to the central aromatic ring.

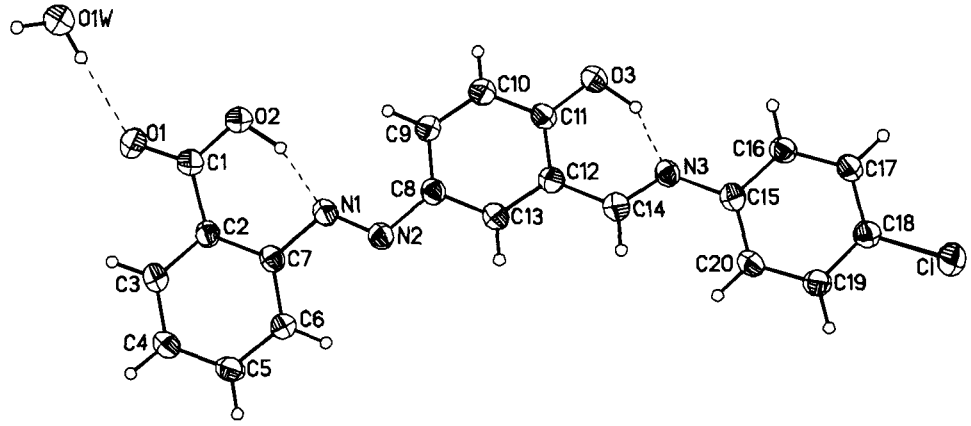

Fig. 2.8 View of the molecule of $L^4HH'.0.5H_2O$, showing the atom-labelling scheme (50% probability ellipsoids)

These quasi-planar molecules forms sheets, parallel to the (100) plane (see Fig. 2.9), that are linked by weak aromatic C-H..O interactions. Adjacent sheets are linked by strong hydrogen bonds to interstitial water molecules (see Fig 2.10, Table 2.6). Bond lengths and angles within the molecule are unremarkable and similar to those found in 4-methylphenyl and 4-bromophenyl analogues (Table 2.3) and related molecules [2,3].

Table 2.6: Hydrogen bonding geometry (Å, °) for $L^4HH'.0.5H_2O$

D-H···A	D-H	H···A	D···A	D-H···A
O(2)-H(2)O···N(1)	0.82	1.83	2.580(5)	152
O(3)-H(3)O···N(3)	0.82	1.81	2.544(5)	148
O(1)W-H(1)W(1)···O(1)	0.852(10)	2.05(3)	2.875(5)	164(8)
C(5)-H(5)A···O(1^{i})	*0.93*	*2.56*	*3.457(7)*	*161*
C(14)-H(14)A···O(1^{ii})W	0.93	2.47	3.364(7)	162
C(19)-H(19)A···O(2^{ii})	0.93	2.59	3.355(6)	140

Primed atoms refer to the molecule in the symmetry related position:
(i)X,1-y, $\frac{1}{2}$+z; (ii)x, y,1+z

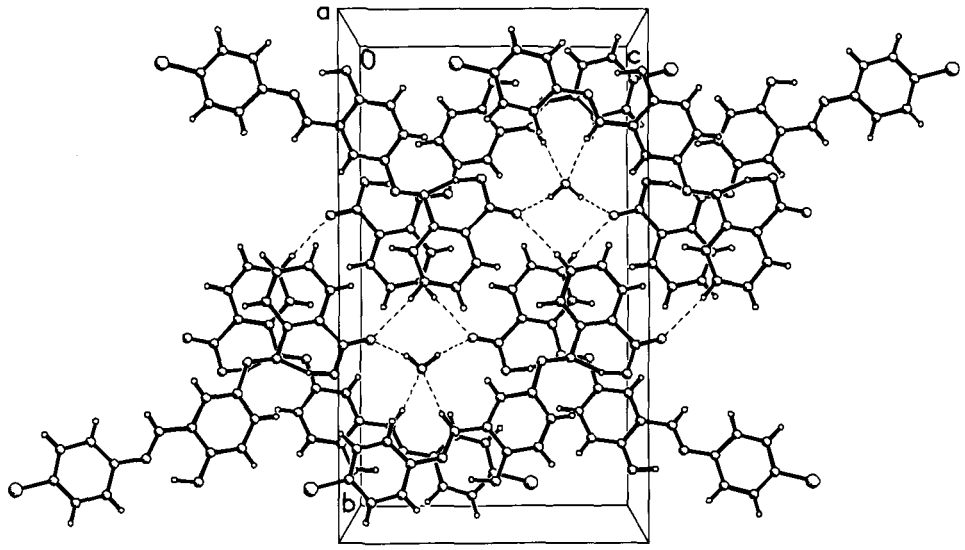

Fig. 2.9 The molecular packing of $L^4HH'.0.5H_2O$, viewed down the *a* axis, perpendicular to the molecular sheets

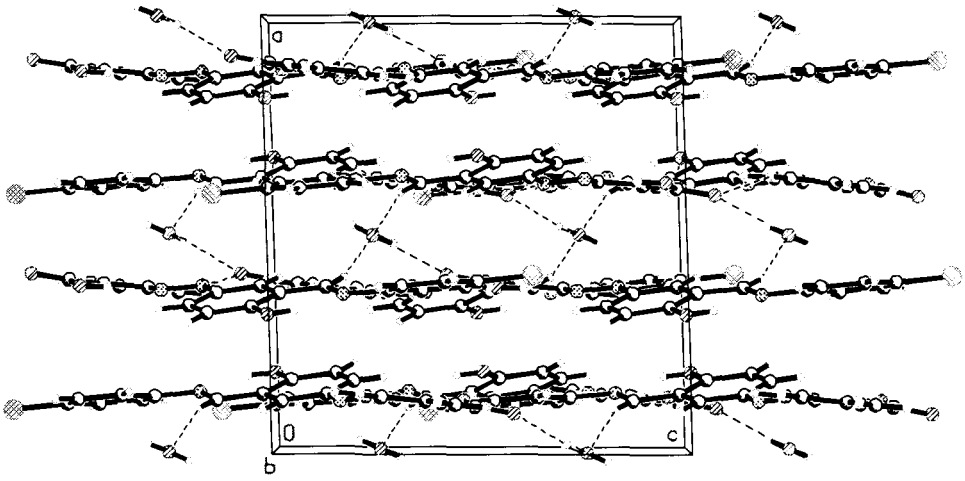

Fig 2.10 The molecular packing of $L^4HH'.0.5H_2O$, viewed down the *b* axis, showing how the atomic sheets are linked by interstitial water molecules

2.6 Experimental

2.6.1 Synthesis of ligands

2.6.1.1 Preparation of 2-[(E)-2-(3-formyl-4-hydroxyphenyl)-1-diazenyl]benzoic acid (L^1HH')

The ligand, L^1HH' was prepared by reacting *o*-carboxybenzenediazonium chloride with salicylaldehyde in alkaline solution under cold conditions by the method described in our earlier report [4]. The synthetic details are given below:

Anthranilic acid (5.0 g, 36.45 mmol) in a mixture of concentrated HCl solution (5 ml) and water (15 ml) was diazotized with cold $NaNO_2$ solution (2.75 g, 39.85 mmol, 12 ml). The cold diazonium salt solution was added slowly to salicylaldehyde (4.45 g, 36.44 mmol), previously dissolved in a NaOH solution (3.0 g, mmol, 30 ml) and held at 0-5 °C in an ice-bath, with vigorous stirring. A deep-red colour developed almost immediately and stirring was continued for 1 h. The reaction mixture was kept overnight at 4 °C, followed by 3 h at room temperature and then acidified with acetic acid. The brown-coloured precipitate was filtered, washed with water and dried *in vacuo*. The crude product was washed thoroughly with hexane, to remove tar-like material and then dissolved in toluene. Several recrystallizations from toluene yielded the product in 50 % yield; m.p.: 177 - 179 °C. Anal. Found. 62.20; H, 3.65; N, 10.35. Calc. for $C_{14}H_{10}N_2O_4$: C, 62.22; H, 3.70; N, 10.37 %.

2.6.1.2 Preparation of 2-{(E)-4-hydroxy-3-[(E)-4-(aryl)iminomethyl]phenyldiazenyl}benzoic acids ($L^{2\text{-}5}HH'$)

A typical procedure is described below.

2.6.1.2.1 Preparation of 2-{(E)-4-hydroxy-3-[(E)-4-chlorophenyliminomethyl]-phenyldiazenyl}benzoic acid (L^4HH')

An equimolar amount of *p*-chloroaniline (0.42 g, 3.36 mmol) in hot absolute ethanol solution (15 ml) was added to a hot toluene (30 ml) containing L^1HH' (0.91 g, 3.36 mmol) and the reaction mixture was refluxed for 5 h. The water formed during the reaction was removed using a Dean-Stark apparatus. The reaction mixture was concentrated to half of the initial solvent volume on a hot plate, cooled to room temperature and was kept overnight in a refrigerator whereupon a dark brown solid precipitated. The precipitate was filtered, washed with absolute ethanol (3 x 5 ml) followed by diethyl ether (2 x 5 ml), and then dried in air. The crude product was washed with hexane to remove any tarry materials and recrystallized from ethanol to yield

pure orange crystalline product (0.78 g, 56 %) of L^4HH'. M. p.: 225-226 °C. Anal. Found. 63.20; H, 3.65; N, 11.13. Calc. for $C_{20}H_{14}N_3O_3Cl$: C, 63.24; H, 3.71; N, 11.06 %.

The other 2-{(*E*)-4-hydroxy-3-[(*E*)-4-(aryl)iminomethyl]phenyldiazenyl}benzoic acids, *viz.*, L^2HH', L^3HH' and L^5HH' were prepared analogously by reacting L^1HH' and appropriate anilines. The characterization data are presented below.

2.6.1.2.2 Preparation of 2-{(E)-4-hydroxy-3-[(E)-4-methylphenyliminomethyl]-phenyldiazenyl}benzoic acid (L^2HH')

Recrystallized from absolute ethanol to give reddish brown precipitate in 70 % yield. m.p.: 199-201 °C. Anal. Found. 69.95; H, 4.65; N, 11.58. Calc. for $C_{21}H_{17}N_3O_3$: C, 70.20; H, 4.76; N, 11.69 %.

2.6.1.2.3 Preparation of 2-{(E)-4-hydroxy-3-[(E)-4-bromophenyliminomethyl]-phenyldiazenyl}benzoic acid (L^3HH')

Recrystallized from absolute ethanol to give orange precipitate in 49 % yield. m.p.: 213-214 °C. Anal. Found. 56.50; H, 3.30; N, 10.01. Calc. for $C_{20}H_{14}N_3O_3Br$: C, 56.60; H, 3.32; N, 9.90 %.

2.6.1.2.4 Preparation of 2-{(E)-4-hydroxy-3-[(E)-4-methoxyphenyliminomethyl]-phenyldiazenyl}benzoic acid (L^5HH')

Recrystallized from absolute ethanol to give dark red precipitate in 54 % yield. m.p.: 174-176 °C. Anal. Found. 67.25; H, 4.60; N, 11.18. Calc. for $C_{21}H_{17}N_3O_4$: C, 67.21; H, 4.56; N, 11.19 %.

2.6.1.3 Preparation of 4-[(E)-2-(3-formyl-4-hydroxyphenyl)-1-diazenyl]benzoic acid (L^6HH')

The ligand, L^6HH' was prepared by reacting *p*-carboxybenzenediazonium chloride with salicylaldehyde in an alkaline solution under cold conditions following the method described earlier for the *ortho*-analogue [4]. The amount of concentrated HCl and water used for the dissolution of the *p*-aminobenzoic acid was 8 and 32 ml, respectively. The crude L^6HH' was obtained after acidification with dil. acetic acid. The light yellow precipitate was filtered, washed with water until the filtrate became neutral and then dried in *vacuo*. The resultant brown product was then washed thoroughly with hexane to remove any tarry materials and dried. The brown

L^6HH' was insoluble in all common organic solvents and water, and consequently could not be recrystallized. The brown precipitate was then re-dissolved in a hot aqueous sodium bicarbonate solution. It was then filtered to remove any undissolved particles and re-precipitated using dil. acetic acid. The precipitate was filtered, washed with water and dried which afforded a bright brown product in 56% yield. m.p.: >275 °C. Anal Found: C, 61.38; H, 3.73; N, 10.26%. Calc. for $C_{14}H_{10}N_2O_4$: C, 62.22; H, 3.70; N, 10.37%.

2.6.2 Chemicals used for the preparations

Salicylaldehyde (Lancaster), anthranilic acid (Spectrochem), *p*-aminobenzoic acid (Sisco) and the substituted anilines (reagent grade) were used without further purification. The solvents used in the reactions /recrystallizations were of AR grade and dried using standard procedures. Toluene was distilled from sodium benzophenone ketyl.

2.6.3 Physical measurements

Carbon, hydrogen and nitrogen analyses were performed with a Perkin Elmer 2400 series II instrument. IR spectra in the range 4000-400 cm^{-1} were obtained on a BOMEM DA-8 FT-IR spectrophotometer with samples investigated as KBr discs. The ^1H- and ^{13}C-NMR spectra of the ligands (L^2HH'-L^6HH') were acquired on a Bruker Avance 500 spectrometer operating at 500.13 and 125.76 MHz, respectively. For the ligand L^1HH', the ^1H- and ^{13}C-NMR spectra were recorded on a Varian Inova 600 spectrometer and measured at 600 and 150 MHz, respectively. The ^1H and ^{13}C chemical shifts were referred to Me_4Si set at 0.00 ppm and $CDCl_3$ set at 77.0 ppm, respectively. Other NMR experiments like correlated spectroscopy (COSY), heteronuclear single-quantum correlation (HMQC) and heteronuclear multiple-bond connectivities (HMBC) were also performed on the same instruments.

2.6.4 X-ray crystallography

Crystals of the ligands suitable for an X-ray crystal-structure determination were obtained from toluene (L^2HH' and L^3HH') and chloroform/ DMSO mixture (L^4HH') by slow evaporation of the solvent at room temperature. The intensity data for L^2HH' and L^3HH' were measured on a Nonius KappaCCD diffractometer using Mo Kα raditaion (λ = 0.71073 Å) at 160 K while L^4HH' was measured on a Bruker P4 diffractometer using Cu Kα raditaion (λ = 1.54178 Å) at 293 K.

The data reduction for L^2HH' and L^3HH' was performed with HKL Denzo and Scalepack [10] while for L^4HH' was with SHELXTL [11].

The data collection and refinement parameters are given in Table 2.2. Views of the structures are shown in Figs. 2.4 (for L^2HH'), 2.6 (for L^3HH') and 2.8 (for L^4HH'). The structure of L^4HH' was solved by SHELXTL [11] while the other structures were solved by direct methods by using SIR92 [12].

In L^2HH' and L^4HH', the asymmetric unit contains one molecule of the carboxylic acid in a general position plus a water molecule that sits on a C_2-axis. The symmetry-unique H-atom of the water molecule and the carboxylic acid H-atom of L^1HH' and L^4HH' were placed in the positions indicated by a difference electron density map and their positions were allowed to refine together with individual isotropic displacement parameters. In L^3HH', the asymmetric unit contains one molecule of the carboxylic acid in a general position plus half of a toluene molecule that is disordered about a centre of inversion, with the centre of gravity of the six-membered ring displaced slightly from the inversion centre. The atoms of one entire toluene molecule were defined with the site occupation factors of the atoms set to 0.5. The atoms of the six-membered ring of the toluene molecule were constrained to an ideal hexagon, while neighbouring atoms within each orientation of the disordered toluene molecule were restrained to have similar atomic displacement parameters.

The non-hydrogen atoms were refined anisotropically. All remaining H-atoms in each structure were placed in geometrically calculated positions and refined using a riding model where each H-atom was assigned a fixed isotropic displacement parameter with a value equal to $1.2U_{eq}$ of its parent atom ($1.5U_{eq}$ for methyl groups). The refinement of each structure was carried out on F^2 using full-matrix least-squares procedures. The calculations were performed using the SHELXL97[13] program for L^2HH' and L^3HH' and SHELXTL [11] program for L^4HH'.

References

[1] D. Revannasiddaiah, N.K. Lokanath, M.A. Sridhar, J.S. Prasad, Z. Kristallogr. **212** (1997) 387.

[2] U. Baumeister, Z. Kosturkiewicz, H. Hartung, D. Demus, W. Weissflog, Liq. Cryst. **7** (1990) 241.

[3] F. Cariati, U. Caruso, A. DeMaria, M. Fusco, B. Panunzi, A. Roviello, A. Tuzi, Inorg. Chim. Acta **357** (2004) 548.

[4] T.S. Basu Baul, S.P. Pyke, K.K. Sarma, E.R.T. Tiekink, Main Group Met. Chem. **19** (1996) 807.

[5] T.S. Basu Baul, K.S. Singh, M. Holčapek, R. Jirásko, E. Rivarola, A. Linden, J. Organomet. Chem. **690** (2005) 4232.

[6] J. Bernstein, R.E. Davis, L. Shimoni, N.-L. Chang, Angew. Chem. **107** (1995) 1689; Angew. Chem. Int. Ed. Engl. **34** (1995) 1555.

[7] A. Linden, T.S. Basu Baul, K.S. Singh, Acta Crystallogr. Sect. **E 62** (2006) o2566.

[8] G.A. Jeffrey, H. Maluszynska, J. Mitra, Int. J. Biol. Macromol. **7** (1985) 336.

[9] R.J. Butcher, T.S. Basu Baul, K.S. Singh, F.E. Smith, Acta Crystallogr. Sect. **E 61** (2005) o1007.

[10] Z. Otwinowski, W. Minor, in: C.W. Carter Jr., R.M. Sweet (Ed.) Methods in Enzymology, Vol. 276, Macromolecular Crystallography, Part A, Academic Press, New York, 1997, pp. 307-326.

[11] G.M. Sheldrick, SHELXTL Version 5.10, Bruker AXS Inc., Madison Wisconsin, USA, 1997.

[12] A. Altomare, G. Cascarano, C. Giacovazzo, A. Guagliardi, M.C. Burla, G. Polidori, M. Camalli, SIR92, J. Appl. Crystallogr. **27** (1994) 435.

[13] G.M. Sheldrick, SHELXL97, Program for the Refinement of Crystal Structures, University of Göttingen, Germany, 1997.

CHAPTER 3

TRIORGANOTIN(IV) COMPLEXES OF 2-[(*E*)-(3-FORMYL-4-HYDROXYPHENYL)-DIAZENYL]- AND 2-{(*E*)-4-HYDROXY-3-[(*E*)-4-(ARYL)IMINOMETYHY]PHENYL- DIAZENYL}- BENZOIC ACIDS: SYNTHESES, CHARECTERIZATION AND STRUCTURES

3.1 Introduction

Salicylaldehyde and their metal derivatives are well established [1-3]. More useful organic reagents having the properties of salicylaldehyde together with other desired features, e.g., having an intense light absorption in the visible region for colorimetric applications, have also been reported. These organic reagents are commonly known as 5-(arylazo)salicylaldehyde (AAS) (systematic name [(*E*)-2-(3-formyl-4-hydroxyphenyl)-1-diazenyl]benzene) and were used by several workers in order to characterize U(VI) [4], Pd(II) [4], Co(II) [5], Cu(II) [6,7], Ni(II) [8], Mn(II) [9], Sn(II) [10] and Sn(IV) [11] complexes in both solid and solution states. A few transition metal complexes also show semi conducting properties in the temperature range 310-340 K [9]. Later, AAS were condensed with mono aromatic amine which resulted in 5-phenylazosalicylidene aniline (PASA) Schiff base and its metal complexes, *viz.*, Fe(III), Co(II), Ni(II) and Cu(II) were prepared and characterized [12]. Recently, a few Cu(II) complexes of some Schiff bases obtained by condensation of AAS with di- and tri-amine have also been reported and in one case the structure of the complex was determined using single crystal X-ray crystallography [13]. Although PASA type ligands have been known for a long time, the extant literature contains no report of the isolation and characterization of metal or organometallic complexes of 2-{(*E*)-4-hydroxy-3-[(*E*)-4-(aryl)iminomethyl]phenyldiazenyl} benzoic acids. These ligands contain a carboxylate group in the *ortho*-position of the diazo-forming aryl moiety of the ASA unit (see Chapter 2 for L^2HH'-L^5HH'), which provides an opportunity for synthesising a wide variety of complexes of the hetero-functional ligand.

Recently, we have been investigating the 2-{(*E*)-4-hydroxy-3-[(*E*)-4-(aryl)iminomethyl]phenyldiazenyl} benzoic acids, which contain both azo and imino linkages. These ligands structurally resemble the *N*-*p*-methoxybenzylidene-*p*-phenylazoaniline system, which is a mesogen and exhibits a nematic liquid-crystal phase [14]. The synthesis of liquid crystals based on organometallic or coordination compounds opens new perspectives in the design of mesogenic molecules. Consequently, there is currently much interest in the synthesis of metal-containing liquid crystals (metallomesogens) owing to the perceived advantages of combining the properties of a liquid crystal system with those of transition metals [15-19]. However, to the best of our knowledge, the literature contains no report of a metallomesogen involving tin(IV). In search of organic ligands/complexes having mesogenic behaviour, we have recently synthesized a number of 2-{(*E*)-4-hydroxy-3-[(*E*)-4-(aryl)iminomethyl]phenyldiazenyl} benzoic acids and efforts have also been made to

characterize these ligands by single crystal X-ray crystallographic techniques, for example, L^2HH' [20], L^3HH' [21] and L^4HH' [22].

In addition, tri-n-butyltin in the form of halides, oxides and acetates, displays a large array of biocidal properties and is used extensively in wood preservatives and in marine anti-fouling paints [23], although there has been considerable environmental concern about their latter use [24]. However, the tri-n-butyltin compounds have not been shown to be neurotoxins, mutagens, teratogens, or carcinogens in humans [25]. Recently, some tri-n-butyltin 5-[(*E*)-2-(aryl)-1-diazenyl]-2-hydroxybenzoates have shown moderate activity towards second larval instar stage of the *Aedes aegypti* [26].

On the other hand, organotin(IV) compounds have been one of the most extensively studied class of antitumour compounds since the observation that triphenyltin(IV) acetate significantly reduced the growth rates of tumours [27,28]. Among the most active organotin(IV) antitumour agents are substituted triphenyltin(IV) benzoates, which exhibited exceptionally high *in vitro* activity against the human mammary tumour MCF-7 and a colon carcinoma, WiDr [29,30].

In addition to their commercial applications, triorganotin(IV) carboxylates present an interesting variety of structural possibilities [31,32]. In line with these developments and as part of a wider study designed to ascertain the reasons for the structural variation found in these systems, we now describe some triorganotin(IV) complexes derived from (i) 2-[(*E*)-2-(3-formyl-4-hydroxyphenyl)-1-diazenyl]benzoic acid (L^1HH') and, (ii) 2-{(*E*)-4-hydroxy-3-[(*E*)-4-(aryl)iminomethyl]phenyldiazenyl}benzoic acids ($L^{2\text{-}5}HH'$). The generic structures of the ligands are shown in Chapter 2.

3.2 Synthesis of triorganotin(IV) complexes

3.2.1 Synthesis of triorganotin(IV) complexes of 2-[(*E*)-2-(3-formyl-4-hydroxyphenyl)-1-diazenyl]benzoic acid (L^1HH')

The 2-[(*E*)-2-(3-formyl-4-hydroxyphenyl)-1-diazenyl]benzoic acid (L^1HH') react with $(^nBu_3Sn)_2O$ in anhydrous toluene in a 2:1 ratio to give compounds of the formulation $^nBu_3SnL^1H$. The triphenyltin(IV) complex was prepared by reacting equimolar amounts of Ph_3SnOH and L^1HH' by following an analogous procedure which afforded the compounds of the formulation $Ph_3SnL^1H.OH_2$ [33]. On the other hand, tribenzyltin(IV) compounds deserve specific comment. Recently, we have investigated the reaction of Bz_3SnCl with sodium 2-[(*E*)-2-(3-formyl-4-

hydroxyphenyl)-1-diazenyl]benzoate, L^1HNa in anhydrous methanol. The reaction proceeded via debenzylation and oxidative decarbonylation [34]. This reaction afforded a cyclic dinuclear

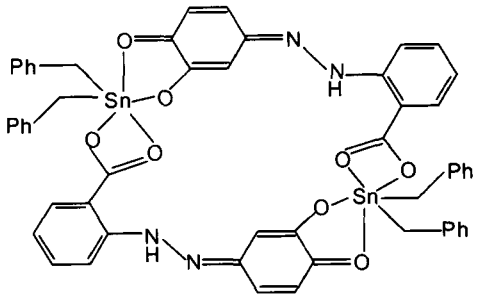

Fig. 3.1. Cyclic dibenzyltin(IV) complex: $[Bz_2\{O_2CC_6H_4\{N(H)\text{-}N{=}(C_6H_3\text{-}4(=O)\text{-}5\text{-}O)\}\text{-}o\}Sn]_2$

dibenzyltin(IV) complex, $[Bz_2\{O_2CC_6H_4\{N(H)\text{-}N{=}(C_6H_3\text{-}4(=O)\text{-}5\text{-}O)\}\text{-}o\}Sn]_2$ (Fig. 3.1, see Chapter 5 for details) instead of the polymeric $Me_3Sn(IV)$ [35] as well as the monomeric $Ph_3Sn(IV)$ [33] analogues. The desired product of composition $Bz_3SnL^1H.OH_2$ was obtained by reacting equimolar amounts of Bz_3SnOH and L^1HH' (1:2) in anhydrous toluene.

The complexes were isolated as orange-red crystalline solids in good yield and purity. They are stable in air and are soluble in common organic solvents. The synthetic details and characterization data are presented in section 3.4 while their spectroscopic data are summarized in section 3.3.

3.2.2 Synthesis of triorganotin(IV) complexes of 2-{(*E*)-4-hydroxy-3-[(*E*)-4-(aryl)imino-methyl]phenyldiazenyl}benzoic acids ($L^{2\text{-}5}HH'$)

The tri-n-butyltin(IV) complexes, $^nBu_3SnL^{2\text{-}5}H$, were synthesized by condensing $^nBu_3SnL^1H$ (see section 3.2.1) with appropriate *p*-substituted anilines in absolute ethanol. However, $^nBu_3SnL^{2\text{-}5}H$ could also be prepared by reacting the appropriate 2-{(*E*)-4-hydroxy-3-[(*E*)-4-(aryl)iminomethyl]phenyldiazenyl}benzoic acids with $(^nBu_3Sn)_2O$ in a 2:1 ratio in anhydrous toluene and the yield of the product was found to be lower. Synthetic convenience led to the choice of the former procedure. The triphenyltin(IV) complexes of composition $Ph_3SnL^{2\text{-}5}H$ were prepared by reacting Ph_3SnOH with the appropriate ligand ($L^{2\text{-}5}HH'$) in a 1:1 ratio in anhydrous toluene.

In a similar way (reactions of Bz_3SnCl with L^1HNa, see section 3.2.1), the reactions of Bz_3SnCl with sodium 2-{(*E*)-4-hydroxy-3-[(*E*)-4-(aryl)iminomethyl]phenyldiazenyl}benzoates, L^2HNa-L^5HNa were attempted under identical reaction conditions in the expectation of obtaining

the corresponding $Bz_3Sn(IV)$ derivatives. Instead, the work-up of the reaction mixture yielded crystals of the same cyclic dibenzyltin(IV) dimer, i.e. $[Bz_2\{O_2CC_6H_4\{N(H)\text{-}N{=}(C_6H_3\text{-}4(=O)\text{-}5\text{-}O)\}\text{-}o\}Sn]_2$ (Fig. 3.1). The melting point, microanalytical, spectroscopic and crystallographic data of the two products were identical. In these reactions, cleavage of the H-C=N-Ar part from the ligand molecule and simultaneous debenzylation was noticed. At present, however, the exact mechanism of the cleavage/rearrangement is not clearly understood. On the other hand, attempted reactions of the L^2HH'-L^5HH' with Bz_3SnOH in anhydrous toluene afforded the desired products $Bz_3SnL^{2\text{-}5}H.OH_2$ in moderate to good yields. Attempted crystallization of these $Bz_3SnL^{2\text{-}5}H.OH_2$ complexes from an anhydrous benzene-methanol mixture again afforded crystals of the dimeric dibenzyltin complex (Fig. 3.1). Hence, the crystallization attempts were made using anhydrous benzene, benzene/hexane or toluene/hexane.

The complexes were isolated as orange to red crystalline solids in good yield and purity. They are stable in air and are soluble in common organic solvents. The synthetic details and characterization data are presented in section 3.4 while their spectroscopic data are summarized in section 3.3.

3.3 Spectroscopic characterization and X-ray crystallography of triorganotin(IV) complexes

This section deals with the spectroscopic characterization of triorganotin(IV) complexes of 2-[(*E*)-2-(3-formyl-4-hydroxyphenyl)-1-diazenyl]benzoic acid (L^1HH') and 2-{(*E*)-4-hydroxy-3-[(*E*)-4-(aryl)imino-methyl]phenyldiazenyl}benzoic acids ($L^{2\text{-}5}HH'$). For convenience of discussion, the tri-n-butyltin(IV), triphenyltin(IV) and tribenzyltin(IV) complexes of L^1HH'-L^5HH' have been dealt separately.

3.3.1 Tri-n-butyltin(IV) complexes of L^1HH'-L^5HH' ($^nBu_3SnL^{1\text{-}5}H$)

The tri-n-butyltin(IV) complexes of 2-[(*E*)-2-(3-formyl-4-hydroxyphenyl)-1-diazenyl]benzoic acid (L^1HH') and 2-{(*E*)-4-hydroxy-3-[(*E*)-4-(aryl)imino-methyl]phenyldiazenyl}benzoic acids ($L^{2\text{-}5}HH'$) have been characterized by IR, ^1H, ^{13}C, ^{119}Sn NMR, ^{119m}Sn Mössbauer and electrospray mass spectrometry (ESI-MS) techniques. The crystal structures of four compounds, *viz.*, $[^nBu_3SnL^1H]_n$ (**1**), $[^nBu_3SnL^2H]_n$ (**2**), $[^nBu_3SnL^4H]_n$ (**4**) and $[^nBu_3SnL^5H]_n$ (**5**) are reported.

3.3.1.1 Infrared data

The diagnostically important infrared absorption frequencies for the carboxylate antisymmetric [ν_{asym}(OCO)] stretching vibration of the ligands (L^1HH'-L^5HH') are recorded in Chapter 2 (section 2.4) while that of their $^nBu_3SnL^{1-5}H$ (**1-5**) complexes are given below. The assignment of the symmetric [ν_{sym}(OCO)] stretching vibration band could not be made owing to the complex pattern of the spectra. The assignment of the band is based on comparison with the spectra of the free ligands. The antisymmetric [ν_{asym}(OCO)] stretching vibrations for the uncomplexed ligands have been detected at 1733 cm^{-1} in L^1HH' and around the 1725 cm^{-1} region for $L^{2-5}HH'$. In the complexes, the carbonyl stretching frequencies are found to be shifted to lower wavenumber which is ascribed to carboxylate coordination in accordance with earlier reports [36,37].

3.3.1.2 ^1H, ^{13}C and ^{119}Sn NMR data

The ^1H- and ^{13}C- NMR data of L^1HH' is reported in our earlier ref. [33] and the signals were assigned by the use of correlated spectroscopy (COSY), heteronuclear single-quantum correlation (HMQC) and heteronuclear multiple-bond connectivities (HMBC) experiments. The conclusions drawn from the ligand assignments were then subsequently extrapolated to the complexes owing to the data similarity. The ^1H and ^{13}C chemical shift assignment of the tri-n-butyltin moiety is straightforward from the multiplicity patterns, resonance intensities and also by examining the $^nJ(^{13}C\text{-}^{119/117}Sn)$ coupling constants [36-38]. The ^1H-NMR integration values were completely consistent with the formulation of the products.

The basic ligand frame-work is shown in Figs. 2.1- 2.2 (Chapter 2) along with the abbreviations and numbering schemes for spectroscopic analyses. Numbering scheme for Sn-^{n}Bu skeleton as shown: $\overset{4^*}{CH_3}—\overset{3^*}{CH_2}—\overset{2^*}{CH_2}—\overset{1^*}{CH_2}—Sn$ and $^nJ(^{13}C\text{-}^{119/117}Sn)$ mean values are given in parentheses. The detailed spectral features for complexes **1-5** are given below:

3.3.1.2.1 $^nBu_3SnL^1H$ (1)

IR (cm^{-1}): 1660 $\nu(OCO)_{asym}$. ^1H-NMR ($CDCl_3$ / 400.13 MHz); δ_H: 11.35 [brs, 1H, OH], 10.02 [s, 1H, C(H)=O], 8.20 [d, 1H, (A) H2], 8.14 [m, 1H, (A) H6], 7.84 [d,1H, (B) H3], 7.49 [m, 3H (B) H4, H5 & H6], 7.10 [d, 1H, (A) H5]; Sn-^{n}Bu: 1.68 [m, 6H, H1*], 1.34 [m, 12H, H2* & H3*], 0.88 [t, 9H, H4*] ppm. ^{13}C-NMR ($CDCl_3$ / 100.62 MHz); δ_C: 196.6 [C(H)=O], 172.7 [COO], 164.1 [(A) C1], 151.7 [(B) C2], 146.4 [(A) C4], 131.9 [(B) C1], 131.2 [(B) C4], 130.8

[(B) C3], 130.3 [(B) C5], 130.2 [(A) C6], 129.9 [(A) C3], 120.5 [(A) C2], 118.7 [(A) C5], 117.7 [(B) C6]; Sn-^{n}Bu: 16.8 (336) [C1*], 27.8 (20) [C2*], 27.3 (64) [C3*], 13.8 (-) [C4*] ppm.

3.3.1.2.2 $^{n}Bu_3SnL^2H$ (2)

IR (cm^{-1}): 1622 $\nu(OCO)_{asym.}$ ^{1}H-NMR ($CDCl_3$ / 400.13 MHz); δ_H: 14.0 [brs, 1H, OH], 8.73 [s, 1H, C(H)=N], 8.04 [d, 1H, (B) H6], 7.99 [dd, 1H, (B) H4], 7.82 [m, 1H, (C) H3], 7.53 [m, 2H (C), H4 & H6], 7.44 [m, 1H, (C) H5], 7.24 [m, 4H, (A) H2, H3, H5 & H6], 7.15 [d, 1H, (B) H3], 2.40 [s, 3H, CH_3]; Sn-^{n}Bu: 1.62 [m, 6H, H1*], 1.30 [m, 12H, H2* & H3*], 0.87 [t, 9H, H4*] ppm. ^{13}C-NMR ($CDCl_3$ / 100.62 MHz); δ_C: 172.5 [COO], 164.3 [(B) C2], 161.0 [C(H)=N], 152.0 [(C) C1], 145.9 [(B) C5], 145.2 [(A) C1], 137.5 [(A) C4], 131.5 [(C) C5], 130.9 [(C) C2], 130.2 [(A) C3 & C5], 129.9 [(C) C4], 129.2 [(C) C3], 128.6 [(B) C6], 127.3 [(B) C4], 121.0 [(A) C2 & C6], 118.9 [(B) C1], 118.1 [(C) C6], 117.8 [(B) C3], 21.1 [CH_3]; Sn-^{n}Bu: 16.8 (342) [C1*], 27.9 (20) [C2*], 27.1 (64) [C3*], 13.6 (-) [C4*] ppm.

3.3.1.2.3 $^{n}Bu_3SnL^3H$ (3)

IR (cm^{-1}): 1618 $\nu(OCO)_{asym.}$ ^{1}H-NMR ($CDCl_3$ / 400.13 MHz); δ_H: 13.60 [brs, 1H, OH], 8.69 [s, 1H, C(H)=N], 8.05 [d, 1H, (B) H6], 8.01 [dd, 1H, (B) H4], 7.82 [m, 1H, (C) H3], 7.56 [part of AA'MM' system, 2H (A), H3 & H5], 7.52 [m, 2H, (C) H4 & H6], 7.44 [m, 1H, (C) H5], 7.19 [part of AA'MM' system, 2H, (A) H2 & H6], 7.12 [d, 1H, (B) H3]; Sn-^{n}Bu: 1.61 [m, 6H, H1*], 1.31 [m, 12H, H2* & H3*], 0.87 [t, 9H, H4*] ppm. ^{13}C-NMR ($CDCl_3$ / 100.62 MHz); δ_C: 172.4 [COO], 164.0 [(B) C2], 162.5 [C(H)=N], 151.9 [(C) C1], 147.0 [(A) C1], 146.0 [(B) C5], 132.7 [(A) C3 & C5], 131.6 [(C) C5], 130.9 [(C) C2], 129.9 [(C) C4], 129.3 [(C) C3], 128.9 [(B) C6], 127.6 [(B) C4], 122.8 [(A) C2 & C6], 120.9 [(A) C4], 118.7 [(B) C1], 118.1 [(C) C6], 117.7 [(B) C3]; Sn-^{n}Bu: 16.8 (362) [C1*], 27.9 (20) [C2*], 27.1 (64) [C3*], 13.6 (-) [C4*] ppm.

3.3.1.2.4 $^{n}Bu_3SnL^4H$ (4)

IR (cm^{-1}): 1616 $\nu(OCO)_{asym.}$ ^{1}H-NMR ($CDCl_3$ / 400.13 MHz); δ_H: 13.60 [brs, 1H, OH], 8.71 [s, 1H, C(H)=N], 8.04 [d, 1H, (B) H6], 8.01 [dd, 1H, (B) H4], 7.82 [m, 1H, (C) H3], 7.51 [m, 1H (C), H6], 7.42 [m, 2H, (C) H4 & H5], 7.25 [m, 4H, (A) H2, H3, H5 & H6], 7.12 [d, 1H, (B) H3]; Sn-^{n}Bu: 1.61 [m, 6H, H1*], 1.31 [m, 12H, H2* & H3*], 0.86 [t, 9H, H4*] ppm. ^{13}C-NMR ($CDCl_3$ / 100.62 MHz); δ_C: 172.6 [COO], 164.0 [(B) C2], 162.4 [C(H)=N], 151.9 [(C) C1], 146.5 [(A) C1], 146.0 [(B) C5], 133.1 [(C) C5], 131.6 [(A) C4], 130.9[(C) C2], 129.9 [(C) C4],

129.7 [(A) C3 & C5], 129.3 [(C) C3], 127.6 [(B), C4 & C6], 122.5 [(A) C2 & C6], 118.7 [(B), C1], 118.1 [(C) C6], 117.7 [(B) C3]; Sn-^{n}Bu: 16.8 (362) [C1*], 27.9 (20) [C2*], 27.1 (64) [C3*], 13.6 (-) [C4*] ppm.

3.3.1.2.5 $^{n}Bu_3SnL^5H$ (5)

IR (cm^{-1}): 1619 $\nu(OCO)_{asym}$. ^{1}H-NMR ($CDCl_3$ / 400.13 MHz); δ_H: 14.0 [brs, 1H, OH], 8.71 [s, 1H, C(H)=N], 8.02 [d, 1H, (B) H6], 7.98 [dd, 1H, (B) H4], 7.82 [m, 1H, (C) H3], 7.51 [m, 2H (C) H4 & H6], 7.43 [m, 1H, (C) H5], 7.32 [part of AA'MM' system, 2H, (A) H2 & H6], 7.11 [d, 1H, (B) H3], 6.97 [part of AA'MM' system, 2H, (A) H3 & H5], 3.85 [s, 1H, OCH_3]; Sn-^{n}Bu: 1.61 [m, 6H, H1*], 1.32 [m, 12H, H2* & H3*], 0.86 [t, 9H, H4*] ppm. ^{13}C-NMR ($CDCl_3$ / 100.62 MHz); δ_C: 172.7 [COO], 164.2 [(B) C2], 159.7 [C(H)=N], 159.3 [(A) C4], 152.0 [(C) C1], 146.0 [(B) C5], 140.7 [(A) C1], 130.9 [(C) C2], 129.9 [(C) C4], 129.2 [(C) C3], 128.5 [(B) C6], 127.0 [(B) C4], 122.4 [(A) C2 & C6], 119.0 [(B) C1], 117.9 [(C) C6], 117.8 [(B) C3], 114.8 [(A) C3 & C5], 55.6 [OCH_3], Sn-^{n}Bu: 16.8 (342) [C1*], 27.9 (20) [C2*], 27.1 (64) [C3*], 13.6 (-) [C4*] ppm.

Four-coordinated tri-n-butyltin compounds, however, exhibit couplings $^1J(^{13}C\text{-}^{119/117}Sn)$ in the range 325-390 Hz, and five-coordinated ones in the range 440-540 Hz [39-42]. The tri-n-butyltin(IV) complexes (**1-5**) of the present investigation exhibit $^1J(^{13}C\text{-}^{119/117}Sn)$ coupling satellites in the range 336-362 Hz in $CDCl_3$ solution, suggesting that the tin atom is four-coordinate in solution. In contrast, a polymeric structure with five-coordinate tin atoms is found in the solid state (see Mössbauer and X-ray crystallography, *vide infra*); this is possibly lost in solution to generate a monomeric four-coordinated tetrahedral structure [38]. The ^{119}Sn-NMR chemical shifts of tri-n-butyltin(IV) complexes in $CDCl_3$ solution are listed in Table 3.1. The complexes exhibit a single sharp resonance at around 116 ppm, consistent with the range specified for tetrahedral triorganotin(IV) compounds [41]. This is further supported by our recent work on analogous triorganotin(IV) azocarboxylates [36-38].

3.3.1.3 ^{119}Sn Mössbauer data

The ^{119}Sn Mössbauer spectra (Table 3.1) of the complexes (**1-5**) were recorded in order to obtain the structure of the complexes in the solid-state. The ratio of the quadrupole splitting value to isomer shift value ($\rho = \Delta/\delta$) can be used to distinguish between the different coordination states

of the central tin atom [43]. Tin compounds which are four coordinate have ρ values less than 1.8 while ρ values larger than 2.1 would indicate compounds with greater than four coordination. As

Table 3.1 ^{119}Sn-NMR data (δ, ppm) and ^{119}Sn Mössbauer parameters (mm s^{-1}) for the tri-n-butyltin(IV) complexes

Complex[a]	^{119}Sn-NMR data[b]	^{119}Sn Mössbauer data[c]				
		δ	Δ	ρ=Δ / δ	Γ_1	Γ_2
^{n}Bu$_3$SnL^{1}H (**1**)	116.6	1.44	3.84	2.7	1.53	1.62
^{n}Bu$_3$SnL^{2}H (**2**)	116.0	1.50	3.79	2.5	1.00	1.01
^{n}Bu$_3$SnL^{3}H (**3**)	116.2	1.52	3.77	2.5	0.95	0.96
^{n}Bu$_3$SnL^{4}H (**4**)	116.1	1.53	3.83	2.5	0.96	0.98
^{n}Bu$_3$SnL^{5}H (**5**)	116.0	1.50	3.80	2.5	1.05	1.05

[a] Complex numbers are in parentheses. [b] In $CDCl_3$ solution.
[c] Parameters: δ, isomer shifts; Δ, quadrupole splitting; Γ_1 and Γ_2: line widths.

can be seen in Table 3.1, all the complexes (**1-5**) have ρ values greater than 2.1 suggesting that the complexes have a coordination number greater than four. Furthermore, the tri-n-butyltin(IV) complexes exhibited Δ values of approximately 3.80 mm s^{-1}. These values are within the range 3.0-4.1 mm s^{-1}, which are consistent with a *trans-* trigonal bipyramidal geometry with a planar Bu_3Sn unit and two axial carboxylate oxygen atoms [44]. Further, the Δ data for complexes **1-5** matches closely with the data of complexes having a *trans*-trigonal bipyramidal geometry in a polymeric structure [37,38], which was subsequently also found here from the crystal structures (see Section 3.3.1.5). The Δ values for the complexes are in the same order of magnitude, suggesting that they adopt the same structural motif.

3.3.1.4 Electrospray mass spectrometry

The tri-n-butyltin(IV) complexes (**1-5**) have been investigated by electrospray mass spectrometry (ESI-MS) and tandem mass spectrometry (MS^n) techniques. The assignments are facilitated by agreement between observed and calculated isotopic patterns and tandem mass spectrometry studies. ESI mass spectra both in the positive- and negative-ion modes were measured using acetonitrile solutions of complexes **1-5** and the results are summarized in Tables 3.2-3.6. The interpretation of the mass spectra is based on previous works on ESI-MS

measurements of organotin(IV) compounds [45-48]. A typical example of an identification approach is illustrated for compound **2** in Fig. 3.2. In the positive-ion mode (Fig. 3.2(a)), the presence of $[M+H]^+$, $[M+Na]^+$ and $[M+K]^+$ enables the unambiguous determination of the molecular weight (MW) for all compounds studied. The presence or absence of a tin atom in individual ions can easily be recognized on the basis of characteristic ten natural tin isotopes with the most abundant ^{120}Sn isotope. All m/z values in Tables 3.2-3.6 are related to the ^{120}Sn isotope. The low mass ions at m/z 288 and 316, shown in Fig. 3.2 (a), do not contain a tin atom and they belong to background impurities not related to the main compound, as confirmed in the subsequent tandem mass spectrometric experiments, where these ions are missing, e.g. the MS/MS spectrum of m/z 672 (Fig 3.2 (b)). The fragment ion $[M+Na-HOSnBu_3]^+$ at m/z 364 is the only ion in the MS/MS spectrum of $[M+Na]^+$. The first-order negative-ion ESI mass spectrum (Fig. 3.2 (c)) shows the deprotonated molecule $[M-H]^-$ and also some fragment ions (see Table 3.3 for details). The other neutral logical losses are found in the MS/MS spectrum of $[M-H]^-$ at m/z 648 (Fig. 3.2 (d)), such as $[M-H-CO_2]^-$ at m/z 604, $[M-H-butane-butene-CO_2]^-$ at m/z 490 and $[M-H-2*butane-butene-CO_2]^-$ at m/z 433. The detailed explanation of all identified fragment ions is given in Tables 3.2-3.6 with several common features. The $[M+Na]^+$ ion is the base peak in all first-order positive-ion

ESI mass spectra, which makes possible an easy MW determination. In all cases, the lower abundant adduct ions with $SnBu_3$ are observed. The $[M-SnBu_3]^-$ ion is the base peak of all first-order negative-ion mass spectra accompanied by the less abundant $[M-H]^-$ ion. For compounds **1-3**, the adduct ion with two hydroxyl groups $[M_{2*OH}-H]^-$ are observed with a lower relative intensity than the $[M-H]^-$ ion. The other neutral logical losses in the tandem mass spectra are butane, butene, CO_2, $HOSnBu_3$, H_2O, etc. The mass spectra of all compounds are in accordance with the suggested structures.

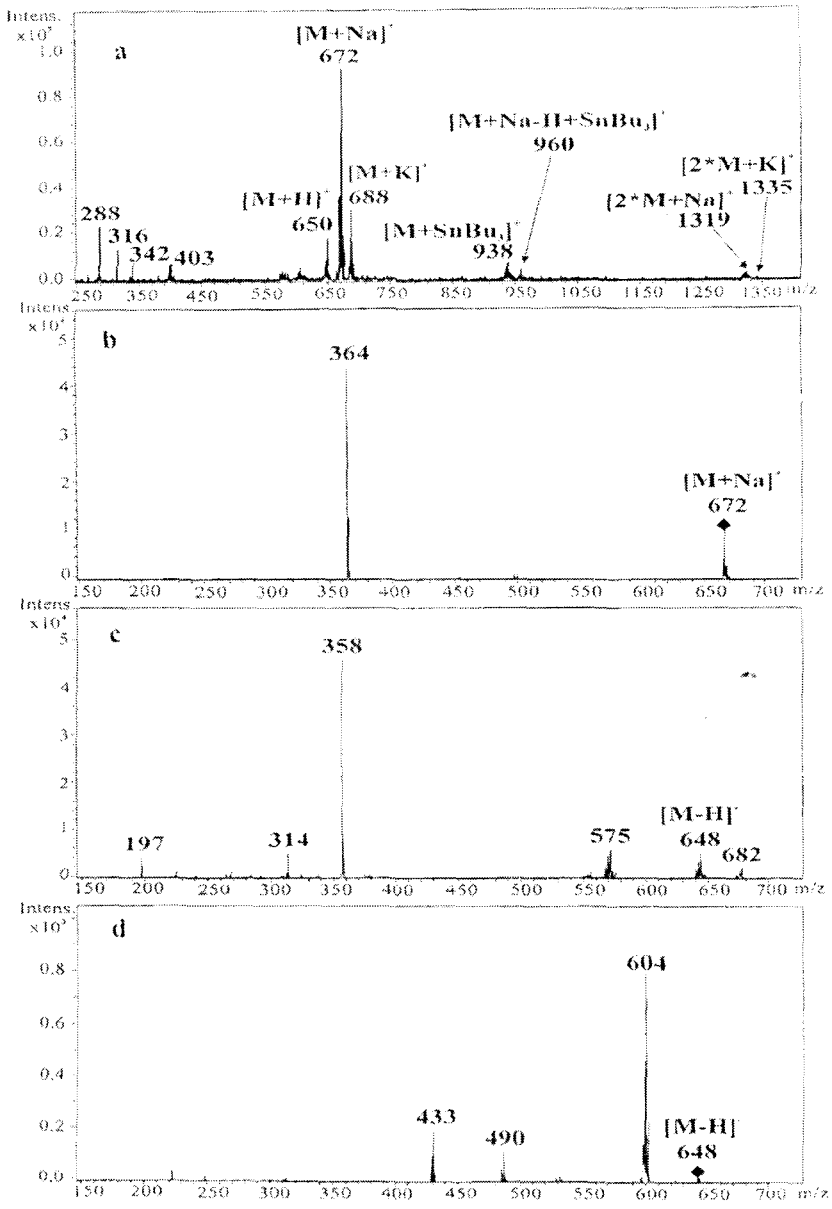

Fig. 3.2 ESI mass spectra of compound **2**: (a) positive-ion first-order spectrum; (b) positive-ion MS-MS of m/z 672; (c) negative-ion first-order spectrum; (d) negative-ion MS-MS spectrum of 648.

Table 3.2 Ions observed in the first-order and tandem mass spectra (MS/MS) using electrospray ionization both in positive-ion and negative-ion modes for compound **1**

m/z	Positive ions	Summary formula	Relative abundance (%)	Observed ions in MS/MS spectra[a]
1739	$[2*M+2*SnBu_3-H+K]^+$	$C_{76}H_{124}N_4O_8Sn_4K$	1	889
1723	$[2*M+Na-2H+2*SnBu_3]^+$	$C_{76}H_{124}N_4O_8Sn_4Na$	4	873
1449	$[2*M+K-H+SnBu_3]^+$	$C_{64}H_{98}N_4O_8Sn_3K$	2	889; 599; 583
1433	$[2*M+Na-H+SnBu_3]^+$	$C_{64}H_{98}N_4O_8Sn_3Na$	17	873; 583
1159	$[2*M+K]^+$	$C_{52}H_{72}N_4O_8Sn_2K$	3	889; 599
1143	$[2*M+Na]^+$	$C_{52}H_{72}N_4O_8Sn_2Na$	27	873; 583
963	$[2*M\text{-butene-}CO_2\text{-Bu}]^+$	$C_{43}H_{55}N_4O_6Sn_2$	9	583; 403
889	$[M+K-H+SnBu_3]^+$	$C_{38}H_{62}N_2O_4Sn_2K$	11	d
873	$[M+Na-H+SnBu_3]^+$	$C_{38}H_{62}N_2O_4Sn_2Na$	10	d
851	$[M+SnBu_3]^+$	$C_{38}H_{63}N_2O_4Sn_2$	46	793; 583; 525; 503; 485; 459; 373; 345; 253
599	$[M+K]^+$	$C_{26}H_{36}N_2O_4SnK$	39	291; 177
583	$[M+Na]^+$	$C_{26}H_{36}N_2O_4SnNa$	100	275; 234; 177
561	$[M+H]^+$	$C_{26}H_{37}N_2O_4Sn$	21	485; 291
403	$[M\text{-butene-}CO_2\text{-Bu}]^+$	$C_{17}H_{19}N_2O_2Sn$	20	345
m/z	Negative ions	Summary formula	Relative abundance (%)	Observed ions in MS/MS spectra[b]
1409	$[2*M+SnBu_3-2H]^-$	$C_{64}H_{97}N_4O_8Sn_3$	3	559; 515
1119	$[2*M-H]^-$	$C_{52}H_{71}N_4O_8Sn_2$	2	559
911	$[M-H+HOSnBu_3+CO_2]^-$	$C_{39}H_{63}N_2O_7Sn_2$	6	559
621	$[M-H+H_2O+CO_2]^-$	$C_{27}H_{37}N_2O_7Sn$	6	559; 269
575[c]	$[M_{carboxyl}-H]^-$	$C_{26}H_{35}N_2O_5Sn$	4	531; 487
559	$[M-H]^-$	$C_{26}H_{35}N_2O_4Sn$	27	515; 401; 344
269	$[M-SnBu_3]^-$	$C_{14}H_9N_2O_4$	100	225
225	$[M-SnBu_3-CO_2]^-$	$C_{13}H_9N_2O_2$	5	d

[a] Interpretation of observed ions in positive-ion tandem mass spectra: m/z 793 $[M+H+SnBu_3\text{-butane}]^+$; m/z 525 $[M+Na\text{-butane}]^+$; m/z 503 $[M+H\text{-butane}]^+$; m/z 485 $[M+H\text{-butane-}H_2O]^+$; m/z 459 $[M+H\text{-butane-}CO_2]^+$; m/z 373 $[M+H\text{-butan-2*butene-}H_2O]^+$; m/z 345 $[M+H\text{-2*butane-butene-}CO_2]^+$; m/z 291 $[M+K\text{-}HOSnBu_3]^+$; m/z 275 $[M+Na\text{-}HOSnBu_3]^+$; m/z 253 $[M+H\text{-}HOSnBu_3]^+$; m/z 177 $[SnBu]^+$.

[b] Interpretation of observed ions in negative-ion tandem mass spectra: m/z 531 $[M_{carboxyl}\text{-H-}CO_2]^-$; m/z 515 $[M\text{-H-}CO_2]^-$; m/z 487 $[M_{carboxyl}\text{-H-2*}CO_2]^-$; m/z 401 $[M\text{-H-}CO_2\text{-butane-butene}]^-$; m/z 344 $[M\text{-}CO_2\text{-3*Bu}]^-$.

[c] Aldehyde group is oxidized to carboxyl group. [d] Not observed.

Table 3.3 Ions observed in the first-order and tandem mass spectra (MS/MS) using electrospray ionization both in positive-ion and negative-ion modes for compound **2**

m/z	Positive ions	Summary formula	Relative abundance (%)	Observed ions in MS/MS spectra[a]
1337	$[2*M+K]^+$	$C_{66}H_{86}N_6O_6Sn_2K$	1	978; 688
1321	$[2*M+Na]^+$	$C_{66}H_{86}N_6O_6Sn_2Na$	4	962; 672
978	$[M+K-H+SnBu_3]^+$	$C_{45}H_{69}N_3O_3Sn_2K$	1	d
962	$[M+Na-H+SnBu_3]^+$	$C_{45}H_{69}N_3O_3Sn_2Na$	4	808; 790; 656; 570; 458
940	$[M+SnBu_3]^+$	$C_{45}H_{70}N_3O_3Sn_2$	8	610; 592; 574; 548; 534; 478; 462; 434; 406; 342; 298
688	$[M+K]^+$	$C_{33}H_{43}N_3O_3SnK$	33	380
672	$[M+Na]^+$	$C_{33}H_{43}N_3O_3SnNa$	100	500; 364
650	$[M+H]^+$	$C_{33}H_{44}N_3O_3Sn$	19	342; 314; 298; 197
m/z	Negative ions	Summary formula	Relative abundance (%)	Observed ions in MS/MS spectra[b]
682	$[M_{2*OH}-H]^-$	$C_{33}H_{44}N_3O_5Sn$	5	358; 314
648	$[M-H]^-$	$C_{33}H_{42}N_3O_3Sn$	12	604; 490; 433
575	$[Bu_3SnOCOC_6H_4N_2C_6H_3(OH)COO]^-$	$C_{26}H_{35}N_2O_5Sn$	14	d
358	$[M-SnBu_3]^-$	$C_{21}H_{16}N_3O_3$	100	314
314	$[M-SnBu_3-CO_2]^-$	$C_{20}H_{16}N_3O$	11	209
197	c	$C_{12}H_9N_2O$	9	d

[a] Interpretation of observed ions in positive-ion tandem mass spectra: m/z 808 $[M+Na-H+SnBu_3-2*butane-butene+H_2O]^+$; m/z 790 $[M+Na-H+SnBu_3-2*butane-butene]^+$; m/z 656 $[M+Na+SnBu_3-OSnBu_3]^+$; m/z 610 $[M-Bu+H_2O]^+$; m/z 592 $[M-Bu]^+$; m/z 574 $[M-Bu-H_2O]^+$; m/z 570 $[M+Na-butan-CO_2]^+$; m/z 548 $[M-Bu-CO_2]^+$; m/z 534 $[M-Bu-butane]^+$; m/z 500 $[M+Na-2*butane-butene]^+$; m/z 478 $[M-Bu-butane-butene]^+$; m/z 462 $[M+H-butane-2*butene-H_2O]^+$; m/z 458 $[M+Na-CO_2-2*butene-butane]^+$; m/z 434 $[M-Bu-butane-butene-CO_2]^+$; m/z 380 $[M+K-HOSnBu_3]^+$; m/z 364 $[M+Na-HOSnBu_3]^+$; m/z 342 $[M+H-HOSnBu_3]^+$; m/z 314 $[M-HOSnBu_3-CO]^+$; m/z 298 $[M+H-HOSnBu_3-CO_2]^+$.

[b] Interpretation of observed ions in negative-ion tandem mass spectra: m/z 604 $[M-H-CO_2]^-$; m/z 490 $[M-H-butane-butene-CO_2]^-$; m/z 433 $[M-H-2*butane-butene-CO_2]^-$; m/z 209 $[M-SnBu_3-CO_2-N_2-benzene]^-$.

[c] Not identified. [d] Not observed.

Table 3.4 Ions observed in the first-order and tandem mass spectra (MS/MS) using electrospray ionization both in positive-ion and negative-ion modes for compound **3**

m/z	Positive ions	Summary formula	Relative abundance (%)	Observed ions in MS/MS spectra[a]
1465	$[2*M+K]^+$	$C_{64}H_{80}N_6O_6Sn_2Br_2K$	0.4	1042; 752
1449	$[2*M+Na]^+$	$C_{64}H_{80}N_6O_6Sn_2Br_2Na$	3	1026; 736; 428
1026	$[M+Na-H+SnBu_3]^+$	$C_{44}H_{66}N_3O_3Sn_2BrNa$	4	968; 872; 854; 810; 720; 634; 550; 522
1004	$[M+SnBu_3]^+$	$C_{44}H_{67}N_3O_3Sn_2Br$	6	946; 674; 656; 638; 612; 406
752	$[M+K]^+$	$C_{32}H_{40}N_3O_3SnBrK$	8	d
736	$[M+Na]^+$	$C_{32}H_{40}N_3O_3SnBrNa$	100	520; 428; 298
177	$[SnBu]^+$	C_4H_9Sn	5	d
m/z	Negative ions	Summary formula	Relative abundance (%)	Observed ions in MS/MS spectra[b]
746	$[M_{2*OH}-H]^-$	$C_{32}H_{41}N_3O_5SnBr$	2	422; 378
712	$[M-H]^-$	$C_{32}H_{39}N_3O_3SnBr$	14	668; 554; 497; 417; 298
422	$[M-SnBu_3]^-$	$C_{20}H_{13}N_3O_3Br$	100	378; 273
378	$[M-SnBu_3-CO_2]^-$	$C_{19}H_{13}N_3OBr$	17	273
197	c	$C_{12}H_9N_2O$	4	d

[a] Interpretation of observed ions in positive-ion tandem mass spectra: m/z 1042 $[M+K-H+SnBu_3]^+$; m/z 968 $[M+Na-H+SnBu_3\text{-butane}]^+$; m/z 946 $[M+SnBu_3\text{-butane}]^+$; m/z 872 $[M+Na-H+SnBu_3\text{-2*butane-butene}+H_2O]^+$; m/z 854 $[M+Na-H+SnBu_3\text{-2*butane-butene}]^+$; m/z 810 $[M+Na-H+SnBu_3\text{-2*butane-butene-}CO_2]^+$; m/z 720 $[M+Na+SnBu_3\text{-OSn}Bu_3]^+$; m/z 674 $[M\text{-Bu}+H_2O]^+$; m/z 656 $[M\text{-Bu}]^+$; m/z 638 $[M\text{-Bu-}H_2O]^+$; m/z 634 $[M+Na\text{-butane-}CO_2]^+$; m/z 612 $[M\text{-Bu-}CO_2]^+$; m/z 550 $[M+Na+SnBu_3\text{-OSn}Bu_3\text{-2*butene-butane}]^+$; m/z 522 $[M+Na\text{-}CO_2\text{-2*butene-butane}]^+$; m/z 520 $[M+Na\text{-2*butane-butene-}CO_2]^+$; m/z 428 $[M+Na\text{-HOSn}Bu_3]^+$; m/z 406 $[M+H\text{-HOSn}Bu_3]^+$.

[b] Interpretation of observed ions in negative-ion tandem mass spectra: m/z 668 $[M\text{-H-}CO_2]^-$; m/z 554 $[M\text{-H-butane-butene-}CO_2]^-$; m/z 497 $[M\text{-H-2*butane-butene-}CO_2]^-$; m/z 417 $[M\text{-H-2*butane-butene-HBr-}CO_2]^-$; m/z 298 $[M\text{-Sn}Bu_3\text{-HBr-}CO_2]^-$; m/z 273 $[M\text{-Sn}Bu_3\text{-}CO_2\text{-}N_2\text{-benzene}]^-$.

[c] Not identified. [d] Not observed.

Table 3.5 Ions observed in the first-order and tandem mass spectra (MS/MS) using electrospray ionization both in positive-ion and negative-ion modes for compound **4**

m/z	Positive ions	Summary formula	Relative abundance (%)	Observed ions in MS/MS spectra[a]
1361	$[2*M+Na]^+$	$C_{64}H_{80}N_6O_6Sn_2Cl_2Na$	5	982; 692
982	$[M+Na-H+SnBu_3]^+$	$C_{44}H_{66}N_3O_3Sn_2ClNa$	3	828; 810; 766; 676; 590; 504; 478
960	$[M+SnBu_3]^+$	$C_{44}H_{67}N_3O_3Sn_2Cl$	6	630; 612; 594; 568; 498; 482; 454; 426; 362
747	c	c	12	d
708	$[M+K]^+$	$C_{32}H_{40}N_3O_3SnClK$	12	d
692	$[M+Na]^+$	$C_{32}H_{40}N_3O_3SnClNa$	100	384; 310
179	$[H_2SnBu]^+$	$C_4H_{11}Sn$	2	d
m/z	Negative ions	Summary formula	Relative abundance (%)	Observed ions in MS/MS spectra[b]
668	$[M-H]^-$	$C_{32}H_{39}N_3O_3SnCl$	54	624; 510; 453; 298
378	$[M-SnBu_3]^-$	$C_{20}H_{13}N_3O_3Cl$	100	334; 229
334	$[M-SnBu_3-CO_2]^-$	$C_{19}H_{13}N_3OCl$	68	297; 229
197	c	$C_{12}H_9N_2O$	11	d

[a] Interpretation of observed ions in positive-ion tandem mass spectra: m/z 828 $[M+Na-H+SnBu_3-2*butane-butene+H_2O]^+$; m/z 810 $[M+Na-H+SnBu_3-2*butane-butene]^+$; m/z 766 $[M+Na-H+SnBu_3-2*butane-butene-CO_2]^+$; m/z 676 $[M+Na+SnBu_3-OSnBu_3]^+$; m/z 630 $[M-Bu+H_2O]^+$; m/z 612 $[M-Bu]^+$; m/z 594 $[M-Bu-H_2O]^+$; m/z 590 $[M+Na-butane-CO_2]^+$; m/z 568 $[M-Bu-CO_2]^+$; m/z 554 $[M-Bu-butane]^+$; m/z 504 $[M+Na+SnBu_3-OSnBu_3-2*butane-butene]^+$; m/z 498 $[M-Bu-butane-butene]^+$; m/z 482 $[M+H-butane-2*butene-H_2O]^+$; m/z 478 $[M+Na-2*butene-butane-CO_2]^+$; m/z 454 $[M-Bu-butane-butene-CO_2]^+$; m/z 400 $[M+K-HOSnBu_3]^+$; m/z 384 $[M+Na-HOSnBu_3]^+$; m/z 362 $[M+H-HOSnBu_3]^+$.

[b] Interpretation of observed ions in negative-ion tandem mass spectra: m/z 624 $[M-H-CO_2]^-$; m/z 510 $[M-H-butane-butene-CO_2]^-$; m/z 453 $[M-H-2*butane-butene-CO_2]^-$; m/z 298 $[M-SnBu_3-HCl-CO_2]^-$; m/z 297; m/z 229 $[M-SnBu_3-CO_2-N_2-benzene]^-$.

[c] Not identified. [d] Not observed.

Table 3.6 Ions observed in the first-order and tandem mass spectra (MS/MS) using electrospray ionization both in positive-ion and negative-ion modes for compound **5**

m/z	Positive ions	Summary formula	Relative abundance (%)	Observed ions in MS/MS spectra[a]
1369	$[2*M+K]^+$	$C_{66}H_{86}N_6O_8Sn_2K$	1	994; 704
1353	$[2*M+Na]^+$	$C_{66}H_{86}N_6O_8Sn_2Na$	4	978; 688; 380
978	$[M+Na-H+SnBu_3]^+$	$C_{45}H_{69}N_3O_4Sn_2Na$	4	920; 824; 806; 762; 672; 586; 500; 472
956	$[M+SnBu_3]^+$	$C_{45}H_{69}N_3O_4Sn_2$	8	626; 608; 590; 564; 550; 478; 450; 422; 358
745	c	c	15	d
704	$[M+K]^+$	$C_{33}H_{43}N_3O_4SnK$	21	d
688	$[M+Na]^+$	$C_{33}H_{43}N_3O_4SnNa$	100	380
666	$[M+H]^+$	$C_{33}H_{44}N_3O_4Sn$	14	358; 330; 314
m/z	Negative ions	Summary formula	Relative abundance (%)	Observed ions in MS/MS spectra[b]
664	$[M-H]^-$	$C_{33}H_{42}N_3O_4Sn$	30	620; 506; 449
374	$[M-SnBu_3]^-$	$C_{21}H_{16}N_3O_4$	100	330; 315
330	$[M-SnBu_3-CO_2]^-$	$C_{20}H_{16}N_3O_2$	9	315
197	c	$C_{12}H_9N_2O$	2	d

[a] Interpretation of observed ions in positive-ion tandem mass spectra: m/z 994 $[M+K-H+SnBu_3]^+$; m/z 920 $[M+Na-H+SnBu_3\text{-butane}]^+$; m/z 824 $[M+Na-H+SnBu_3\text{-}2*\text{butane-butene}+H_2O]^+$; m/z 806 $[M+Na-H+SnBu_3\text{-}2*\text{butane-butene}]^+$; m/z 762 $[M+Na-H+SnBu_3\text{-}2*\text{butane-butene-}CO_2]^+$; m/z 672 $[M+Na+SnBu_3\text{-}OSnBu_3]^+$; m/z 626 $[M\text{-}Bu+H_2O]^+$; m/z 608 $[M\text{-}Bu]^+$; m/z 590 $[M\text{-}Bu\text{-}H_2O]^+$; m/z 586 $[M+Na\text{-butane-}CO_2]^+$; m/z 564 $[M\text{-}Bu\text{-}CO_2]^+$; m/z 550 $[M\text{-}Bu\text{-butane}]^+$; 500 $[M+Na+SnBu_3\text{-}OSnBu_3\text{-}2*\text{butane-butene}]^+$; m/z 478 $[M+H\text{-butane-}2*\text{butene-}H_2O]^+$; m/z 472 $[M+Na\text{-}2*\text{butane-butene-}CO_2]^+$; m/z 450 $[M\text{-}Bu\text{-butane-butene-}CO_2]^+$; m/z 380 $[M+Na\text{-}HOSnBu_3]^+$; m/z 358 $[M+H\text{-}HOSnBu_3]^+$; m/z 330 $[M+H\text{-}HSnBu_3\text{-}CO_2]^+$; m/z 314 $[M+H\text{-}HOSnBu_3\text{-}CO_2]^+$.

[b] Interpretation of observed ions in negative-ion tandem mass spectra: m/z 620 $[M\text{-}H\text{-}CO_2]^-$; m/z 506 $[M\text{-}H\text{-butane-butene-}CO_2]^-$; m/z 449 $[M\text{-}H\text{-}2*\text{butane-butene-}CO_2]^-$; m/z 315 $[M\text{-}SnBu_3\text{-}CH_4\text{-}CO_2]^-$.

[c] Not identified. [d] Not observed.

3.3.1.5 X-ray crystallography

Crystals of the tri-n-butyltin(IV) complexes suitable for an X-ray crystal-structure determination were obtained from hexane ($[^nBu_3SnL^1H]_n$ (**1**)), hexane/dichloromethane ($[^nBu_3SnL^2H]_n$ (**2**)) and hexane/chloroform mixture ($[^nBu_3SnL^4H]_n$ (**4**) and $[^nBu_3SnL^5H]_n$ (**5**)), by slow evaporation of the solvent at room temperature. The crystal structures of four of the tri-n-butyltin(IV) complexes **1** [49], **2** [50], **4** [49] and **5** [51] have been determined. The data collection and refinement parameters are given in Table 3.7.

Table 3.7 Crystallographic data and structure refinement parameters for the tributyltin(IV) complexes **1**, **2**, **4** and **5**

	1	**2**	**4**	**5**
Empirical formula	$C_{26}H_{36}N_2O_4Sn$	$C_{33}H_{33}N_3O_3Sn$	$C_{32}H_{40}ClN_3O_3Sn$	$C_{33}H_{43}N_3O_4Sn$
Formula weight	559.18	648.32	668.74	664.32
Crystal size (mm)	0.05 × 0.15 × 0.22	0.10 × 0.17 × 0.32	0.17 × 0.25 × 0.27	0.15 × 0.20 × 0.27
Crystal shape	Plate	Prism	Prism	Prism
Temperature (K)	160(1)	160(1)	160(1)	160(1)
Crystal system	Triclinic	Monoclinic	Monoclinic	Triclinic
Space group	$P\bar{1}$	$P2_1/n$	$P2_1/n$	$P\bar{1}$
a (Å)	20.4071(4)	14.1439(2)	14.1136(2)	10.2502(2)
b (Å)	23.8710(4)	9.9908(2)	9.9787(1)	13.2405(2)
c (Å)	26.1342(4)	23.2964(4)	23.2971(3)	23.4197(4)
α (°)	86.3718(9)	90	90	88.548(1)
β (°)	66.9966(8)	105.1374(9)	105.3959(7)	86.0704(9)
γ (°)	67.0400(7)	90	90	88.992(1)
V (Å^3)	10730.4(3)	3177.8(1)	3163.31(7)	3169.6(1)
Z	16	4	4	4
Dx (g cm^{-3})	1.384	1.355	1.404	1.392
μ (mm^{-1})	0.983	0.839	0.927	0.845
Transmission factors (min, max)	0.711, 0.969	0.752, 0.929	0.780, 0.860	0.739, 0.888
$2\theta_{max}$ (°)	50	55	60	55
Reflections measured	176976	66753	71033	62292
Independent reflections (R_{int})	37789 (0.121)	7243 (0.075)	9248 (0.062)	14479 (0.056)
Reflection with $I > 2\sigma(I)$	21227	5802	7081	11074
Number of parameters	2619	409	390	810
Number of restraints	2805	77	18	114
$R(F)$ ($I > 2\sigma(I)$ reflns)	0.056	0.0367	0.034	0.041
$wR(F^2)$ (all data)	0.148	0.088	0.082	0.088
$GOF(F^2)$	1.02	1.06	1.01	1.07
max, min $\Delta\rho$ (e/Å^3)	1.07, -0.74	1.15, -0.62	1.08, -0.59	1.17, -0.77

All the four structures conform to the same motif in which the carboxylate O atoms of a single aryl ligand bridge two Sn atoms and the pattern then repeats itself to give a continuous single-stranded polymeric structure, as illustrated in Figs. 3.3 (for **1**), 3.4 & 3.5 (for **2**), 3.6 & 3.7 (for **4**) and 3.8 (for **5**) (see Scheme 3.1 for line diagrams).

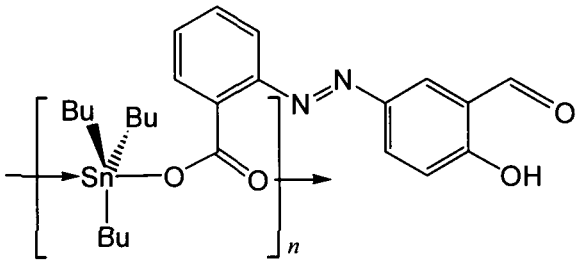

(**1**)

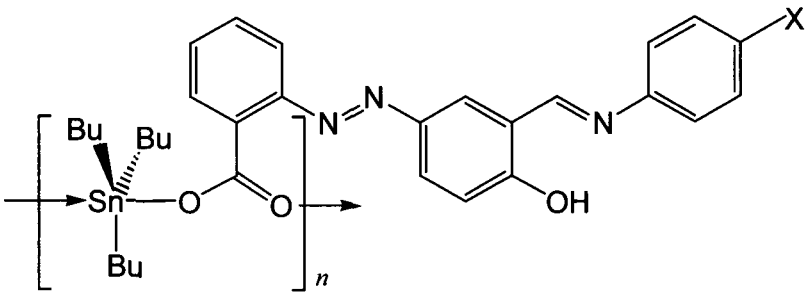

(X = -CH_3 (**2**), -Cl (**4**), -OCH_3 (**5**))

Scheme 3.1 A line diagram showing polymeric structures of $[Bu_3SnLH]_n$ complexes

The Sn atoms in each structure have a slightly distorted *trans*-R_3SnO_2 trigonal bipyramidal coordination geometry with equatorial butyl groups and carboxylate O atoms occupying axial positions, one being from each of two aryl ligands. The carboxylate C–O bond lengths are not equivalent, which shows some distinction between the carbonyl and carboxylic acid O atoms. Correspondingly, the Sn–O bond lengths involving these O atoms are also not equivalent, with the Sn–O bond to the carbonyl O atom being the longer, as would be expected on electronic grounds. Selected geometric parameters for the tri-n-butyltin(IV) complexes are given in Table 3.8 except for **1** (corresponding parameters for **1** are equivalent with **4**). The length of the intramolecular Sn···O(2) separation in **2** (3.1371(18) Å), **4** (3.138(2) Å), and **5** (3.221(2) Å)) is similar for the corresponding interactions in **1**. Although these distances are well inside the sum of the van der Waals radii of the Sn and O atoms (*ca.* 3.6 Å), there does not appear to be any significant distortion of the trigonal bipyramidal coordination geometry as a result of this contact.

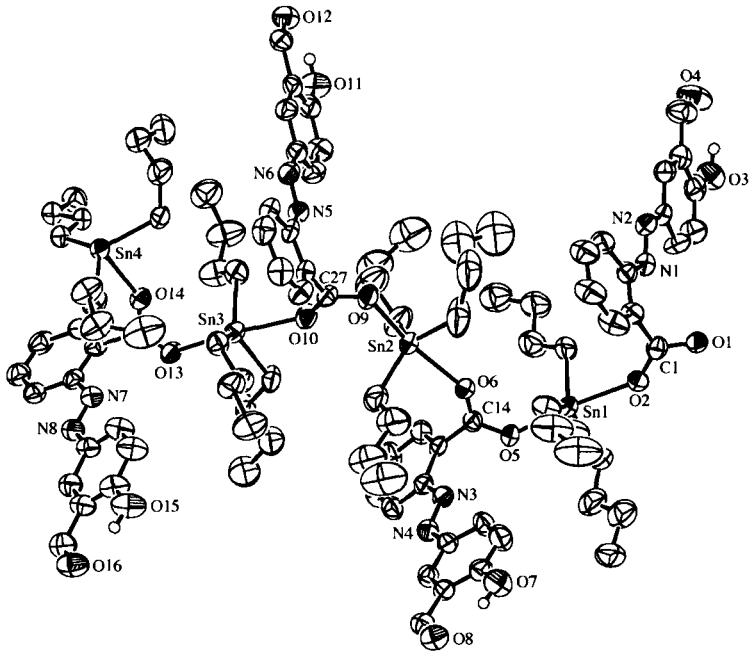

Fig.3.3 One of the two symmetry-independent three-unit segments of the polymeric $[Bu_3SnL^1H]_n$ chain in the asymmetric unit of **1** (50% probability ellipsoids).

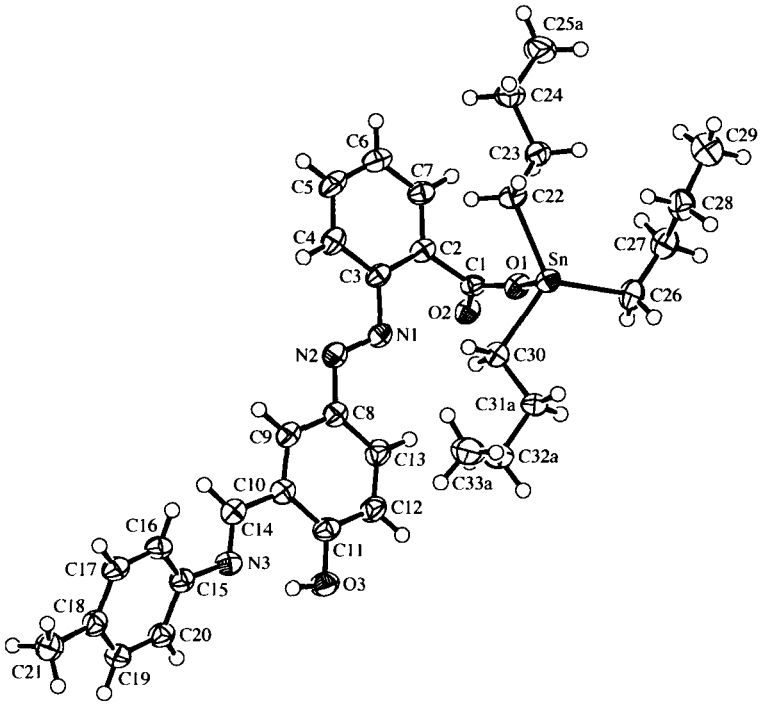

Fig. 3.4 View of the asymmetric unit of **2**, showing the atom-labelling scheme (50% probability ellipsoids). Only one conformation of the disordered *n*-butyl groups is shown.

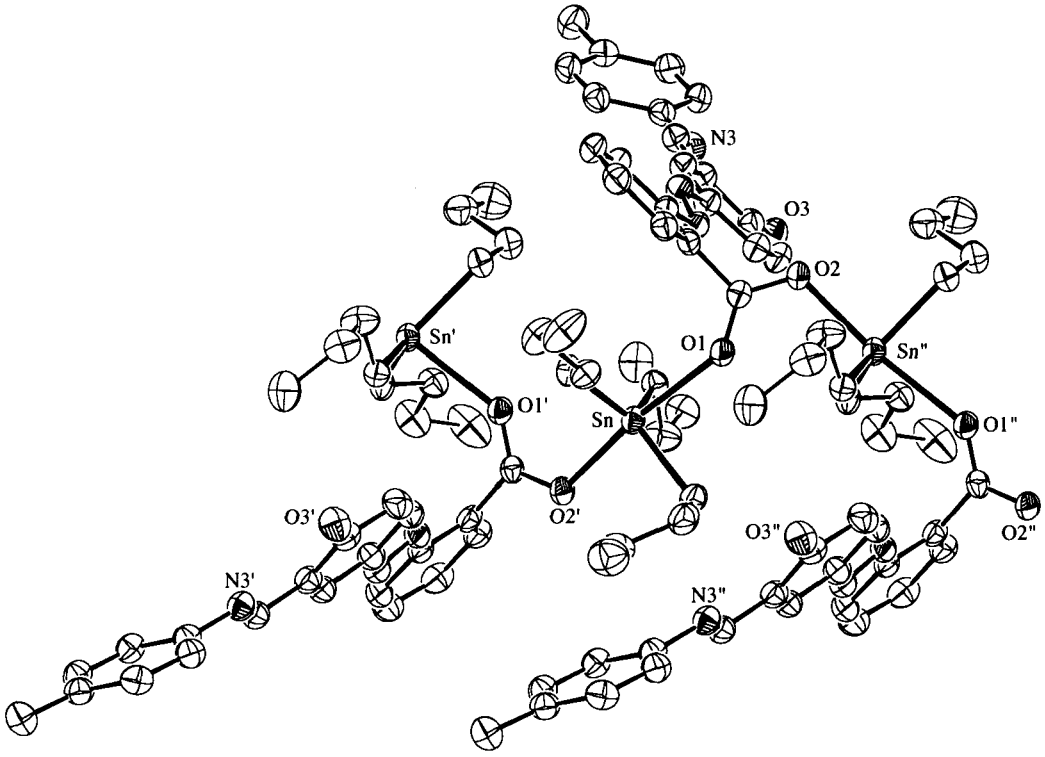

Fig. 3.5 A three-unit segment of the polymeric $[Bu_3SnL^2H]_n$ chain in **2** (50% probability ellipsoids). H atoms have been omitted for clarity.

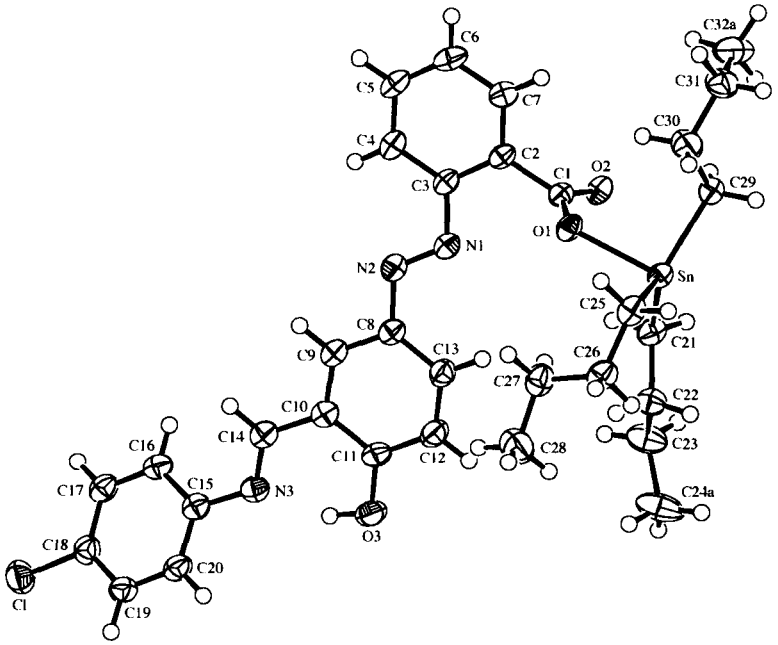

Fig. 3.6 The asymmetric unit of $[Bu_3SnL^4H]_n$ **4** showing the atom-labelling scheme (50% probability ellipsoids).

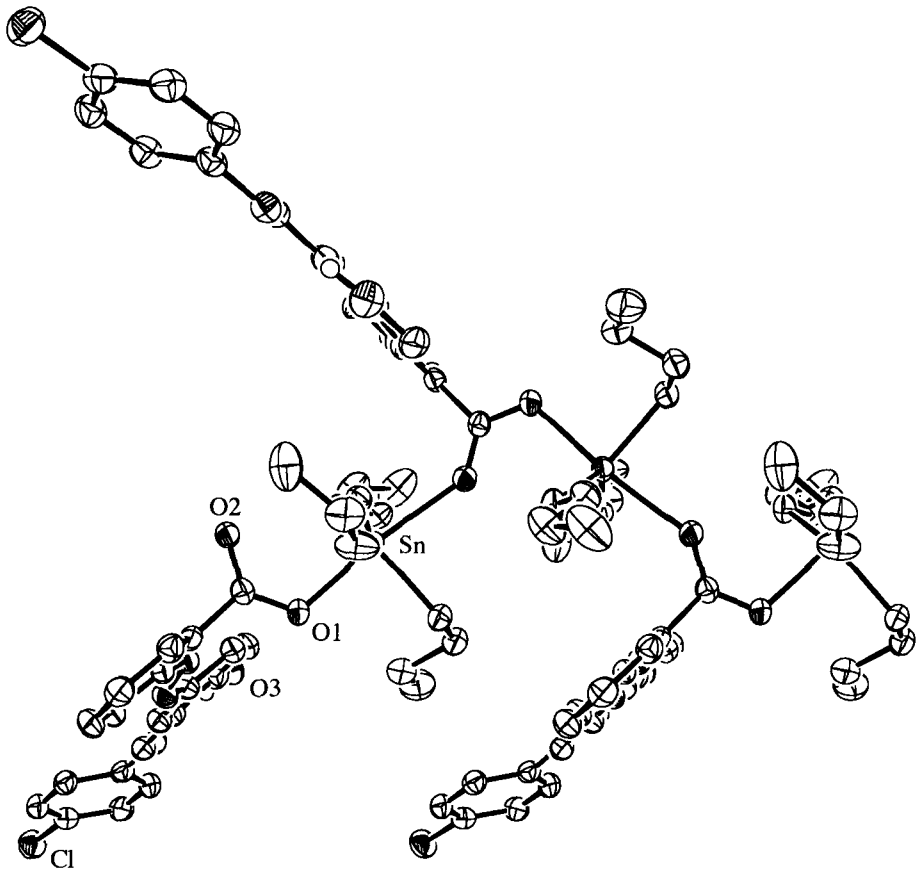

Fig. 3.7 A three-unit segment of the polymeric $[Bu_3SnL^4H]_n$ chain in **4** (50% probability ellipsoids).

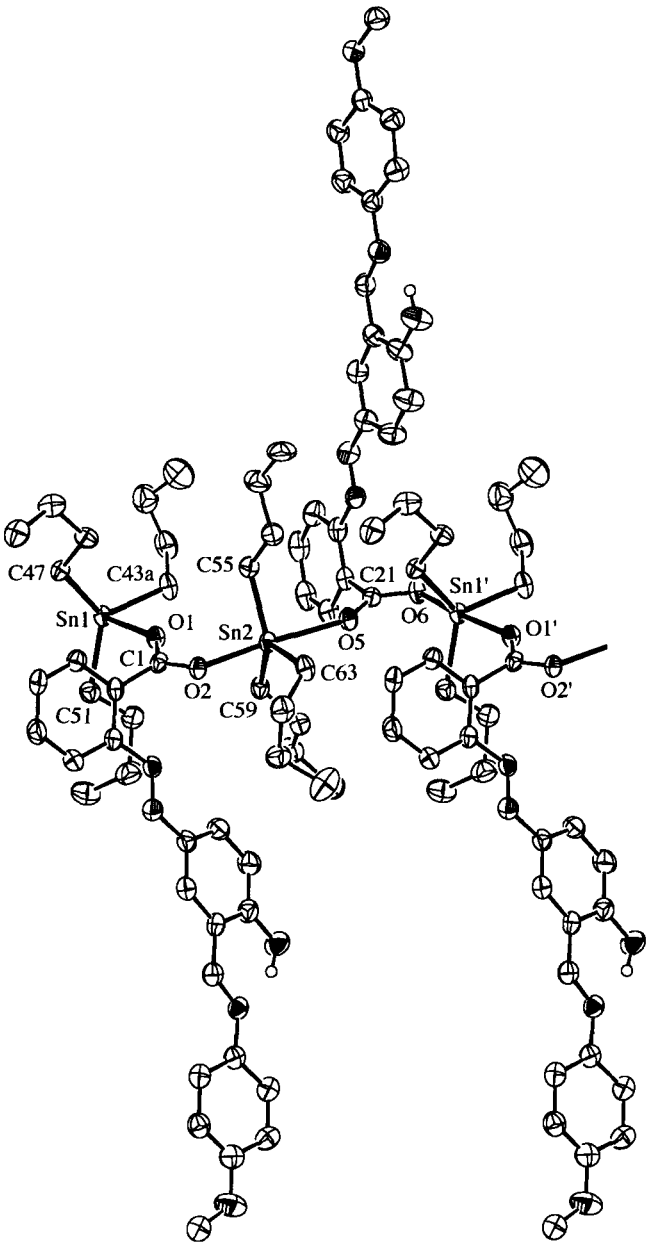

Fig. 3.8 A segment of the polymeric $[Bu_3SnL^5H]_n$ chain in **5** showing the asymmetric unit plus one additional $[Bu_3SnL^5H]$ unit (50% probability ellipsoids, only one of the disordered conformations of the ligands is shown).

Table 3.8 Selected bond lengths (Å) and angles (°) for the tributyltin(IV) complexes[a] **2**, **4** and **5**

Geometric Parameter	**2**	Geometric Parameter	**4**	Geometric Parameter	**5**
Sn-O(1)	2.456(18)	Sn-O(1)	2.213(2)	Sn(1)-O(1)	2.425(2)
Sn-O(2)^{i}	2.2087(18)	Sn-O(2)^{i}	2.454(2)	Sn(1)-O(6)^{i}	2.218(2)
Sn-O(1)^{i}	3.1371(18)	Sn···O(2)	3.138(2)	Sn(1)···O(5)^{i}	3.172(2)
Sn-C(22)	2.149(3)	Sn-C(21)	2.143(2)	Sn(1)-C(47)	2.145(3)
Sn-C(26)	2.148(2)	Sn-C(25)	2.147(2)	Sn(1)-C(43a)	2.150(4)
Sn-C(30)	2.135(3)	Sn-C(29)	2.134(2)	Sn(1)-C(51)	2.133(3)
O(1)-Sn-O(2)^{i}	173.26(6)	O(1)-Sn-O(2)^{i}	173.19(5)	O(1)-Sn(1)-O(6)^{i}	173.89(7)
O(1)-Sn-C(22)	89.32(9)	O(1)-Sn-C(21)	96.25(7)	O(1)-Sn(1)-C(47)	91.1(1)
O(1)-Sn-C(26)	84.17(9)	O(1)-Sn-C(25)	89.68(8)	O(1)-Sn(1)-C(43a)	83.6(3)
O(1)-Sn-C(30)	86.40(9)	O(1)-Sn-C(29)	93.12(7)	O(1)-Sn(1)-C(51)	86.0(1)
O(2)^{i}-Sn-C(22)	96.22(9)	O(2)^{i}-Sn-C(21)	89.80(7)	O(6)^{i}-Sn(1)-C(47)	93.0(1)
O(2)^{i}-Sn-C(26)	89.67(9)	O(2)^{i}-Sn-C(25)	84.55(7)	O(6)^{i}-Sn(1)-C(43a)	90.4(3)
O(2)^{i}-Sn-C(30)	93.88(9)	O(2)^{i}-Sn-C(29)	86.19(7)	O(6)^{i}-Sn(1)-C(51)	95.6(1)
C(22)-Sn-C(26)	121.0(11)	C(21)-Sn-C(25)	120.58(9)	C(43a)-Sn(1)-C(47)	119.4(2)
C(22)-Sn-C(30)	122.01(11)	C(21)-Sn-C(29)	122.68(9)	C(47)-Sn(1)-C(51)	122.6(1)
C(26)-Sn-C(30)	115.99(11)	C(25)-Sn-C(29)	115.88(9)	C(43a)-Sn(1)-C(51)	117.1(2)

[a] Atom labels with superscript ^{i} refer to atoms from the next symmetry-related ligand in the polymeric chain.

In **2** and **4**, the asymmetric unit of the crystal structure contains just one of the principle chemical units, which then repeats to form the polymeric structure. By contrast, the asymmetric unit in **1** contains two symmetry-independent fragments of the polymer, with each fragment being comprised of four repeats of the principle chemical unit. Thus there are eight symmetry-independent Sn atoms in the structure. In **5**, the asymmetric unit contains two repeats of the principal chemical unit and the structure is built from adjacent $SnBu_3$ moieties bridged by the two carboxylate oxygen atoms of a single aryl ligand, with the pattern then continuing indefinitely.

The hydroxy group in each ligand forms an intraligand hydrogen bond with the adjacent aldehyde O atom in **1** and with the adjacent imino N atom in **2**, **4** and **5**. Some of the butyl groups in each structure are disordered, as is common for complexes involving the Bu_3Sn core (see Section 3.4). In **5**, the methoxy methyl group of one of the two symmetry-independent carboxylate ligands is also disordered over two conformations, which differ by an approximately 180° rotation about the C(ring)–O bond.

The structures of all the tri-n-butyltin(IV) complexes correspond with the type **II** polymeric motif described by Willem et al. for related R_3SnO_2CR' compounds [38] and the general description of the structure of $[Me_3Sn(O_2CR')]_n$ (R' = 2-[(*E*)-2-(2-hydroxy-5-methylphenyl)-1-diazenyl]benzoate) given there applies equally well to **1, 2, 4** and **5**. As in the earlier report [38], the polymeric chain in the structures of both **1** and **4** propagates in a 2_1 screw fashion, with this being a crystallographic 2_1 screw axis in the case of **2** and **4** and a non-crystallographic pseudo-2_1 screw axis in **1** and **5**.

In **1**, the eight symmetry-independent Sn···Sn distances range from 5.1288(9) to 5.548(1) Å. In **2,** The repeat Sn···Sn distances in **2** and **4** are 5.2583(3) Å and 5.2601(2) Å, respectively while in **5** are 5.3520(3) and 5.3200(3) Å, which agrees very well with the mean repeat distance found in other type **II** carboxylate-bridged triorganotin species of 5.19 ± 0.21 Å [38], i.e., the repeat distance is independent of the nature of the tin-bound substituents and carboxylate residues.

The polymeric structures of **1**, **2**, **4**, and **5** contrast with the ESI-MS data, where the polymeric ions have only low relative abundances in the positive ion ESI-MS and are totally absent in the negative ion ESI-MS which may be caused by easy fragmentation of polymeric species and decomposition of polymers upon dissolution.

3.3.2 Triphenyltin(IV) complexes of L^1HH'-L^5HH' ($Ph_3SnL^{1-5}H$)

The triphenyltin(IV) complex of formulation $Ph_3SnL^1H.OH_2$ is obtained by the azeotropic dehydration of a mixture of Ph_3SnOH and 2-[(*E*)-2-(3-formyl-4-hydroxyphenyl)-1-diazenyl]benzoic acid (L^1HH') in a 1:1 molar ratio in an anhydrous toluene. The structure of the complex was confirmed by X-ray diffraction and NMR (^1H and ^{13}C) studies by Basu Baul *et al.* [33]. ^{119}Sn- NMR, ^{119m}Sn Mössbauer and electrospray mass spectrometry (ESI-MS) data for $Ph_3SnL^1H.OH_2$ have now been obtained and included for convenience of discussion.

The triphenyltin(IV) complexes of 2-{(*E*)-4-hydroxy-3-[(*E*)-4-(aryl)imino-methyl]phenyldiazenyl}benzoic acids ($L^{2-5}HH'$) have been characterized by IR, ^1H, ^{13}C, ^{119}Sn NMR, ^{119m}Sn Mössbauer and electrospray mass spectrometry (ESI-MS) techniques. The crystal structures of three compounds, *viz.*, $[Ph_3SnL^2H]_n$ (**2**), $[Ph_3SnL^3H]_n$ (**3**) and $[^nPh_3SnL^5H]_2$ (**5**) are reported.

3.3.2.1 Infrared data

The diagnostically important infrared absorption frequencies for the carboxylate antisymmetric [ν_{asym}(OCO)] stretching vibration of the triphenyltin complexes (**2-5**) are given below. The assignment of the symmetric [ν_{sym}(OCO)] stretching vibration band could not be made owing to the complex pattern of the spectra. The antisymmetric [ν_{asym}(OCO)] stretching vibration band of the uncomplexed ligands ($L^{2-5}HH'$) appears at ~1725 cm^{-1} [49]. In the triphenyltin(IV) complexes, the carbonyl stretching frequency appears at ~1620 cm^{-1}. The shift of the band relative to its position for the free ligand is ascribed to carboxylate coordination in accordance with earlier reports [49,36,37].

3.3.2.2 ^1H, ^{13}C and ^{119}Sn NMR data

The ^1H- and ^{13}C- NMR data of $L^{2-5}HH'$ are reported in our earlier ref. [49] and are also presented in Chapter 2. The conclusions drawn from the ligand assignments were then subsequently extrapolated to the complexes owing to the data similarity. The ^1H- and ^{13}C-chemical shift assignments (listed below) of the triphenyltin moiety are straightforward from the multiplicity patterns, resonance intensities and also by examining the $^nJ(^{13}C\text{-}^{119/117}Sn)$ coupling constants [36-38]. The ^1H-NMR integration values were completely consistent with the

formulation of the products. The ^{119}Sn-NMR chemical shifts of the triphenyltin(IV) complexes (**2-5**) in $CDCl_3$ solution are listed in Table 3.9. The complexes exhibit a single sharp resonance at *ca.* -109 ppm, suggesting that the complexes are isostructural in solution where the tin atom is four-coordinate [36,38,40]. In contrast, the solid-state polymeric structures found for complexes **2** and **3**, and the dimeric structure observed for complex **5** reveal five-coordinate tin atoms (vide infra). It is anticipated that the multi-nuclear structures break down in solution to generate a monomeric four-coordinate tetrahedral structure [38].

The basic ligand frame-work is shown in Figs. 2.1- 2.2 along with the abbreviations and numbering schemes for spectroscopic analyses. Numbering scheme for Sn-Ph skeleton as shown below:

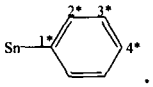

The detailed spectral features for complexes **1-5** are given below:

3.3.2.2.1 $Ph_3SnL^1H.OH_2$ (1)

ESI-MS data: MW = 620 (Ph_3SnL^1H). Positive-ion MS: m/z 659 $[M+K]^+$, 100%; m/z 643 $[M+Na]^+$; m/z 463. MS/MS of m/z 659: m/z 581 $[M+K\text{-benzene}]^+$; m/z 537 $[M+K\text{-}CO_2\text{-benzene}]^+$; m/z 503 $[M+K\text{-}2*\text{benzene}]^+$; m/z 291 $[M+K\text{-}HOSnPh_3]^+$. MS/MS of m/z 643: m/z 565 $[M+Na\text{-benzene}]^+$; m/z 521 $[M+Na\text{-}CO_2\text{-benzene}]^+$; m/z 487 $[M+Na\text{-}2*\text{benzene}]^+$; m/z 351 $[SnPh_3]^+$; m/z 275 $[M+Na\text{-}HOSnPh_3]^+$; m/z 270. Negative-ion MS: m/z 619 $[M-H]^-$; m/z 439 $[Ph_3SnCl+Cl+H_2O]^-$; m/z 269 $[L^1H]^-$, 100%; m/z 225 $[L^1H\text{-}CO_2]^-$; m/z 197 $[L^1H\text{-}CO\text{-}CO_2]^-$. MS/MS of m/z 619: m/z 575 $[M\text{-}H\text{-}CO_2]^-$; m/z 547 $[M\text{-}H\text{-}CO\text{-}CO_2]^-$. MS/MS of m/z 439: m/z 351 $[Ph_3Sn]^-$. MS/MS of m/z 269: m/z 225 $[L^1H\text{-}CO_2]^-$; m/z 197 $[L^1H\text{-}CO\text{-}CO_2]^-$. MS/MS of m/z 225: m/z 197 $[L^1H\text{-}CO\text{-}CO_2]^-$. MS/MS of m/z 197: m/z 170 $[L^1H\text{-}CO\text{-}CO_2\text{-}N_2]^-$; m/z 92 $[L^1H\text{-}CO\text{-}CO_2\text{-}N_2\text{-benzene}]^-$.

3.3.2.2.2 Ph_3SnL^2H (2)

IR (cm^{-1}): 1619 $\nu(OCO)_{asym.}$ ^{1}H-NMR ($CDCl_3$ / 400.13 MHz); δ_H: 14.0 [brs, 1H, OH], 8.38 [s, 1H, C(H)=N], 7.91 [d, 1H, (B) H6], 7.81 [m, 2H, (B) H4 & (C) H3], 7.57 [m, 2H, (C) H4 & H6], 7.41 [m, 1H (C) H5], 7.28 [part of AA'BB' system, 2H, (A) H2 & H6], 7.19 [part of AA'BB' system, 2H, (A) H3 & H5], 6.99 [d, 1H (B) H3], 2.41 [s, 3H, CH_3]; Sn-Ph: 7.75 [m, 6H, H2*], 7.41 [m, 9H, H3* & H4*] ppm. ^{13}C-NMR ($CDCl_3$ / 100.62 MHz); δ_C: 174.6 [COO], 164.4 [(B) C2], 161.2 [C(H)=N], 152.0 [(C) C1], 145.7 [(B) C5], 145.1 [(A) C1], 138.4 [(A) C4], 131.6

[(C) C5], 130.5 [(C) C2], 130.1 [(A) C3 & C5], 129.2 [(C) C4], 128.6 [(C) C3], 128.3 [(B) C6], 127.9 [(B) C4], 121.1 [(A) C2 & C6], 118.8 [(B) C1], 118.7 [(C) C6], 118.1 [(B) C3], 21.1 [CH_3]; Sn-Ph: 137.5 [C1*], 136.9 [C2*], 130.1 [C4*], 128.9 [C3*] ppm. MW = 709. Positive-ion MS: m/z 1457 $[2*M+K]^+$; m/z 1441 $[2*M+Na]^+$; m/z 1060 $[M+SnPh_3]^+$; m/z 748 $[M+K]^+$, 100%; m/z 732 $[M+Na]^+$; m/z 710 $[M+H]^+$. MS/MS of m/z 1457: m/z 1100 $[M+K+HSnPh_3]^+$; m/z 748 $[M+K]^+$. MS/MS of m/z 1441: m/z 1084 $[M+Na+HSnPh_3]^+$; m/z 732 $[M+Na]^+$. MS/MS of m/z 1060: m/z 982 $[M\text{-benzene}+SnPh_3]^+$; m/z 904 $[M\text{-}2*\text{benzene}+SnPh_3]^+$; m/z 650 $[M\text{-Ph}+H_2O]^+$; m/z 632 $[M\text{-Ph}]^+$; m/z 588 $[M\text{-Ph}\text{-}CO_2]^+$; m/z 554 $[M\text{-Ph-benzene}]^+$. MS/MS of m/z 732: m/z 364 $[M+Na\text{-}HOSnPh_3]^+$. MS/MS of m/z 710: m/z 632 $[M\text{-benzene}+H]^+$; m/z 588 $[M+H\text{-benzene}\text{-}CO_2]^+$; m/z 554 $[M+H\text{-}2*\text{benzene}]^+$; m/z 342 $[M+H\text{-}HOSnPh_3]^+$. Negative-ion MS: m/z 720 $[L^1H+Ph_2SnCl_2+H_2O]^-$; m/z 708 $[M\text{-}H]^-$; m/z 553; m/z 439 $[Ph_3SnCl+Cl+H_2O]^-$; m/z 358 $[L^1H]^-$, 100%; m/z 314 $[L^1H\text{-}CO_2]^-$; m/z 269 $[L^5H]^-$. MS/MS of m/z 720: m/z 358 $[L^1H]^-$; m/z 314 $[L^1H\text{ -}CO_2]^-$. MS/MS of m/z 708: m/z 664 $[M\text{-}H\text{-}CO_2]^-$. MS/MS of m/z 439: m/z 351 $[Ph_3Sn]^-$. MS/MS of m/z 358: m/z 314 $[L^1H\text{ -}CO_2]^-$.

3.3.2.2.3 Ph_3SnL^3H (3)

IR (cm^{-1}): 1622 $\nu(OCO)_{asym}$. ^{1}H-NMR ($CDCl_3$ / 400.13 MHz); δ_H: 13.5 [brs, 1H,OH], 8.47 [s, 1H, C(H)=N], 7.91 [d, 1H, (B) H6], 7.82 [m, 2H, (B) H4 & (C) H3], 7.56 [m, 3H, (C) H4, H5 & H6], 7.41 [part of AA'MM' system, 2H (A) H2 & H6], 7.12 [part of AA'MM' system, 2H (A) H3 & H5], 6.90 [d, 1H, (B) H3]; Sn-Ph: 7.75 [m, 6H, H2*], 7.41 [m, 9H, H3* & H4*] ppm. ^{13}C-NMR ($CDCl_3$ / 100.62 MHz); δ_C: 174.3 [COO], 164.0 [(B) C2], 162.7 [C(H)=N], 152.2 [(C) C1], 146.9 [(B) C5], 145.8 [(A) C1], 132.6 [(A) C3 & C5], 131.6 [(C) C5], 130.5 [(C) C2], 129.3 [(A) C4], 129.2 [(C) C3], 128.4 [(B) C4], 122.9 [(A) C2 & C6], 120.9 [(A) C4], 118.7 [(B) C1], 118.6 [(C) C6], 118.1 [(B) C3]; Sn-Ph: 138.4 [C1*], 136.9 [C2*], 130.2 [C4*], 128.9 [C3*]. MW = 773. Positive-ion MS: m/z 1585 $[2*M+K]^+$; m/z 1569 $[2*M+Na]^+$; m/z 812 $[M+K]^+$, 100%; m/z 796 $[M+Na]^+$; m/z 463. MS/MS of m/z 1585: m/z 1164 $[M+K+HSnPh_3]^+$; m/z 812 $[M+K]^+$. MS/MS of m/z 1569: m/z 1148 $[M+Na+HSnPh_3]^+$; m/z 796 $[M+Na]^+$. MS/MS of m/z 796: m/z 428 $[M+Na\text{-}HOSnPh_3]^+$. Negative-ion MS: m/z 772 $[M\text{-}H]^-$; m/z 439 $[Ph_3SnCl+Cl+H_2O]^-$; m/z 422 $[L^2H]^-$, 100%; m/z 378 $[L^2H\text{-}CO_2]^-$; m/z 269 $[L^5H]^-$. MS/MS of m/z 772: m/z 728 $[M\text{-}H\text{-}CO_2]^-$. MS/MS of m/z 439: m/z 351 $[Ph_3Sn]^-$. MS/MS of m/z 422: m/z 378 $[L^2H\text{-}CO_2]^-$.

3.3.2.2.4 Ph_3SnL^4H (4)

IR (cm^{-1}): 1616 $\nu(OCO)_{asym}$. ^{1}H-NMR ($CDCl_3$ / 400.13 MHz); δ_H: 13.6 [brs, 1H, OH], 8.31 [s, 1H, C(H)=N], 7.91 [d, 1H, (B) H6], 7.83 [m, 2H, (B) H4 & (C) H3], 7.57 [m, 2H, (C) H4 & H6], 7.42 [m, 3H (A) H2 & H6 and (C) H5], 7.19 [part of AA'BB' system, 2H, (A) H3 & H5], 7.0 [d, 1H, (B) H3]; Sn-Ph: 7.75 [m, 6H, H2*], 7.42 [m, 9H, H3* & H4*] ppm. ^{13}C-NMR ($CDCl_3$ / 100.62 MHz); δ_C: 174.5 [COO], 164.0 [(B) C2], 162.6 [C(H)=N], 152.2 [(C) C1], 146.4 [(B) C5], 145.8 [(A) C1], 138.4 [(A) C4], 131.6 [(C) C5], 130.6 [(C) C2], 130.2 [(A) C3 & C5], 129.7 [(C) C4], 129.2 [(C) C3], 128.6 [(B) C6], 128.4 [(B) C4] 122.5 [(A) C2 & C6], 118.6 [(B) C1], 118.3 [(C) C6], 118.1 [(B) C3]; Sn-Ph: 138.4 [C1*], 136.9 [C2*], 130.2 [C4*], 128.9 [C3*] ppm. MW = 729. Positive-ion MS: m/z 1497 $[2*M+K]^+$; m/z 1481 $[2*M+Na]^+$; m/z 768 $[M+K]^+$, 100%; m/z 752 $[M+Na]^+$; m/z 463. MS/MS of m/z 1499: m/z 1120 $[M+K+HSnPh_3]^+$; m/z 768 $[M+K]^+$. MS/MS of m/z 1483: m/z 1104 $[M+Na+HSnPh_3]^+$; m/z 752 $[M+Na]^+$. MS/MS of m/z 752: m/z 384 $[M+Na-HOSnPh_3]^+$; m/z 351 $[SnPh_3]^+$. Negative-ion MS: m/z 728 $[M-H]^-$; m/z 439 $[Ph_3SnCl+Cl+H_2O]^-$; m/z 378 $[L^3H]^-$, 100%; m/z 334 $[L^3H-CO_2]^-$; m/z 269 $[L^5H]^-$. MS/MS of m/z 728: m/z 684 $[M-H-CO_2]^-$. MS/MS of m/z 439: m/z 351 $[Ph_3Sn]^-$. MS/MS of m/z 378: m/z 334 $[L^3H-CO_2]^-$.

3.3.2.2.5 Ph_3SnL^5H (5)

IR (cm^{-1}): 1619 $\nu(OCO)_{asym}$. ^{1}H-NMR ($CDCl_3$ / 400.13 MHz); δ_H: 14.0 [brs, 1H, OH], 8.48 [s, 1H, C(H)=N], 7.91 [d, 1H, (B) H6], 7.80 [m, 2H, (B) H4 & (C) H3], 7.57 [m, 2H, (C) H4 & H6], 7.40 [m, 1H (C) H5], 7.26 [part of AA'MM' system, 2H, (A) H2 & H6], 6.98 [m, 3H, (A) H3 & H5 and (B) H3], 3.89 [s, 3H, OCH_3]; Sn-Ph: 7.75 [m, 6H, H2*], 7.40 [m, 9H, H3* & H4*] ppm. ^{13}C-NMR ($CDCl_3$ / 100.62 MHz); δ_C: 174.8 [COO], 164.2 [(B) C2], 159.9 [C(H)=N], 159.4 [(A) C4], 152.3 [(C) C1], 145.6 [(B) C5], 140.6 [(A) C1], 131.6 [(C) C5], 130.6 [(C) C2], 129.2 [(C) C4], 128.6 [(C) C3], 128.1 [(B) C6], 127.7 [(B) C4], 122.4 [(A) C2 & C6], 118.9 [(B) C1], 118.7 [(C) C6], 118.0 [(B) C3], 114.8 [(A) C3 & C5], 55.6 [OCH_3]; Sn-Ph: 138.4 [C1*], 136.9 [C2*], 130.2 [C4*], 128.9 [C3*] ppm. MW = 725. Positive-ion MS: m/z 1489 $[2*M+K]^+$; m/z 1473 $[2*M+Na]^+$; m/z 1076 $[M+SnPh_3]^+$; m/z 764 $[M+K]^+$, 100%; m/z 748 $[M+Na]^+$; m/z 726 $[M+H]^+$. MS/MS of m/z 1489: m/z 1116 $[M+K+HSnPh_3]^+$; m/z 764 $[M+K]^+$. MS/MS of m/z 1473: m/z 1100 $[M+Na+HSnPh_3]^+$; m/z 748 $[M+Na]^+$. MS/MS of m/z 1076: m/z 998 $[M-benzene+SnPh_3]^+$; m/z 920 $[M-2*benzene+SnPh_3]^+$; m/z 666 $[M-Ph+H_2O]^+$; m/z 648 $[M-Ph]^+$; m/z 604 $[M-Ph-CO_2]^+$. m/z 570 [M-Ph-benzene]$^+$. MS/MS of m/z 764: m/z 686 $[M+K-benzene]^+$; m/z 642 $[M+K-benzene-CO_2]^+$; m/z 396 $[M+K-HOSnPh_3]^+$; m/z 270. MS/MS of m/z 748: m/z

626 $[M+Na\text{-}benzene\text{-}CO_2]^+$; m/z 380 $[M+Na\text{-}HOSnPh_3]^+$. MS/MS of m/z 726: m/z 648 [M+H-benzene]$^+$; m/z 604 $[M+H\text{-}benzene\text{-}CO_2]^+$; m/z 570 [M+H-2*benzene]$^+$; m/z 358 $[M+H\text{-}HOSnPh_3]^+$. Negative-ion MS: m/z 1099 [M+ligand]$^-$; m/z 736 $[L^4H+Ph_2SnCl_2+H_2O]^-$; m/z 724 $[M\text{-}H]^-$; m/z 553; m/z 439 $[Ph_3SnCl+Cl+H_2O]^-$; m/z 374 $[L^4H]^-$, 100%; m/z 330 $[L^4H\text{-}CO_2]^-$; m/z 269 $[L^5H]^-$. MS/MS of m/z 1099: m/z 374 $[L^4H]^-$. MS/MS of m/z 736: m/z 374 $[L^4H]^-$; m/z 330 $[L^4H\text{-}CO_2]^-$; m/z 315 $[L^4H\text{-}CO_2\text{-}CH_3]^-$. MS/MS of m/z 724: m/z 680 $[M\text{-}CO_2]^-$; m/z 665 $[M\text{-}CO_2\text{-}CH_3]^-$. MS/MS of m/z 439: m/z 351 $[Ph_3Sn]^-$. MS/MS of m/z 374: m/z 330 $[L^4H\text{-}CO_2]^-$; m/z 315 $[L^4H\text{-}CO_2\text{-}CH_3]^-$.

Table 3.9 ^{119}Sn-NMR data (δ, ppm) and ^{119}Sn Mössbauer parameters (mm s^{-1}) for the triphenyltin(IV) complexes **1-5**

Complex[a]	^{119}Sn-NMR data[b]	^{119}Sn Mössbauer data[c]				
		δ	Δ	ρ =Δ / δ	Γ_1	Γ_2
$Ph_3SnL^1H.OH_2$ (**1**)	- 109.7	1.24	3.00	2.42	0.90	0.92
Ph_3SnL^2H (**2**)	- 109.8	1.27	3.05	2.40	0.85	0.91
Ph_3SnL^3H (**3**)	- 109.7	1.26	2.97	2.36	0.88	0.87
Ph_3SnL^4H (**4**)	- 109.8	1.25	2.98	2.38	0.84	0.80
Ph_3SnL^5H (**5**)	-108.0	1.30	3.30	2.53	0.84	0.95

[a] Complex numbers are in parentheses. [b] In $CDCl_3$ solution.
[c] Parameters: δ, isomer shifts; Δ, quadrupole splitting; Γ_1 and Γ_2: line widths.

3.3.2.3 ^{119}Sn Mössbauer data

The ^{119}Sn Mössbauer results from the triphenyltin(IV) complexes are listed in Table 3.9. The ratio of the quadrupole splitting (Δ) value to isomer shift (δ) value ($\rho = \Delta/\delta$) can be used to distinguish between the different coordination states of the central tin atom [43]. Tin compounds which are four coordinate have ρ values less than 1.8 while ρ values larger than 2.1 would indicate compounds with greater than four coordination. All the complexes have similar δ, Δ parameters and ρ values greater than 2.1 suggesting that the complexes are isostructural with a coordination number greater than four. Furthermore, the triphenyltin(IV) complexes exhibited Δ values of ~3.00 mm s^{-1} which correspond with a trigonal bipyramidal geometry around the tin atom [44,52,53] and is in agreement with structures determined from X-ray crystallography (see

Section 3.3.2.5) after ignoring the long Sn···O contact, which has no effect on the trigonal bipyramidal geometry.

3.3.2.4 Electrospray mass spectrometry

The ESI mass spectra of the triphenyltin(IV) complexes (**1-5**; see Section 3.3.2) are very complex due to the formation of various unexpected adducts and the presence of a wide range of fragment ions in the first-order mass spectra, which complicates the interpretation of the spectra [54-58]. The assignments of the individual ions are therefore based on the combination of measurements of positive-ion, negative-ion and multistage tandem mass spectrometric (MS^n) experiments, which provide the most comprehensive and reliable results for the structure confirmation [45-48]. The typical ions in the first-order positive-ion ESI mass spectra are the sodium and potassium ion adducts with the molecule, which is used for the determination of the molecular weights (MW) of the organotin(IV) compounds **1-5**. Moreover, the dimeric ions $[2*M+K]^+$ and $[2*M+Na]^+$ with significantly lower relative abundances are present as well. The presence of these dimeric ions, together with their tandem mass spectra, is a useful tool for the confirmation of the MW. The formation of other unusual adducts is observed, such as adducts with the triphenyltin fragment ion (e.g., $[M\text{-benzene}+SnPh_3]^+$), water or Ph_2SnCl_2. The correctness of these assignments was supported by comparison of the theoretical and experimental isotopic distributions and tandem mass spectrometric experiments. The formation of similar adducts has already been reported in the literature [54]. The base peaks of the first-order negative ESI mass spectra are the $[ligand]^-$ ions (i.e., $[M\text{-}SnPh_3]^-$ written in the different notation), which are formed by cleavage of the most labile bond between the tin and oxygen atoms. The deprotonated molecule $[M\text{-}H]^-$ is also observed in the spectra and confirm the MS assignment. The characteristic neutral losses in the tandem mass spectra, such as CO, CO_2, acetic acid, benzene, $HOSnPh_3$, etc., show the presence of these functionalities in the structures.

3.3.2.5 X-ray crystallography

Crystals of the triphenyltin(IV) complexes suitable for an X-ray crystal-structure determination were obtained from chloroform ($[Ph_3SnL^2H]_n$ (**2**)), benzene/hexane ($[Ph_3SnL^3H]_n$ (**3**)) and benzene ($[Ph_3SnL^1H]_2$ (**5**)) by slow evaporation of the solvent at room temperature. The crystal structures of three of the triphenyltin(IV) complexes **2**, **3** and **5** [20] have been determined. The data collection and refinement parameters are given in Table 3.10.

Table 3.10 Crystallographic data and structure refinement parameters for the triphenyltin(IV) complexes **2**, **3** and **5**

	2	**3**	**5**
Empirical formula	$C_{39}H_{31}N_3O_3Sn$	$C_{38}H_{28}BrN_3O_3Sn$	$C_{78}H_{62}N_6O_8Sn_2$
Formula weight	708.29	773.16	1448.58
Crystal size (mm)	0.10 × 0.12 × 0.35	0.05 × 0.22 × 0.27	0.05 × 0.20 × 0.25
Crystal shape	Tablet	Plate	Plate
Temperature (K)	273(1)	160(1)	160(1)
Crystal system	Monoclinic	Monoclinic	Triclinic
Space group	$P2_1/c$	$P2_1/c$	$P\bar{1}$
a (Å)	9.5782(1)	9.9665(1)	9.3588(3)
b (Å)	15.7608(2)	15.5199(2)	11.1570(3)
c (Å)	22.0905(3)	21.4797(2)	16.0416(5)
α (°)	90	90	79.173(2)
β (°)	98.8889(7)	101.2908(8)	80.388(1)
γ (°)	90	90	77.642(2)
V (Å^3)	3294.73(7)	3258.16(6)	1592.98(8)
Z	4	4	1
D_x (g cm^{-3})	1.428	1.576	1.510
μ (mm^{-1})	0.817	2.056	0.849
Transmission factors (min, max)	0.820, 0.932	0.581, 0.912	0.835, 0.980
$2\theta_{max}$ (°)	55	60	60
Reflections measured	72870	78938	41734
Independent reflections (R_{int})	7563 (0.068)	9509 (0.094)	9281 (0.079)
Reflections with $I > 2\sigma(I)$	5519	7292	6941
Number of parameters	420	419	429
$R(F)$ ($I > 2\sigma(I)$ reflns)	0.036	0.038	0.043
$wR(F^2)$ (all data)	0.093	0.094	0.091
GOF(F^2)	1.05	1.04	1.03
max, min $\Delta\rho$ (e/Å^3)	0.95, -0.65	0.90, -1.31	0.54, -1.15

The crystal structures of all the three complexes are illustrated in Figs. 3.9 & 3.10 (for **2**), 3.11 & 3.12 (for **3**) and 3.13 (for **5**) (see Scheme 3.2 for line diagrams).

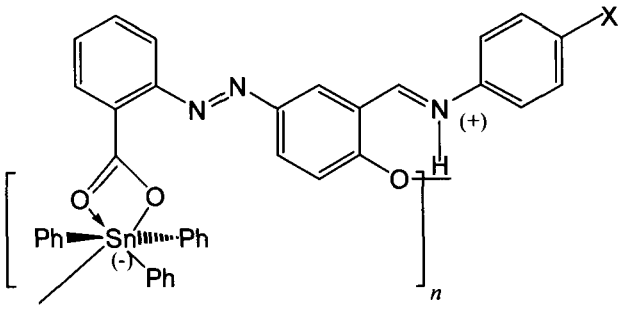

(X = -CH_3 (**2**), -Br (**3**))

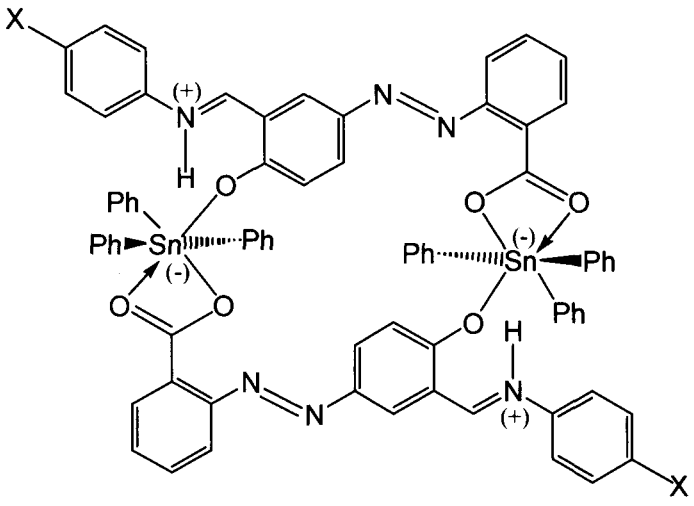

(X = -OCH_3 (**5**))

Scheme 3.2 A line diagram showing polymeric- $[Ph_3SnL^2H]_n$ (**2**), $[Ph_3SnL^3H]_n$ (**3**) and dimeric- $[Ph_3SnL^5H]_2$ (**5**) structures of complexes

The crystal structures of triphenyltin(IV) complexes **2** and **3** are isostructural and the principal geometric parameters do not differ significantly (Table 3.11). Both compounds exhibit the same polymeric *trans*-R_3SnO_2 structural motif, in which adjacent $SnPh_3$ moieties are bridged by a single carboxylate ligand *via* one carboxylate O-atom and the phenoxide O-atom, with the pattern then continuing indefinitely, as illustrated in Figs. 3.11 and 3.12. Each

Sn-atom has a slightly distorted trigonal bipyramidal coordination geometry with equatorial phenyl groups and the carboxylate and phenoxide O atoms from two different carboxylate ligands occupying axial positions. A polymeric structure with a similar mode of coordination and geometry about the Sn-atom was observed in $Ph_3Sn(2\text{-}OHC_6H_4C(H)=NCH_2COO)_n$ [52]. The carbonyl O-atom of the carboxylate group of the carboxylate ligand in **2** and **3** also coordinates very weakly to the Sn-atom *via* long Sn···O(2) bonds of 3.071(2) and 3.092(2) Å, respectively. Although these long Sn···O(2) distances are well inside the sum of the van der Waals radii of the Sn and O atoms (*ca.* 3.6 Å), there does not appear to be any major distortion of the trigonal bipyramidal Sn-coordination geometry as a result of this contact. Similar additional weak Sn···O coordination was also observed in the structures of related polymeric $[^nBu_3SnLH]_n$ derivatives [49,51].

Table 3.11 Selected bond lengths (Å) and angles (°) for **2**, **3** and **5** [a]

	2	**3**	**5**
Sn-O(1)	2.155(2)	2.163(2)	2.161(2)
Sn-O(3)^i	2.380(2)	2.370(2)	2.367(2)
Sn···O(2)	3.071(2)	3.092(2)	3.253(2)
Sn-C(22)	2.130(3)	2.136(3)	2.133(3)
Sn-C(28)	2.141(3)	2.138(3)	2.145(3)
Sn-C(34)	2.142(3)	2.144(3)	2.141(3)
O(1)-Sn-O(3)^i	170.70(7)	172.71(7)	173.11(6)
O(1)-Sn-C(22)	90.38(9)	89.42(8)	100.36(8)
O(1)-Sn-C(28)	89.17(9)	89.26(8)	95.38(9)
O(1)-Sn-C(34)	97.25(9)	96.38(8)	83.01(8)
O(3)^i-Sn-C(22)	86.42(9)	89.74(8)	83.98(8)
O(3)^i-Sn-C(28)	84.74(8)	84.75(8)	87.23(8)
O(3)^i-Sn-C(34)	91.31(9)	89.50(8)	90.31(8)
C(22)-Sn-C(28)	118.8(1)	118.2(1)	117.5(1)
C(22)-Sn-C(34)	132.9(1)	132.9(1)	115.1(1)
C(28)-Sn-C(34)	107.8(1)	108.6(1)	126.7(1)

[a] Atom labels with superscript "i" refer to atoms from (i) the next symmetrically-related ligand in the polymeric chain for **2** and **3** (Symmetry code: $1-x, \frac{1}{2}+y, \frac{1}{2}-z$) and (ii) the centrosymmetrically related ligand in the dinuclear moiety for **5** (Symmetry code: $-x, 1-y, 1-z$)

Although the same slightly distorted trigonal bipyramidal *trans*-R_3SnO_2 structural motif is found in complex **5**, the polymeric structures found for **2** and **3** are not repeated in the structure of **5**. Instead, the structure of **5** consists of discrete cyclic centrosymmetric dimers with two Ph_3Sn entities being bridged by two carboxylate anions through their carboxylate and phenoxide O-atoms (Fig. 3.13). Despite the dimerization instead of polymerization, the coordination geometry about the Sn-atom is virtually the same as that found for complexes **2** and **3** (Table 3.11), including the presence of the additional weak Sn···O(2) interaction of 3.253(2). The tin atom coordination geometry found for complexes **2**, **3** and **5** is in good agreement with that inferred from ^{119m}Sn Mössbauer spectroscopy (see Section 3.3.2).

The bridging of the Sn-atoms *via* one carboxylate and the phenoxide O-atoms of the carboxylate ligand in the structures of complexes **2**, **3** and **5** is in stark contrast to the mode present in the structures of the related polymeric $[^nBu_3SnLH]_n$ derivatives [49,51], where both carboxylate O-atoms are involved in the bridge and the phenolic O-atom is non-coordinating. As the LH ligands are closely related in all of these structures, the change in ligand coordination mode must be influenced by the steric influence of the core R_3Sn moiety. The flexible and less bulky Bu_3Sn moieties allow coordination by both carboxylate O-atoms of the carboxylate ligand, so that there is only a short O-C-O spacer between adjacent Sn-atoms. In such arrangements, known as the type **II** polymeric motif for R_3SnO_2CR' compounds [38], the Sn···Sn distance has been found to be in the range of 5.1-5.6 Å [49,59]. The more bulky arrangement caused by the phenyl groups about the Ph_3Sn core does not allow sufficient room for adjacent Sn-atoms to be separated by only an O-C-O spacer, so the much larger 11 atom spacer offered by the use of the phenoxide O-atom as the second coordinating atom of the ligand in complexes **2**, **3** and **5** is preferred. The coordination mode observed in complexes **2**, **3** and **5** results in much larger Sn···Sn distances of 8.2725(3), 8.0508(3) and 7.9219(4) Å, respectively. These results suggest that the preferred coordination mode of 2-{(*E*)-4-hydroxy-3-[(*E*)-4-(aryl)imino-methyl]phenyldiazenyl}benzoic acids ($L^{2\text{-}5}HH'$) and related ligands is *via* both carboxylate O-atoms when steric conditions permit.

The carboxylate ligand in complexes **2**, **3** and **5** is in a zwitterionic form similar to that found for the structure of L^2HH' [20] (see Chapter 2 for X-ray results), as the H-atom was clearly located and refined to a position close to the imine N-atom, rather than being near to the phenolic O-atom. The N(3)-H and H···O(3) distances are in the range 0.77-0.83 Å and 1.92-1.95 Å and show that the imine N-H group forms an intramolecular hydrogen bond with the phenoxide O(3) atom. The zwitterionic nature of the ligand in these triphenyltin(IV) complexes is in contrast to

the arrangement found in the tri-n-butyltin(IV) analogues where the phenolic H-atom remains associated with the phenolic O-atom [49,51]. The preference for the formation of the zwitterionic form of the ligand in complexes **2**, **3** and **5** may be a result of the coordination of the phenoxide O-atom to the Sn-atom, whereas the phenolic O-atom is not involved in coordination in the tri-n-butyltin(IV) analogues. Nonetheless, zwitterionic forms are quite commonly encountered in similar systems [52,60-62].

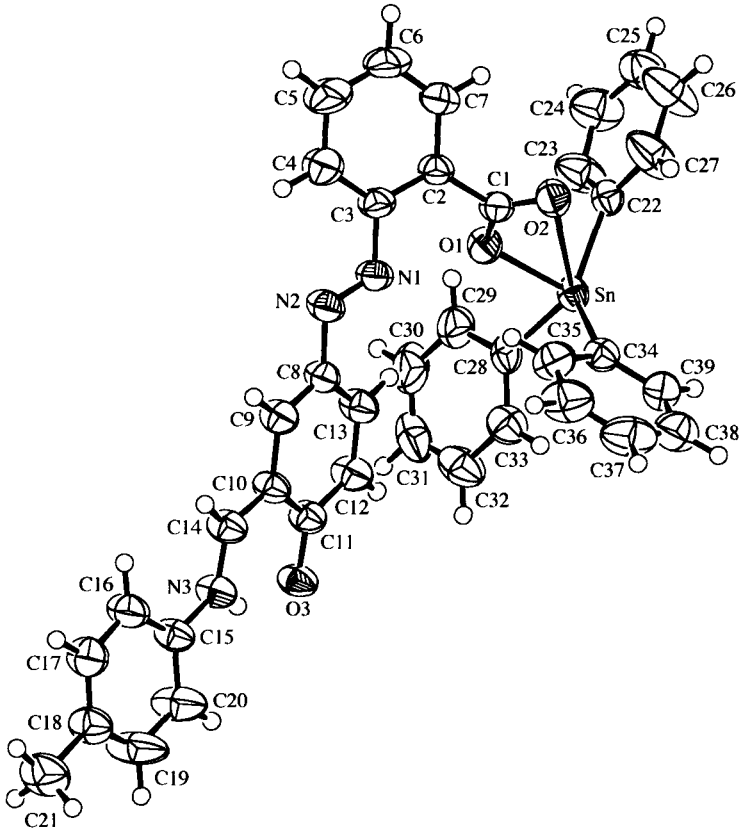

Fig. 3.9 The asymmetric unit of $[Ph_3SnL^2H]_n$ **(2)** showing the atom-labelling scheme (50% probability ellipsoids).

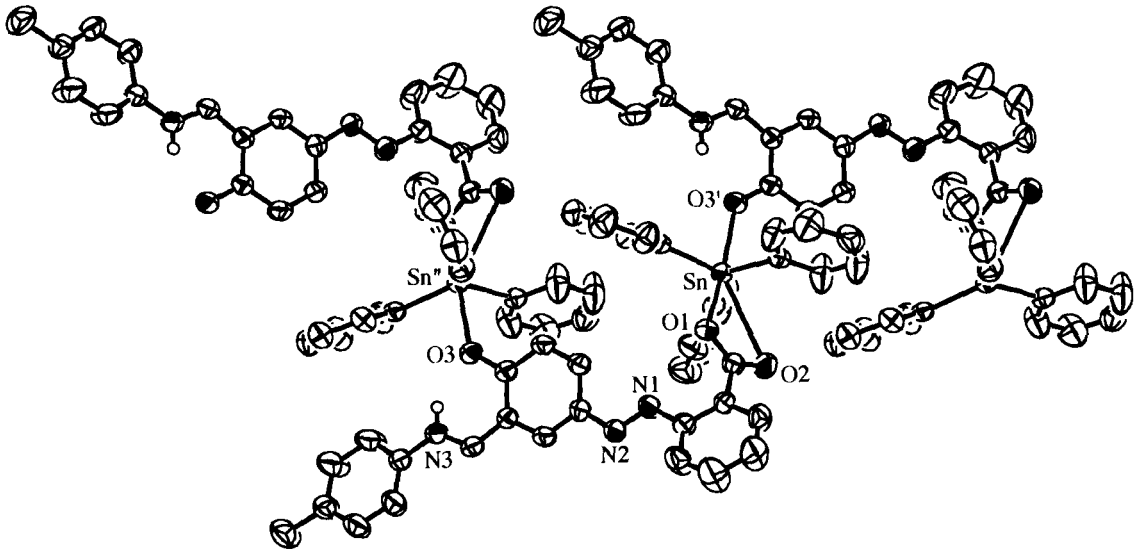

Fig. 3.10 A three-unit segment of the polymeric $[Ph_3SnL^2H]_n$ chain in **2** (50% probability ellipsoids).

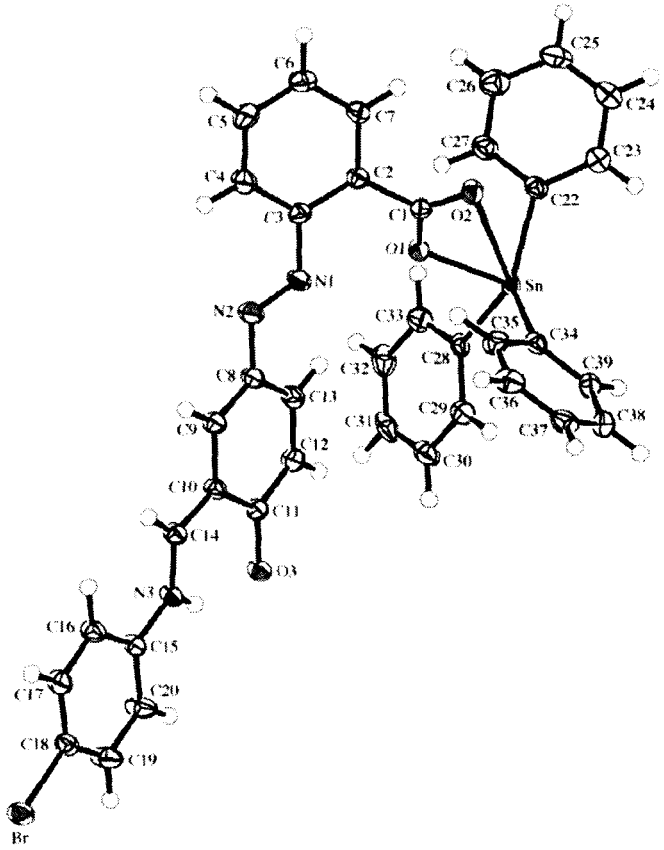

Fig. 3.11 The asymmetric unit of $[Ph_3SnL^3H]_n$ (**3**) showing the atom-labelling scheme (50% probability ellipsoids).

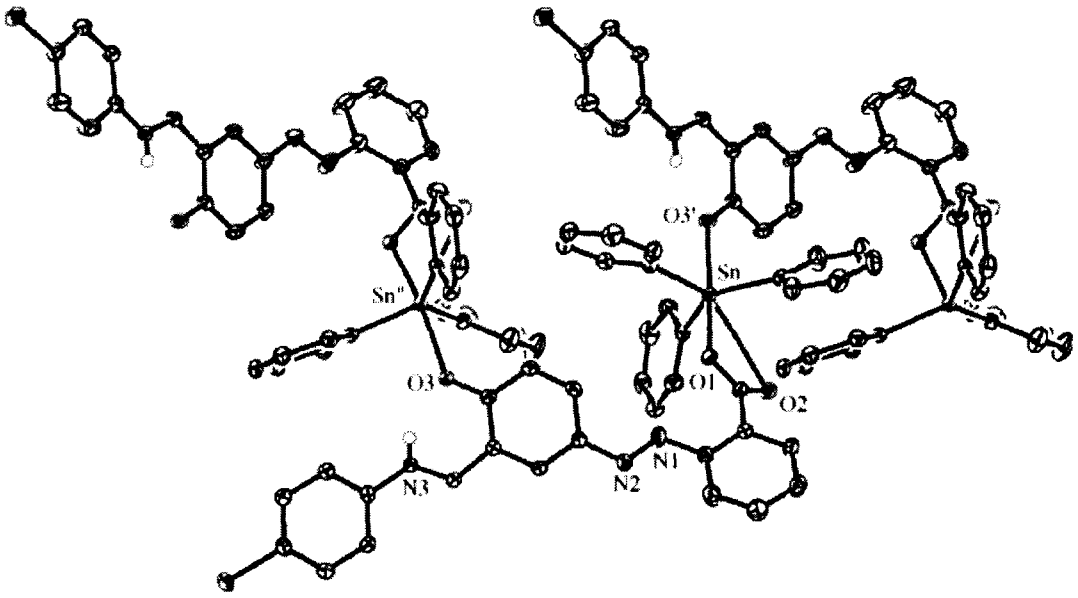

Fig. 3.12 A three-unit segment of the polymeric $[Ph_3SnL^3H]_n$ chain in **3** (50% probability ellipsoids).

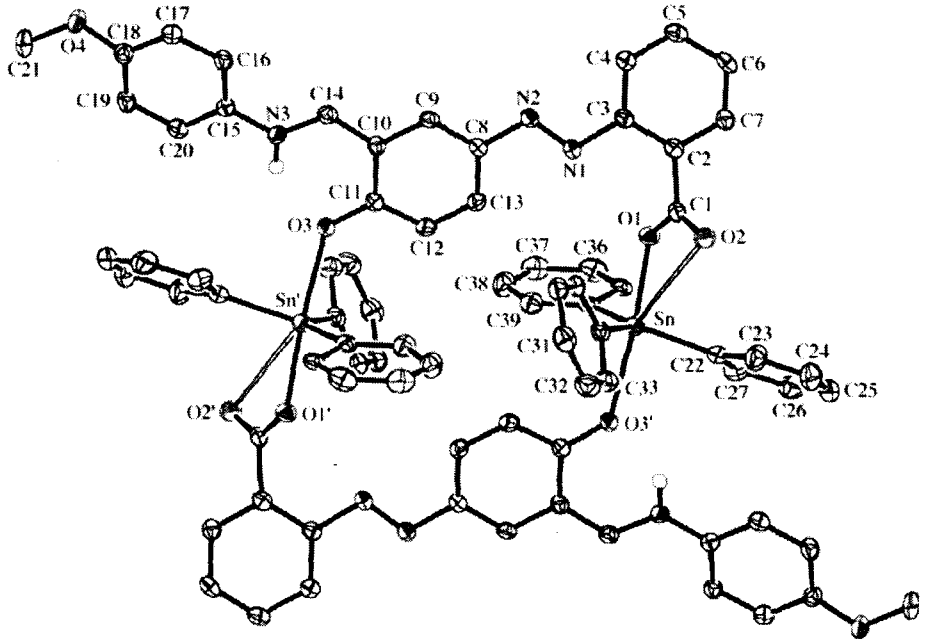

Fig. 3.13 The cyclic dinuclear moiety of $[Ph_3SnL^5H]_2$ (**5**) with the atom-labelling scheme (50% probability ellipsoids).

3.3.3 Tribenzyltin(IV) complexes of L^1HH'-L^5HH' ($Bz_3SnL^{1-5}H$)

The tribenzyltin(IV) complexes of 2-[(*E*)-2-(3-formyl-4-hydroxyphenyl)-1-diazenyl]benzoic acid (L^1HH') and 2-{(*E*)-4-hydroxy-3-[(*E*)-4-(aryl)imino-methyl]phenyldiazenyl}benzoic acids ($L^{2-5}HH'$) have been characterized by IR, ^1H, ^{13}C, ^{119}Sn NMR and ^{119m}Sn Mössbauer spectroscopic techniques. The crystal structures of two compounds, *viz.*, $Bz_3SnL^4H.OH_2$ (**4**) and $Bz_3SnL^5H.OH_2$ (**5**) are reported.

3.3.3.1 Infrared data

The diagnostically important infrared absorption frequencies for the carboxylate antisymmetric [ν_{asym}(OCO)] stretching vibration of the complexes are given below. The assignment of the symmetric [ν_{sym}(OCO)] stretching vibration band could not be made owing to the complex pattern of the spectra. The assignment of the band is based on comparison with the spectra of the free ligands. The antisymmetric [ν_{asym}(OCO)] stretching vibrations for the uncomplexed ligands have been detected at 1733 cm^{-1} in L^1HH' [33] and around the 1725 cm^{-1} region for $L^{2-5}HH'$ [49]. In the complexes, the carbonyl stretching frequencies are found to be shifted to lower wavenumber, which is ascribed to carboxylate coordination in accordance with earlier reports [20,49,36,37].

3.3.3.2 ^1H, ^{13}C and ^{119}Sn NMR data

The ^1H- and ^{13}C- NMR data of L^1HH' and $L^{2-5}HH'$ have been reported earlier [49,33] and the conclusions drawn from the ligand assignments were then subsequently extrapolated to the complexes owing to the data similarity for at least a few signals. The ^1H-NMR integration values were completely consistent with the formulation of the products. Individual assignments of the ^1H- and ^{13}C- signals of the tribenzyltin(IV) moiety and most parts of the ligand skeleton could not be made owing to serious signal overlap resulting in complex patterns. The ^{119}Sn-NMR chemical shifts of the tribenzyltin(IV) complexes (**2-5**) in $CDCl_3$ solution are listed in Table 3.12. The complexes exhibit a single sharp resonance at around -10.0 ppm, suggesting that the complexes are isostructural in solution. The ^{119}Sn-NMR resonances fall within the range from +55.0 to -25.0 ppm, which is usually indicative of four-coordinate tribenzyltin(IV) species in solution [63]. This indicates that the five-coordinate structure of the solid (see X-ray discussion, *vide infra*) breaks up in solution [64], presumably by loss of the water ligand.

The basic ligand frame-work is shown in Figs. 2.1- 2.2 along with the abbreviations and numbering schemes for spectroscopic analyses. The detailed spectral features for complexes **1-5** are given below:

3.3.3.2.1 $Bz_3SnL^1H.OH_2$ (1)

IR (cm^{-1}): 1659 $\nu(OCO)_{asym.}$ ^{1}H-NMR ($CDCl_3$ / 400.13 MHz); δ_H: 11.3 [brs, 1H, OH, D_2O exchangeable], 9.78 [s, 1H, C(H)=O], 2.68 [s, 6H, CH_2: Bz_3Sn], 6.72-7.60 [complex multiplets, 22H, remaining ligand and Bz_3Sn protons], ppm. ^{13}C-NMR ($CDCl_3$ / 100.62 MHz); δ_C: 196.5 [C(H)=O], 174.9 [CO_2], not detected [C-OH], 24.2 [CH_2: Bz_3Sn], 116.3-161.2 [complex nature of the remaining ligand and Bz_3Sn carbon signals which could not be identified with certainty owing to poor signal to noise ratio], ppm.

3.3.3.2.2 $Bz_3SnL^2H.OH_2$ (2)

IR (cm^{-1}): 1619 ν $(OCO)_{asym.}$ ^{1}H-NMR ($CDCl_3$ / 400.13 MHz); δ_H: 13.1 [brs, 1H, OH, D_2O exchangeable], 8.45 [s, 1H, C(H)=N], 2.69 [s, 6H, CH_2: Bz_3Sn], 2.42 [s, 3H, CH_3], 6.70-8.10 [26 H, remaining ligand and Bz_3Sn protons], ppm. ^{13}C-NMR ($CDCl_3$ / 100.62 MHz); δ_C: 174.9 [CO_2], 164.5 [C-OH], 160.8 [C(H)=N], 24.3 [CH_2: Bz_3Sn], 20.9 [CH_3], 151.9, 145.7, 144.9, 138.6, 137.3, 131.3, 129.9, 129.1, 128.6, 128.3, 127.8, 127.2, 124.5, 120.9, 118.9, 118.1, 117.8 [remaining ligand and Bz_3Sn carbon signals], ppm.

3.3.3.2.3 $Bz_3SnL^3H.OH_2$ (3)

IR (cm^{-1}): 1619 ν $(OCO)_{asym.}$ ^{1}H-NMR ($CDCl_3$ / 400.13 MHz); δ_H: 13.5 [brs, 1H, OH, D_2O exchangeable], 8.43 [s, 1H, C(H)=N], 2.63 [s, 6H, CH_2: Bz_3Sn], 6.70-7.99 [26 H, remaining ligand and Bz_3Sn protons], ppm. ^{13}C-NMR ($CDCl_3$ / 100.62 MHz); δ_C173.4 [CO_2], 164.1 [C-OH], 162.3 [C(H)=N], 24.3 [CH_2: Bz_3Sn], 151.9, 146.6, 145.8, 138.5, 132.5, 131.4, 129.9, 129.5, 129.3, 128.8, 127.9, 127.0, 124.6, 122.8, 120.8, 118.8, 118.2, 117.6 [remaining ligand and Bz_3Sn carbon signals], ppm.

3.3.3.2.4 $Bz_3SnL^4H.OH_2$ (4)

IR (cm^{-1}): 1617 ν $(OCO)_{asym.}$ ^{1}H-NMR ($CDCl_3$ / 400.13 MHz); δ_H: 13.6 [brs, 1H, OH, D_2O exchangeable], 8.49 [s, 1H, C(H)=N], 2.69 [s, 6H, CH_2: Bz_3Sn], 6.70-8.05 [26 H, remaining ligand and Bz_3Sn protons], ppm. ^{13}C-NMR ($CDCl_3$ / 100.62 MHz); δ_C: 173.2 [CO_2], 163.9 [C-OH], 162.2 [C(H)=N], 24.3 [CH_2: Bz_3Sn], 151.7, 146.1, 145.8, 139.8, 138.4, 132.8, 131.2, 129.9,

129.4, 129.2, 128.6, 127.8, 126.8, 124.5, 122.2, 118.7, 117.9, 117.5 [remaining ligand and Bz_3Sn carbon signals], ppm.

3.3.3.2.5 $Bz_3SnL^5H.OH_2$ (5)

IR (cm^{-1}): 1617 ν $(OCO)_{asym}$. ^{1}H-NMR ($CDCl_3$ / 400.13 MHz); δ_H: 14.1 [brs, 1H, OH, D_2O exchangeable)] 8.53 [s, 1H, C(H)=N], 3.84 [s, 3H, OCH_3], 2.69 [s, 6H, CH_2: Bz_3Sn], 6.70-8.03 [26 H, remaining ligand and Bz_3Sn protons], ppm. ^{13}C-NMR ($CDCl_3$ / 100.62 MHz); δ_C: 173.2 [CO_2], 164.3 [C-OH], 159.5 [C(H)=N], 55.5 [OCH_3], 24.3 [CH_2: Bz_3Sn], 151.9, 145.8, 140.5, 138.6, 131.3, 130.3, 129.9, 129.2, 128.6, 128.4, 126.8, 124.5, 122.3, 119.1, 117.9, 117.7, 114.7 [remaining ligand and Bz_3Sn carbon signals], ppm.

Table 3.12 ^{119}Sn-NMR data (δ, ppm) and ^{119}Sn Mössbauer parameters (mm s^{-1}) for the tribenzyltin(IV) complexes **1-5**

Complex[a]	^{119}Sn-NMR data[b]	^{119}Sn Mössbauer data[d]		
		δ	Δ	ρ=Δ / δ
$Bz_3SnL^1H.OH_2$ (1)	c	1.04	2.51	2.4
$Bz_3SnL^2H.OH_2$ (2)	- 10.5	1.39	3.07	2.2
$Bz_3SnL^3H.OH_2$ (3)	- 9.82	1.27	2.76	2.2
$Bz_3SnL^4H.OH_2$ (4)	-10.2	1.14	2.99	2.6
$Bz_3SnL^5H.OH_2$ (5)	-10.48	1.39	3.13	2.3

[a] Complex numbers are in parentheses. [b] In $CDCl_3$ solution. [c] Not detected owing to poor solubility.
[d] Parameters: δ, isomer shifts; Δ, quadrupole splitting; Γ_1 and Γ_2: line widths.

3.3.3.3 ^{119}Sn Mössbauer data

The ^{119}Sn Mössbauer results from the tribenzyltin(IV) complexes are listed in Table 3.12. The ratio of the quadrupole splitting (Δ) value to the isomer shift (δ) value (ρ = Δ/δ) can be used to distinguish between the different coordination states of the central tin atom [43]. Tin compounds which are four coordinate have ρ values less than 1.8 while ρ values larger than 2.1 would indicate compounds with greater than four coordination. Complexes **2-5** (slightly lower in the case of **1**) have similar δ, Δ parameters and the ρ values are greater than 2.1 suggesting that the complexes are isostructural with a coordination number greater than four. Trigonal bipyramidal triorganotin(IV) complexes with organic groups in the equatorial plane [65] have

been reported to have Δ values between 3.00 – 4.00 mm s^{-1}. This value has also been found to change as a function of the axial bond distances [65]. The tribenzyltin(IV) complexes in the present investigation exhibited Δ values of ~3.00 mm s^{-1} which correspond with a trigonal bipyramidal geometry around the tin atom with equatorial benzyl groups [44,64,66,67] and is in agreement with the structures determined by X-ray crystallography (see below).

3.3.3.4 X-ray crystallography

Crystals of the tribenzyltin(IV) complexes suitable for an X-ray crystal-structure determination were obtained from a toluene/hexane ($Bz_3SnL^4H.OH_2$ (**2**)) and benzene/hexane ($Bz_3SnL^5H.OH_2$ (**5**)) by slow evaporation of the solvent at room temperature. The crystal structures of two of the tribenzyltin(IV) complexes **4** and **5** [68] have been determined. The data collection and refinement parameters are given in Table 3.13.

The crystal structures of the complexes **4** and **5** are illustrated in Figs. 3.14 and 3.15 while their molecular packing showing the intra- and inter-molecular hydrogen bonding are shown in Figs. 3.16 and 3.17, respectively (see Scheme 3.3 for line diagram).

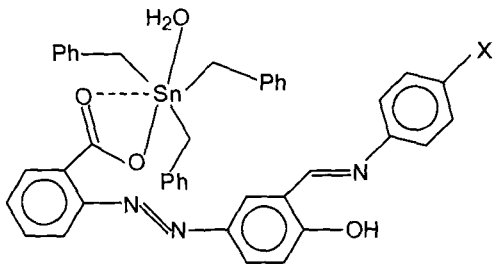

(X = -Cl (**4**), -OCH_3 (**5**))

Scheme 3.3 Structures of the complexes **4** and **5**

The crystal structures of complexes **4** and **5** are very similar and the principal geometric parameters do not differ significantly (Table 3.14). In contrast to the polymeric tri-n-butyltin(IV) [49-51] and polymeric and dimeric triphenyltin(IV) [20] analogues (Schemes 3.1 and 3.2), both of the tribenzyltin(IV) complexes, **4** and **5**, exhibit the same monomeric *trans*-R_3SnO_2 structural motif, as illustrated in Figs. 3.14 and 3.15. The structures are also shown in Scheme 3.3 for clarity. The Sn atom has a slightly distorted trigonal bipyramidal coordination geometry with equatorial benzyl groups and the axial positions occupied by an O atom from the

carboxylate ligand and the O atom from the water ligand. A monomeric structure with a similar mode of coordination and geometry about the Sn atom was observed in the triphenyltin(IV)

Table 3.13 Crystallographic data and structure refinement parameters for the tribenzyltin(IV) complexes **4** and **5**

	4	**5**
Empirical formula	$C_{41}H_{36}ClN_3O_4Sn$	$C_{42}H_{39}N_3O_5Sn$
Formula weight	788.80	784.39
Crystal size (mm)	0.10 x 0.17 x 0.32	0.12 x 0.17 x 0.28
Crystal shape	Tablet	Prism
Temperature (K)	160(1)	160(1)
Crystal system	Monoclinic	Monoclinic
Space group	$P2_1/n$	$P2_1/n$
a (Å)	12.5388(1)	13.1825(2)
b (Å)	22.6661(2)	21.9417(4)
c (Å)	14.1787(2)	14.3594(2)
β (°)	114.8089(5)	115.9489(8)
V (Å^3)	3657.78(7)	3734.7(1)
Z	4	4
D_x (g cm^{-3})	1.432	1.395
μ (mm^{-1})	0.817	0.732
Transmission factors (min, max)	0.804; 0.925	0.759;0.916
$2\theta_{max}$ (°)	60	55
Reflections measured	88212	82555
Independent reflections (R_{int})	10662 (0.068)	8548 (0.091)
Reflections with $I > 2\sigma(I)$	8172	6020
Number of parameters	463	474
$R(F)$ ($I > 2\sigma(I)$ reflns)	0.037	0.039
$wR(F^2)$ (all data)	0.090	0.091
GOF(F^2)	1.05	1.05
max, min $\Delta\rho$ (e/Å^3)	1.61, -0.92	1.52, 0.67

complex of the pre-ligand i.e. $Ph_3SnL^1H.OH_2$ [33]. The carbonyl O atom of the carboxylate ligand in **4** and **5** also coordinates very weakly to the Sn atom with long Sn···O(2) distances of 3.056(2) and 3.008(2) Å, respectively. Although the Sn···O(2) distances are well inside the sum of the van der Waals radii of the Sn and O atoms (*ca.* 3.6 Å), there does not appear to be any major distortion of the principal trigonal bipyramidal Sn-coordination geometry as a result of

Table 3.14 Selected bond lengths (Å) and angles (°) for **4** and **5**

	4	**5**
Sn-O(1)	2.150(1)	2.164(2)
Sn-O(4)	2.399(2)	2.396(2)
Sn···O(2)	3.056(2)	3.008(2)
Sn-C(21)	2.150(2)	2.151(3)
Sn-C(28)	2.148(2)	2.147(3)
Sn-C(35)	2.143(2)	2.139(3)
O(1)-C(1)	1.278(3)	1.288(3)
O(2)-C(1)	1.238(3)	1.234(3)
N(1)-N(2)	1.252(3)	1.254(3)
N(1)-C(3)	1.425(3)	1.421(4)
N(2)-C(8)	1.429(3)	1.429(4)
O(1)-Sn-O(4)	173.58(6)	172.64(8)
O(1)-Sn-C(21)	89.12(8)	89.05(9)
O(1)-Sn-C(28)	96.40(8)	96.4(1)
O(1)-Sn-C(35)	99.12(7)	98.98(9)
O(4)-Sn-C(21)	85.22(8)	84.1(1)
O(4)-Sn-C(28)	83.66(8)	84.2(1)
O(4)-Sn-C(35)	86.13(7)	86.58(9)
C(21)-Sn-C(28)	118.19(9)	114.9(1)
C(21)-Sn-C(35)	116.35(9)	117.9(1)
C(28)-Sn-C(35)	123.18(9)	124.9(1)
Sn-O(1)-C(1)	116.4(1)	114.1(2)
N(2)-N(1)-C(3)	114.3(2)	115.3(2)
N(1)-N(2)-C(8)	113.2(2)	113.2(2)
O (1)-C(1)-O(2)	123.6(2)	123.5(2)
O (1)-C(1)-C(2)	117.0(2)	116.7(2)
O (2)-C(1)-C(2)	119.4(2)	119.8(2)

this contact. Similar additional weak Sn···O coordination was also observed in the structures of related polymeric $[R_3SnLH]_n$ (R = ^{n}Bu, Ph) derivatives [20,49-51]. The Sn atom coordination geometry found for complexes **4** and **5** is in good agreement with that inferred from ^{119m}Sn Mössbauer spectroscopy (vide supra).

In complexes **4** and **5**, the phenoxy H atom forms an intramolecular hydrogen bond with the imine N atom, thereby creating a loop with a graph set motif [69] of S(6). The H atoms of the water ligand form intermolecular hydrogen bonds with the phenoxy O atom of one neighbouring molecule and with the weakly coordinating carboxylate O atom of a different neighbouring molecule (Table 3.15).

Table 3.15 Hydrogen bonding geometry (Å, °) for **4**[a] and **5**[b]

D-H···A	D-H	H···A	D···A	D-H···A
O(3)-H(3)···N(3)	0.90(3) (0.95(5))	1.72(3) (1.69(5))	2.562(3) (2.572(4))	155 (3) (151(4))
O(4)-H(41)···O(3')	0.80(4) (0.79(3))	1.98(4) (1.89(3))	2.783(3) (2.678(3))	172 (4) (171(3))
O(4)-H(42)···O(2")	0.83(4) (0.84(4))	1.85(4) (1.97(4))	2.668(3) (2.779(3))	174 (3) (162(4))

Primed atoms refer to the molecule in the following symmetry related positions:

For **4**: ' $\frac{1}{2}-x, \frac{1}{2}+y, \frac{1}{2}-z$ and " $x-\frac{1}{2}, \frac{1}{2}-y, z-\frac{1}{2}$

For **5**: ' $x, \frac{1}{2}-y, z-\frac{1}{2}$ and " $1-x, \frac{1}{2}+y, \frac{1}{2}-z$

The H-bonding geometrical parameters for complex **5** are in parentheses.

The former interaction links the molecules into extended chains which run parallel to the [0 1 0] direction and can be described by a graph set motif of C(14). The latter interaction links the molecules into extended chains which can be described by a graph set motif of C(4) and which run parallel to the [1 0 1] direction in **4** and the [0 0 1] direction in **5**. Together, the intermolecular interactions link the molecules into two-dimensional networks. In the case of **4**, these networks lie parallel to the (1 0 -1) plane (Fig. 3.16), while in **5**, they lie parallel to the (1 0 0) plane (Fig. 3.17).

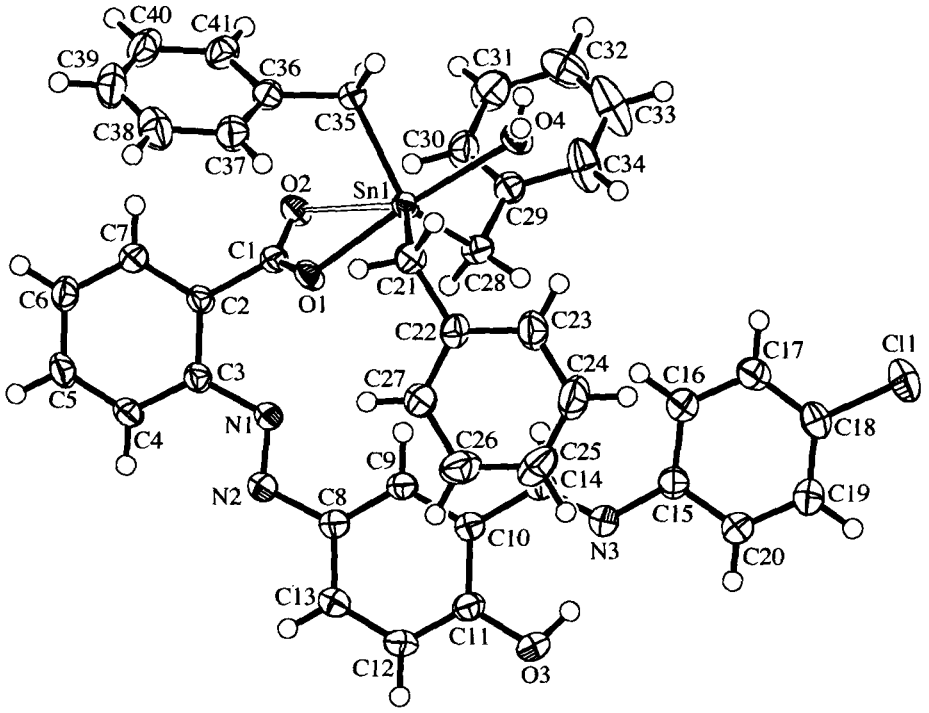

Fig. 3.14 The molecular structure of $Bz_3SnL^4H.OH_2$ (**4**) showing the atom-labelling scheme (50% probability ellipsoids).

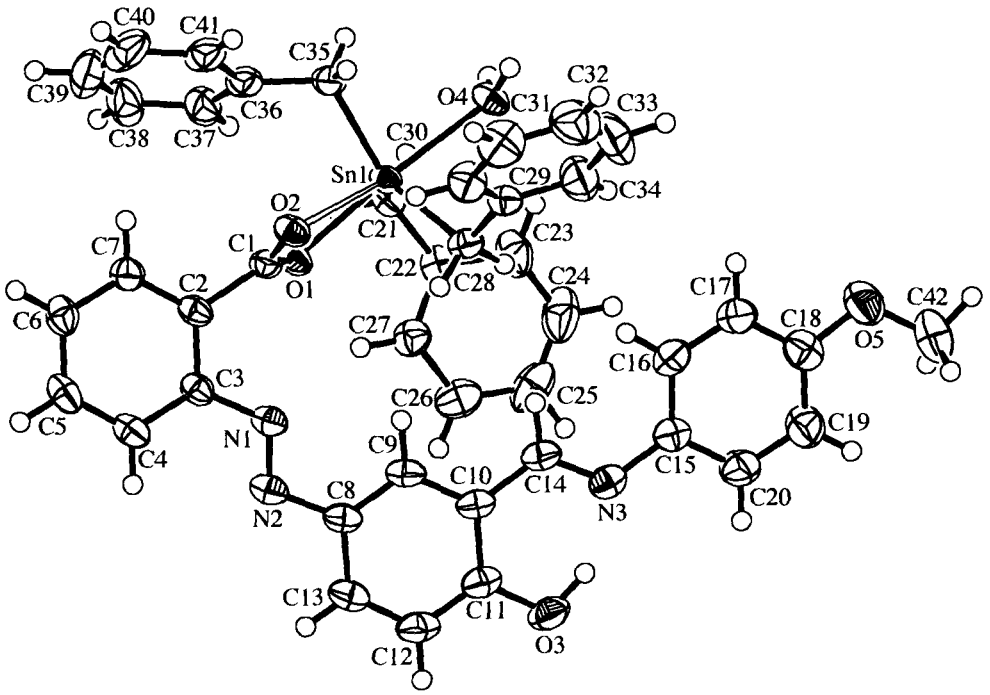

Fig. 3.15 The molecular structure of $Bz_3SnL^5H.OH_2$ (**5**) showing the atom-labelling scheme (50% probability ellipsoids).

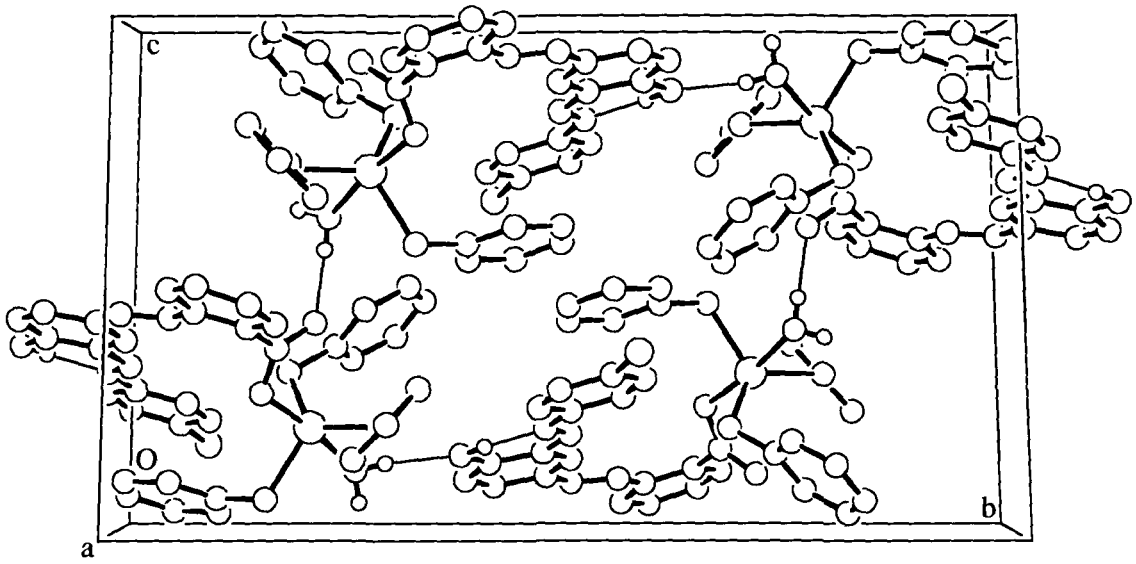

Fig. 3.16 The molecular packing of $Bz_3SnL^4H.OH_2$ **(4)** showing the intra- and inter-molecular hydrogen bonding

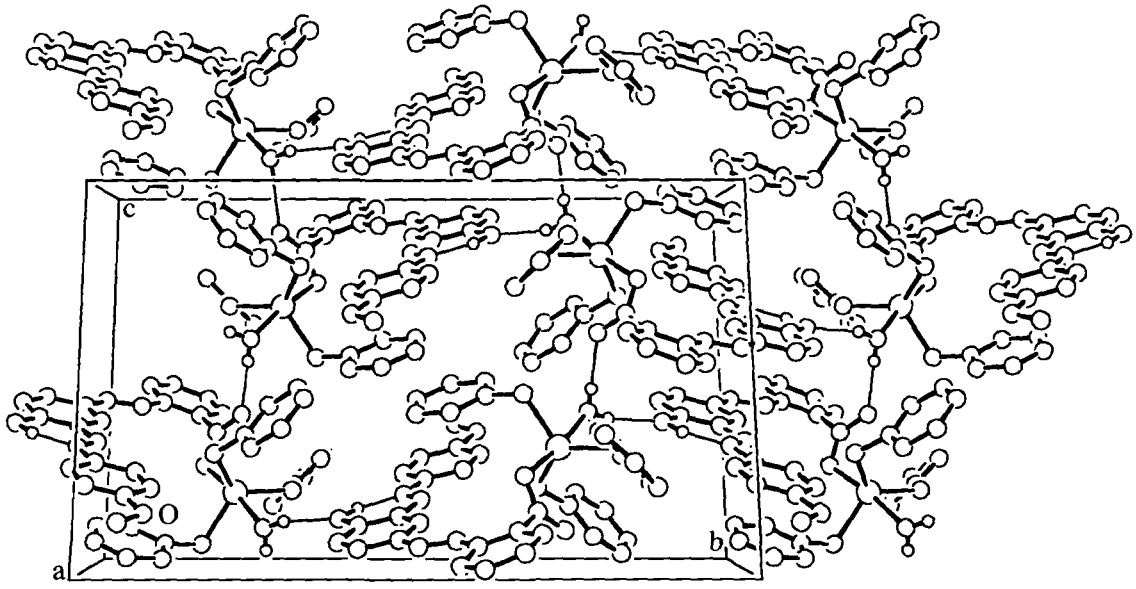

Fig. 3.17 The molecular packing of $Bz_3SnL^5H.OH_2$ **(5)** showing the intra- and inter-molecular hydrogen bonding

3.4 Experimental

3.4.1 Synthesis of ligands

The ligands *viz.*, 2-[(*E*)-2-(3-formyl-4-hydroxyphenyl)-1-diazenyl]benzoic acid (L^1HH') [33] and 2-{(*E*)-4-hydroxy-3-[(*E*)-4-(aryl)imino-methyl]phenyldiazenyl}benzoic acids ($L^{2-5}HH'$) [49] used for synthesizing triorganotin(IV) complexes are described in Chapter 2 (see section 2.6).

3.4.2 Synthesis of triorganotin(IV) complexes

The synthesis of triorganotin(IV) complexes, viz., tri-n-butyltin(IV), triphenyltin(IV) and tribenzyltin(IV) complexes are described in sequel along with the characterization data.

3.4.2.1 Synthesis of tri-n-butyltin(IV) complexes

Two typical methods are described below.

3.4.2.1.1 Synthesis of $^nBu_3SnL^1H$ (**1**)

The compound was synthesized by mixing L^1HH' (0.90 g, 3.33 mmol) and $(^nBu_3Sn)_2O$ (1.0 g, 1.67 mmol) in 50 ml of anhydrous toluene, in a 100 ml flask equipped with a Dean-Stark moisture trap and a water cooled condensor. The reaction mixture was refluxed for 7 h. The solvent was then distilled off to dryness and the residue was dried *in vacuo*. The solid mass was washed with hexane (2 x 5 ml) under cold conditions and was recrystallized from hexane to yield orange crystals of the desired product. Yield (0.74 g, 79 %). M. p.: 63-64 °C. Anal. Found: C, 55.76; H, 6.39; N, 5.20. Calc. for $C_{26}H_{36}N_2O_4Sn$: C, 55.84; H, 6.48; N, 5.00 %.

3.4.2.1.2 Synthesis of $^nBu_3SnL^4H$ (**4**)

$^nBu_3SnL^1H$ (0.79 g, 1.41 mmol) in absolute ethanol (30 ml) was added dropwise to a hot stirred ethanolic solution (20 ml) containing *p*-chloroaniline (0.18 g, 1.41 mmol). The reaction mixture was then refluxed using a Dean-Stark moisture trap and water cooled condenser for 3 h and filtered while hot. The filtrate was collected and the volatiles were removed using a rotary evaporator. The residue was dried *in vacuo*, washed with hexane (2 x 1 ml), extracted into chloroform and filtered. The crude product was obtained after evaporation and this was then recrystallized from chloroform-hexane mixture (1:1, v/v) to yield orange crystals of the desired product. Yield (0.83 g, 82.4 %). M. p.: 88-90 °C. Anal. Found: C, 57.40; H, 6.19; N, 6.20. Calc. for $C_{32}H_{40}ClN_3O_3Sn$: C, 57.43; H, 6.02; N, 6.27 %.

The other tri-n-butyltin complexes of ligands, *viz.*, L^2HH', L^3HH' and L^5HH' were prepared by reacting $^nBu_3SnL^1H$ and appropriate anilines by following analogous procedure. The characterization data of the complexes are given below.

3.4.2.1.3 $^nBu_3SnL^2H$ (2)

Yield: 80 %. M. p.: 89-91 °C. Anal. Found: C, 61.20; H, 6.75; N, 6.53. Calc. for $C_{33}H_{43}N_3O_3Sn$: C, 61.10; H, 6.68; N, 6.47 %.

3.4.2.1.4 $^nBu_3SnL^3H$ (3)

Yield: 78 %. M. p.: 86-88 °C. Anal. Found: C, 53.80; H, 5.60; N, 5.98. Calc. for $C_{32}H_{40}BrN_3O_3Sn$: C, 53.86; H, 5.65; N, 5.88 %.

3.4.2.1.5 $^nBu_3SnL^5H$ (5)

Yield: 93 %. M. p.: 84-86 °C. Anal. Found: C, 59.73; H, 6.49; N, 6.50. Calc. for $C_{33}H_{43}N_3O_4Sn$: C, 59.63; H, 6.52; N, 6.32 %.

3.4.2.2 Synthesis of triphenyltin(IV) complexes

A typical method is described below.

3.4.2.2.1 Synthesis of $Ph_3SnL^1H.OH_2$ (1)

This complex was prepared by reacting equimolar amounts of Ph_3SnOH and L^1HH'[33].

3.4.2.2.2 Synthesis of Ph_3SnL^2H (2)

Compound **2** was synthesized by reacting L^2HH' (0.73 g, 2.04 mmol) and Ph_3SnOH (0.75 g, 2.04 mmol) in 50 ml of anhydrous toluene in a 100 ml flask equipped with a Dean-Stark moisture trap and water-cooled condenser. The reaction mixture was refluxed for 9 h and filtered while hot. The filtrate was collected and the volatiles were removed using a rotary evaporator. The residue was dried *in vacuo*, washed with hexane (3 x 5 ml), extracted into chloroform and filtered. The crude product was obtained after evaporation and this was then recrystallized from chloroform to yield orange crystals of the desired product. Yield (0.50 g, 34.5%); M. p.: 138-40 °C. Anal. Found: C, 66.12; H, 4.45; N, 6.02. Calc. for $C_{39}H_{31}N_3O_3Sn$: C, 66.09; H, 4.40; N, 5.92%.

The other triphenyltin complexes (**3-5**) were prepared by reacting Ph_3SnOH with the appropriate ligand (L^3HH', L^4HH' and L^5HH') by following an analogous procedure. The characterization data of the complexes are given below.

3.4.2.2.3 Ph_3SnL^3H (**3**)

Red crystals of compound **3** were obtained from a benzene-hexane mixture (1:3 v/v). Yield: 37.3%; M. p.: 132-134 °C. Anal. Found: C, 59.10; H, 3.70; N, 5.40. Calc. for $C_{38}H_{28}BrN_3O_3Sn$: C, 58.99; H, 3.64; N, 5.42%.

3.4.2.2.4 Ph_3SnL^4H (**4**)

Orange crystals of compound **4** were obtained from a benzene-hexane mixture (1:3 v/v). Yield: 35.6%; M. p.: 146-148 °C. Anal. Found: C, 62.40; H, 3.90; N, 5.80. Calc. for $C_{38}H_{28}ClN_3O_3Sn$: C, 62.61; H, 3.87; N, 5.76%.

3.4.2.2.5 Ph_3SnL^4H (**5**)

Red-brown crystals of compound **5** were obtained from benzene. Yield: 38%; M. p.: 136-138 °C. Anal. Found: C, 64.60; H, 4.27; N, 5.80. Calc. for $C_{39}H_{31}N_3O_4Sn$: C, 64.67; H, 4.30; N, 5.80%.

3.4.2.3 Synthesis of tribenzyltin(IV) complexes

A typical method is described below.

3.4.2.3.1 Synthesis of $Bz_3SnL^1H.OH_2$ (**1**)

Compound **1** was synthesized by reacting L^1HH' (0.38 g, 1.40 mmol) and Bz_3SnOH (0.58 g, 1.41 mmol) in 50 ml of anhydrous toluene in a 100 ml flask equipped with a Dean-Stark moisture trap and water-cooled condenser. The reaction mixture was refluxed for 8 h and filtered while hot. The filtrate was collected and the volatiles were removed using a rotary evaporator. The residue was dried *in vacuo*, washed with hexane thoroughly, extracted into benzene and filtered. The crude product was obtained after evaporation and this was then recrystallized from benzene to yield dark-red crystals of the desired product. Yield (0.36 g, 39%); M. p.: 73-75 °C. Anal Found: C, 61.48; H, 4.53; N, 4.29%. Calc.for $C_{35}H_{32}N_2O_5Sn$: C: 61.85; H: 4.70, N: 4.12%.

The other tribenzyltin(IV) complexes (**2-5**) were prepared by reacting Bz_3SnOH with the

appropriate ligand (L^2HH'-L^5HH') following an analogous procedure. The characterization data of the complexes are given below.

3.4.2.3.2 $Bz_3SnL^2H.OH_2$ (**2**)

Orange-red crystals of compound **2** was obtained from a benzene-hexane mixture (1:3 v/v). Yield: 79%; M. p.: 96-98 °C. Anal Found: C, 65.42; H, 4.83; N, 5.49%. Calc. for $C_{42}H_{39}N_3O_4Sn$: C, 65.62; H, 5.11; N, 5.46 %.

3.4.2.3.3 $Bz_3SnL^3H.OH_2$ (**3**)

Red crystals of compound **3** were obtained from a benzene-hexane mixture (1:3 v/v). Yield: 64%; M. p.: 72-74 °C. Anal. Found: C, 60.19; H, 4.26; N, 5.18%. Calc.for $C_{41}H_{36}BrN_3O_4Sn$: C, 59.09; H, 4.35; N, 5.04%.

3.4.2.3.4 $Bz_3SnL^4H.OH_2$ (**4**)

Red crystals of compound **4** were obtained from a toluene-hexane mixture (1:3 v/v). Yield: 49%; M. p.: 71-73 °C. Anal. Found: C, 62.01; H, 4.49; N, 5.40%. Calc.for $C_{41}H_{36}ClN_3O_4Sn$: C, 62.43; H, 4.59; N, 5.33%.

3.4.2.3.5 $Bz_3SnL^5H.OH_2$ (**5**)

Red crystals of compound **5** were obtained from a benzene-hexane mixture (1:3 v/v). Yield: 75%; M. p.: 74-76 °C. Anal. Found: C, 64.50; H, 4.89; N, 5.28%. Calc. for $C_{42}H_{39}N_3O_5Sn$: C, 64.30; H, 5.01; N, 5.36%.

3.4.3 Chemicals used for the preparations

$(Bu_3Sn)_2O$ (Merck) was used as such. Ph_3SnOH was prepared from Ph_3SnCl (Fluka) by following the literature method [71]. Bz_3SnOH was prepared as described by Sisido *et al.* [72]. The solvents used in the reactions were of AR grade and were dried using standard procedures. The solvents used in the reactions were of AR grade and dried using standard procedures. Toluene was distilled from sodium benzophenone ketyl.

3.4.4 Physical measurements

Carbon, hydrogen and nitrogen analyses were performed with a Perkin Elmer 2400 series II instrument. IR spectra in the range 4000-400 cm^{-1} were obtained on a BOMEM DA-8 FT-IR spectrophotometer with samples investigated as KBr discs. The ^{1}H-, ^{13}C- and ^{119}Sn-NMR spectra were recorded on a Bruker AMX 400 spectrometer and measured at 400.13, 100.62 and 149.18 MHz respectively. The ^{1}H, ^{13}C and ^{119}Sn chemical shifts were referred to Me_4Si set at 0.00 ppm, $CDCl_3$ set at 77.0 ppm and Me_4Sn set at 0.00 ppm respectively.

The ^{119}Sn Mössbauer spectra of the triorganotin(IV) complexes, viz., $^{n}Bu_3SnL^{1\text{-}5}H$ (**1-5**) and $Bz_3SnL^{1\text{-}5}H.OH_2$ (**1-5**) *in the solid-state were recorded using a Model MS-900 (Ranger* Scientific Co., Burleson, TX) spectrometer in the acceleration mode with a moving source geometry. A 5 mCi $Ca^{119m}SnO_3$ source was used, and counts of 30,000 or more were accumulated for each spectrum. The spectra were measured at 80 K using a liquid-nitrogen cryostat (CRYO Industries of America, Inc., Salem, NH). The velocity was calibrated at ambient temperature using a composition of $BaSnO_3$ and tin foil (splitting 2.52 mm s^{-1}). The resultant spectra were analyzed using the Web Research software package (Web Research Co., Minneapolis, MN). The Mössbauer spectra of triphenyltin(IV) complexes, $Ph_3SnL^{1}H.OH_2$ (**1**) and $Ph_3SnL^{2\text{-}5}H$ (**2-5**) were recorded on solid samples at liquid nitrogen temperature by using a conventional constant acceleration spectrometer, coupled with a multichannel analyser (a.e.n., Ponteranica (BG), Italy) equipped with a cryostat Cryo (RIAL, Parma, Italy). A $Ca^{119}SnO_3$ Mössbauer source, 10 mCi (from Ritverc, St Petersburg, Russia) moving at room temperature with constant acceleration in a triangular waveform was used. The velocity calibration was made using a ^{57}Co Mössbauer source, 10 mCi, and an iron foil as absorber (from Ritverc, St Petersburg, Russia).

Positive-ion and negative-ion electrospray ionization (ESI) mass spectra of triorganotin(IV) complexes, viz., $^{n}Bu_3SnL^{1\text{-}5}H$ (**1-5**), $Ph_3SnL^{1}H.OH_2$ (**1**) and $Ph_3SnL^{2\text{-}5}H$ (**2-5**) were measured on an ion trap analyzer Esquire 3000 (Bruker Daltonics, Bremen, Germany) in the mass range m/z 50-1600. The samples were dissolved in 100% acetonitrile (HPLC grade, Merck, Darmstadt, Germany) and analyzed by direct infusion at a flow rate of 5 µl/min. The ion source temperature was 300°C, the tuning parameter compound stability 100%, the flow rate and pressure of nitrogen were 4 l/min and 10 psi, respectively. The selected precursor ions were further analyzed by tandem mass spectrometry (MS/MS) experiments under the following conditions: isolation width m/z = 8 for ions containing one tin atom and m/z = 12 for ions containing more tin atoms, and the collision amplitude was in the range 0.7 - 1.0 V depending on the precursor ion stability.

3.4.5 X-ray crystallography

3.4.5.1 Tri-n-butyltin(IV) complexes

Crystals of the tri-n-butyltin(IV) complexes suitable for an X-ray crystal-structure determination were obtained from hexane ($[^nBu_3SnL^1H]_n$ (**1**)), hexane/dichloromethane ($[^nBu_3SnL^2H]_n$ (**2**)) and hexane/chloroform mixture ($[^nBu_3SnL^4H]_n$ (**4**) and $[^nBu_3SnL^5H]_n$ (**5**)), by slow evaporation of the solvent at room temperature. The crystal structures of four of the tri-n-butyltin(IV) complexes **1** [49], **2** [50], **4** [49] and **5** [51] have been determined. The data collection and refinement parameters are given in Table 3.7.

All measurements were made at low temperature on a Nonius Kappa CCD diffractometer [72] with graphite-monochromated Mo$K\alpha$ radiation (λ = 0.71073 Å) and an Oxford Cryosystems Cryostream 700 cooler. Data reduction was performed with HKL Denzo and Scalepack [73]. The intensities were corrected for *Lorentz* and polarization effects, and an empirical absorption correction based on the multi-scan method [74] was applied. Equivalent reflections were merged. The structure of **1** was solved by employing heavy-atom Patterson methods [75], followed by the Fourier expansion routine of DIRDIF94 [76], **2** and **4** were solved by direct methods using SIR92 [77] while that of **5** was solved by SHELXS97 [78] which revealed the positions of all non-hydrogen atoms. In each structure, the non-hydrogen atoms were refined anisotropically, while employing restraints when necessary as described below.

In **1**, there are two symmetry-independent fragments of the polymer in the asymmetric unit, with each fragment being comprised of four repeats of the principle chemical unit. The root-mean-square fit of the atoms of one fragment to those of the other is 0.17 Å. This close fit, plus the equivalence of the unit cell parameters β and γ, and the similarity of the unit cell parameters b and c, suggests that the independent fragments are almost related by a superstructure. If parameters b and c were identical, the structure could be defined in the higher symmetry space group $C2/c$, where only one fragment would need to be defined in the asymmetric unit. However, the difference between the unit cell parameters b and c means that the superstructure relationship is only approximate. This was confirmed in a test of the atomic coordinates for a relationship from a higher symmetry space group using the program PLATON [79], which indicated that additional crystallographic symmetry was not present. Nine of the 24 unique butyl groups in the structure are disordered over two conformations. Two sets of overlapping positions were defined for all atoms of one butyl group, for the terminal propyl segment of five butyl groups and for the terminal ethyl segment of another three butyl groups. Refinement of the site occupation factors of the disordered groups indicated that most disordered conformations are approximately equally occupied. Similarity restraints were applied to the chemically equivalent bond lengths and angles

within all butyl groups, including the ordered ones. Bond length restraints were also applied to any Sn–C bonds involving a disordered butyl C atom. Furthermore, neighbouring atoms within and between each conformation of the disordered butyl groups and within the ordered butyl groups were restrained to have similar atomic displacement parameters.

In **4**, the terminal methyl groups in two of the butyl ligands are disordered over two conformations. The refinement of constrained site occupation factors for the two orientations yielded values of 0.63(3) and 0.61(1) for the major conformation of each disordered group. Similarity restraints were applied to the chemically equivalent bond lengths involving disordered C atoms and neighbouring disordered atoms were restrained to have similar atomic displacement parameters.

In **2**, the terminal methyl group in one of the butyl ligands and the terminal propyl segment of another butyl ligand are disordered over two conformations. Two sets of overlapping positions were defined for the disordered atoms and the refinement of constrained site occupation factors yielded values of 0.52(5) and 0.71(1), respectively, for the major conformations of the disordered groups. Similarity restraints were applied to the chemically equivalent bond lengths and angles involving disordered C-atoms, while neighbouring disordered atoms were restrained to have similar atomic displacement parameters.

In **5**, there are two symmetry-independent repeats of the principle chemical unit in the asymmetric unit of this one-dimensional polymeric structure. The atomic coordinates were tested carefully for a relationship from a higher symmetry space group using the program PLATON [79] but none could be found. The terminal methyl group of one butyl ligand on one of the unique Sn-atoms is disordered over two conformations, as are all atoms of one butyl ligand on the other Sn-atom and one of the methoxy methyl groups. Refinement of constrained site occupation factors for the two orientations of these groups yielded values of 0.57(9), 0.659(6) and 0.519(9), respectively, for the major conformations. Similarity and bond lengths restraints were applied to the chemically equivalent bond lengths and angles involving disordered C atoms, while neighbouring atoms within and between each conformation of the disordered groups were restrained to have similar atomic displacement parameters.

The hydroxy H atom in **4** was placed in the position indicated by a difference electron density map and its position was allowed to refine together with an isotropic displacement parameter. All of the remaining H atoms in all the four structures were placed in geometrically calculated positions and refined using a riding model where each H atom was assigned a fixed isotropic displacement parameter with a value equal to $1.2U_{eq}$ of its parent atom ($1.5U_{eq}$ for the methyl and hydroxy groups). The orientation of each hydroxy O–H vector in **1** was optimised to

correspond with the direction that would bring the H atom closest to the nearest hydrogen bond acceptor. Refinement of each structure was carried out on F^2 using full-matrix least-squares procedures, which minimized the function $\Sigma w(F_o^2 - F_c^2)^2$. Corrections for secondary extinction were not applied. One reflection, whose intensity was considered to be an extreme outlier, was omitted from the final refinement in the case of **1**. All calculations were performed using the SHELXL97 [80] program.

3.4.5.2 Triphenyltin(IV) complexes

Crystals of the triphenyltin(IV) complexes suitable for an X-ray crystal-structure determination were obtained from chloroform ($[Ph_3SnL^2H]_n$ (**2**)), benzene/hexane ($[Ph_3SnL^3H]_n$ (**3**)) and benzene ($[Ph_3SnL^1H]_2$ (**5**)) by slow evaporation of the solvent at room temperature. The crystal structures of three of the triphenyltin(IV) complexes **2**, **3** and **5** [20] have been determined. The data collection and refinement parameters are given in Table 3.10.

All measurements were made at low temperature (except for **2**, the crystals of which did not survive cooling to 160 K) on a Nonius KappaCCD diffractometer [72] with graphite-monochromated Mo Kα radiation (λ = 0.71073 Å) and an Oxford Cryosystems Cryostream 700 cooler. Data reduction was performed with HKL Denzo and Scalepack [73]. The intensities were corrected for *Lorentz* and polarization effects, and an empirical absorption correction based on the multi-scan method [74] was applied. Equivalent reflections were merged. The structure of **5** was solved by heavy-atom Patterson methods [75], followed by the Fourier expansion routine of DIRDIF94 [76]. The other structures were solved by direct methods by using SIR92 [77]. For each structure, the non-hydrogen atoms were refined anisotropically.

In **5**, the dinuclear molecule sits across a crystallographic centre of inversion. The H-atom of the protonated imine group of **2**, **3** and **5** were placed in the positions indicated by a difference electron density map and their positions were allowed to refine together with individual isotropic displacement parameters. All remaining H-atoms in each structure were placed in geometrically calculated positions and refined using a riding model where each H-atom was assigned a fixed isotropic displacement parameter with a value equal to $1.2U_{eq}$ of its parent atom ($1.5U_{eq}$ for methyl groups). The refinement of each structure was carried out on F^2 using full-matrix least-squares procedures, which minimized the function $\Sigma w(F_o^2\text{-}F_c^2)^2$. Three reflections, whose intensities were considered to be extreme outliers, were omitted from the final refinement of **2**. All calculations were performed using the SHELXL97 [80] program.

3.4.5.3 Tribenyltin(IV) complexes

Crystals of the tribenzyltin(IV) complexes suitable for an X-ray crystal-structure determination were obtained from a toluene/hexane ($Bz_3SnL^4H.OH_2$ (**2**)) and benzene/hexane ($Bz_3SnL^5H.OH_2$ (**5**)) by slow evaporation of the solvent at room temperature. The crystal structures of two of the tribenzyltin(IV) complexes **4** and **5** [68] have been determined. The data collection and refinement parameters are given in Table 3.14.

All measurements were made at low temperature on a Nonius KappaCCD diffractometer [72] with graphite-monochromated MoKα radiation (λ = 0.71073 Å) and an Oxford Cryosystems Cryostream 700 cooler. Data reduction was performed with HKL Denzo and Scalepack [73]. The intensities were corrected for *Lorentz* and polarization effects, and an empirical absorption correction based on the multi-scan method [74] was applied. The structures were solved by direct methods by using SIR92 [77]. For each structure, the non-hydrogen atoms were refined anisotropically. The water ligand and phenoxy H atoms were placed in the positions indicated by a difference electron density map and their positions were allowed to refine together with individual isotropic displacement parameters. All remaining H atoms in each structure were placed in geometrically calculated positions and refined using a riding model where each H atom was assigned a fixed isotropic displacement parameter with a value equal to $1.2U_{eq}$ of its parent atom ($1.5U_{eq}$ for methyl group in **5**). The refinement of each structure was carried out on F^2 using full-matrix least-squares procedures, which minimized the function $\Sigma w(F_o^2-F_c^2)^2$. A correction for secondary extinction was applied in the case of complex **5**. One reflection, whose intensity was considered to be an extreme outlier, was omitted from the final refinement of **4**. All calculations were performed using the SHELXL97[80] program.

References

[1] L.E. Maley, D.P. Mellor, Nature **159** (1974) 370.

[2] M. Calvin, K.W. Wilson, J. Am. Chem. Soc. **67** (1945) 2003.

[3] D.G. Vartak, K.R. Menon, J. Inorg. Nucl. Chem. **31** (1969) 3341.

[4] P.N. Mohan Das, C.P. Trivedi, J. Indian Chem. Soc. **49** (1972) 739.

[5] K.G. Deshmukh, R.A. Bhobe, Curr. Science **46** (1977) 67.

[6] K.G. Deshmukh, R.A. Bhobe, J. Indian Chem. Soc. **54** (1977) 375.

[7] A.A. Khandar, Z.Rezvani, Polyhedron **18** (1998) 129.

[8] K.G. Deshmukh, R.A. Bhobe, J. Inorg. Nucl. Chem. **40** (1978) 135.

[9] L. Pardeshi, A. Rasheed, R.A. Bhobe, J. Indian Chem. Soc. **57** (1980) 388.

[10] K.K. Sarma, T.S. Basu Baul, D.D. Mishra, Synth. React. Inorg. Met-Org. Chem. **23** (1993) 1277.

[11] K.K. Sarma, T.S. Basu Baul, E. Rivarola, R.P. Agrawal, Polyhedron **13** (1994) 2217.

[12] M.A. Pujar, T.D. Bharamagoudar, J. Indian Chem. Soc. **57** (1980) 462.

[13] A.A. Khandar, K. Nejati, Polyhedron **19** (2000) 607.

[14] D. Revannasiddaiah, N.K. Lokanath, M.A. Sridhar, J.S. Prasad, Z. Kristallogr. **212** (1997) 387.

[15] S.A. Hudson and P.M. Maitlis, Chem. Rev. **93** (1993) 861.

[16] A-M. Giroud-Godquin, P.M. Maitlis, Angew. Chem., Int. Ed. Engl. **30** (1991) 375.

[17] P. Espinet, M.A. Esteruelas, L.A. Oro, J.L. Serrano, E. Sola, Coord. Chem. Rev. **117** (1992) 215.

[18] D.W. Bruce, in: D.W. Bruce and D. O'Hare (Ed.), Inorganic Materials, Wiley, Chichester, 1992.

[19] A.P. Polishchuk, T.V. Timofeeva, Russ. Chem. Rev. **62** (1993) 291.

[20] T.S. Basu Baul, K.S. Singh, M. Holčapek, R. Jirásko, E. Rivarola, A. Linden, J. Organomet. Chem. **690** (2005) 4232.

[21] A Linden, T.S. Basu Baul, K.S. Singh, Acta Crystallogr. Sect. E62 (2006) o2566.

[22] R.J. Butcher, T.S. Basu Baul, K.S. Singh, F.E. Smith, Acta Crystallogr. Sect. **E 61** (2005) o1007

[23] S.J. de Mora, in: S.J. de Mora (Ed.), Tributyltin: Case Study of an Environmental Contaminant, Cambridge University Press, London, 1996, pp. 1 - 20.

[24] P.E. Gibbs, G.W. Bryan, in: S.J. de Mora (Ed.), Tributyltin: Case Study of an Environmental Contaminant, Cambridge University Press, London, 1996, pp. 212 - 236.

[25] R.F. Bennett, in: S.J. de Mora (Ed.), Tributyltin: Case Study of an Environmental Contaminant, Cambridge University Press, London, 1996, pp. 21 - 61.

[26] T.S. Basu Baul, S. Dhar, E. Rivarola, F.E. Smith, R. Butcher, X. Song, M. McCain, G. Eng, Appl. Organomet. Chem. **17** (2003) 261.

[27] M. Gielen, P. Lelieveld, D. de Vos, R. Willem, in: M. Gielen (Ed.), Metal Based Antitumour Drug, vol. 2, Freund Publication, Tel Aviv, 1992, pp. 29-54.

[28] M. Gielen, E.R.T. Tiekink, in: M. Gielen, E.R.T. Tiekink (Ed.), Metallotherapeutic Drug and Metal-Based Diagnostic Agents, chapter 22: ^{50}Sn Tin Compounds and their Therapeutic Potential, Wiley, 2005, pp 421-439.

[29] M. Gielen, R. Willem, M. Biesemans, M. Boualam, A. El Khloufi, D. de Vos, Appl. Organomet. Chem. **6** (1992)287.

[30] M. Boualam, M. Gielen, A. El Khloufi, D. de Vos, R. Willem, (Pharmachemie B.V.) Eur. Pat. 91202746.3-October 1991.

[31] E.R.T. Tiekink, Appl. Organomet. Chem. **5**, (1991) 1.

[32] E.R.T. Tiekink, Trends Organomet. Chem. **1** (1994) 71.

[33] T.S. Basu Baul, S.M. Pyke, K.K. Sarma, E.R.T. Tiekink, Main Group Met. Chem. **19** (1996) 807.

[34] T.S. Basu Baul, K.S. Singh, A. Lyčka, M. Holčapek, A. Linden, J. Organomet. Chem. **690** (2005) 1581.

[35] T.S. Basu Baul, E.R.T. Tiekink, Z. Kristallogr. NCS, **212** (1997) 363.

[36] T.S. Basu Baul, S. Dhar, N. Kharbani, S.M. Pyke, R. Butcher, F.E. Smith, Main Group Met. Chem. **22** (1999) 413.

[37] T.S. Basu Baul, S. Dhar, S.M. Pyke, E.R.T. Tiekink, E. Rivarola, R. Butcher, F.E. Smith, J. Organomet. Chem. **633** (2001) 7.

[38] R. Willem, I. Verbruggen, M. Gielen, M. Biesemans, B. Mahieu, T.S. Basu Baul, E.R.T. Tiekink, Organometallics **17** (1998) 5758.

[39] J. Holeček, M. Nádvorník, K. Handlir, A. Lyčka, J. Organomet. Chem. **241** (1983) 177.

[40] M. Nádvorník, J. Holeček, K. Handlir, A. Lyčka, J. Organomet. Chem. **275** (1984) 43.

[41] A. Lyčka, J. Holeček, M. Nádvorník, K. Handlir, J. Organomet. Chem. **280** (1985) 323.

[42] J. Holeček, K. Handlir, M. Nádvorník, A. Lyčka, J. Organomet. Chem. **258** (1983) 147.

[43] J.J. Zuckerman, In: F.G.A. Stone, R. West (Eds.), Advances in Organometallic Chemistry, Academic Press, New York, 1970, Vol 9, p. 21.

[44]R. Barbieri, F. Huber, L. Pellerito, G. Ruisi, A. Silvestri, in: P.J. Smith (Ed.), Chemistry of Tin: ^{119}Sn Mössbauer Studies on Tin Compounds, Blackie, London, 1998, pp. 496 - 540.

[45] A. Růžička, L. Dostál, R. Jambor, V. Buchta, J. Brus, I. Císařová, M. Holčapek, J. Holeček, Appl. Organomet. Chem. **16** (2002) 315.

[46] R. Jambor, L. Dostál, A. Růžička, I. Císařová, J. Brus, M. Holčapek, J. Holeček, Organometallics **21** (2002) 3996.

[47] A. Růžička, A. Lyčka, R. Jambor, P. Novák, I. Císařová, M. Holčapek, M. Erben, J. Holeček, Appl. Organomet. Chem. **17** (2003) 168.

[48] L. Kolářová, M. Holčapek, R. Jambor, L. Dostál, A. Růžička, M. Nádvorník, J. Mass Spectrom. **39** (2004) 621.

[49] T.S. Basu Baul, K.S. Singh, X. Song, A. Zapata, G. Eng, A. Lyčka, A. Linden, J. Organomet. Chem. **689** (2004) 4702.

[50] A. Linden, T.S. Basu Baul, K.S. Singh, Acta Crystallogr. **E61** (2005) m2711.

[51] T.S. Basu Baul , K.S. Singh, M. Holčapek, R. Jirásko, A. Linden, X. Song, A. Zapata, G. Eng, Appl. Organomet. Chem. **19** (2005) 935.

[52] T.S. Basu Baul, S. Dutta, E. Rivarola, R. Butcher, F.E. Smith, J. Organomet. Chem. **654** (2002) 100.

[53] G.M. Bancroft, R.H. Platt, Adv. Inorg. Chem. Radiochem. **15** (1972) 59.

[54] G. Lawson, R.H. Dahm, N. Ostah, E.D. Woodland, Appl. Organomet. Chem. **10** (1996) 125.

[55] E. Gonzáles-Toledo, R. CompaZó, M.D. Prat, M. Granados, J. Chromatogr. A. **946** (2002) 1.

[56] T.L. Jones-Lepp, K.E. Varner, M. McDaniel, L. Riddick, Appl. Organomet. Chem. **13** (1999) 881.

[57] D. Dakternieks, H. Zhu, E.R.T. Tiekink, R. Colton, J. Organomet. Chem. **476** (1994) 33.

[58] J. Beckmann, M. Henn, K. Jurkschat, M. Schürmann, Organometallics **21** (2002) 192.

[59] S.W. Ng, C. Wei, V.G. Kumar Das, J. Organomet. Chem. **345** (1988) 59.

[60] J.P. Charland, F.L. Lee, E.G. Gabe, L.E. Khoo, F.E. Smith, Inorg. Chim. Acta **130** (1987) 55.

[61] J.J. Bullock, M.F.C. Ladd, D.C. Povey, H.A. Tajmir-Raihi, Acta Crystallogr. **B35** (1979) 2013.

[62] M.E. Kamwaya, L.E. Khoo, Acta Crystallogr. **C 41** (1985) 1027.

[63] A. Lyčka, J. Jirman, A. Kolonicny, J. Holeček, J. Organomet. Chem. **333** (1987) 305.

[64] T.S. Basu Baul, C. Masharing, E. Rivarola, F.E. Smith, R. Butcher, Str. Chem., in the press.

[65]A.G. Davies, P.J. Smith, in: G. Wilkinson G, F.G.A. Stone, E.W. Abel (Eds.), Comprehensive Organometallic Chemistry, vol. 2, Pergamon Press, New York, NY, 1982, p. 519.

[66] T.S. Basu Baul, S. Dutta, E. Rivarola, R. Butcher, F.E. Smith, J. Organomet. Chem. **654** (2002) 100.

[67] G.M. Bancroft, R.H. Platt, Adv. Inorg. Chem. Radiochem. **15** (1972) 59.

[68] T.S. Basu Baul, K.S. Singh, A. Linden, X. Song, G. Eng, J. Organomet. Chem., submitted for publication.

[69] J. Bernstein, R.E. Davis, L. Shimoni, N.-L. Chang, Angew. Chem. **107** (1995) 1689; Angew. Chem. Int. Ed. Engl. **34** (1995) 1555.

[70] B. Kushlefsky, I. Simmons, A. Ross, Inorg. Chem. **2** (1963) 187.

[71] K. Sisido, T. Takeda, J. Kinigawa, J. Am. Chem. Soc. **83** (1961) 538.

[72] R. Hooft, Kappa *CCD Collect Software*, Nonius BV, Delft, The Netherlands, 1999.

[73] Z. Otwinowski, W. Minor, in: C.W. Carter Jr., R.M. Sweet (Ed.) Methods in Enzymology, Vol. 276, Macromolecular Crystallography, Part A, Academic Press, New York, 1997, pp. 307-326.

[74] R.H. Blessing, Acta Crystallogr. **A 51** (1995) 33.

[75] P.T. Beurskens, G. Admiraal, G. Beurskens, W.P. Bosman, S. Garcia-Granda, R.O. Gould, J.M.M Smits, C. Smykalla, PATTY: The DIRDIF program system, Technical Report of the Crystallography Laboratory, University of Nijmegen, The Netherlands, 1992.

[76] P.T. Beurskens, G. Admiraal, G. Beurskens, W.P. Bosman, R. de Gelder, R. Israel, J.M. M. Smits, DIRDIF94: The DIRDIF program system, Technical Report of the Crystallography Laboratory, University of Nijmegen, The Netherlands, 1994.

[77] A. Altomare, G. Cascarano, C. Giacovazzo, A. Guagliardi, M.C. Burla, G. Polidori, M. Camalli, SIR92, J. Appl. Crystallogr. **27** (1994) 435.

[78] G.M. Sheldrick, SHELXS97, Program for the Solution of Crystal Structures, University of Göttingen, Germany, 1997.

[79] A.L. Spek, PLATON, Program for the Analysis of Molecular Geometry, University of Utrecht, The Netherlands, 2003.

[80] G.M. Sheldrick, SHELXL97, Program for the Refinement of Crystal Structures, University of Göttingen, Germany, 1997.

CHAPTER 4

TRIORGANOTIN(IV) COMPLEXES OF 4-[(*E*)-(3-FORMYL-4-HYDROXYPHENYL)-DIAZENYL]- AND 4-{(*E*)-4-HYDROXY-3-[(*E*)-4-(ARYL)IMINOMETYHY]PHENYL- DIAZENYL}-BENZOIC ACIDS: SYNTHESES, CHARECTERIZATION AND STRUCTURES

4.1 Introduction

Organotin(IV) complexes of 2-[(*E*)-2-(3-formyl-4-hydroxyphenyl)-1-diazenyl]benzoic acid [1-5] and 2-{(*E*)-4-hydroxy-3-[(*E*)-4-(aryl)iminomethyl]phenyldiazenyl}benzoic acids [3,5-8] have been studied in great detail which are discussed in Chapter 3 due to their various structural motifs (Scheme 4.1 (**I-III**)) as well as for their important role in understanding Sn(IV) coordination chemistry in solution as well as in the solid state. In addition, this class of compounds has shown promise as larvicides against various species of mosquito (see Chapter 6). For example, n-butyltin(IV) azo carboxylates, *viz.*, tri-n-butyltin(IV) 5-[(*E*)-2-(aryl)-1-diazenyl]-2-hydroxybenzoates and tri-n-butyltin(IV) 2-[(*E*)-2-(3-formyl-4-hydroxyphenyl)-1-diazenyl]benzoate have been investigated for their toxicites against both the *Aedes aegypti (Ae. aegypti)* and *Anopheles stephensi (An. stephensi)* mosquito larvae. The results indicated that these compounds have shown moderate [9] to good [3] activities, respectively. The latter compounds were further condensed with primary aromatic amines to obtain the tri-n-butyltin(IV) 2-{(*E*)-4-hydroxy-3-[(*E*)-4-(aryl)iminomethyl]phenyldiazenyl}benzoates (Chapter 3). The activities for these compounds were found to be lower and correlated with the size of the molecules (Chapter 6) [6].

In view of this, and in search of better candidates for the control of various mosquito larvae, the present study details the synthesis and characterization of the pre-ligand i.e. 4-[(*E*)-2-(3-formyl-4-hydroxyphenyl)-1-diazenyl]benzoic acid (L^6HH', Fig. 4.1a) and the triorganotin(IV) complexes of the corresponding condensed ligands, i.e. 4-{(*E*)-4-hydroxy-3-[(*E*)-4-(aryl)iminomethyl]phenyldiazenyl}benzoic acids ($L^{7\text{-}10}HH'$, Fig. 4.1b). The generic structures of each of the ligands are shown in Chapter 2.

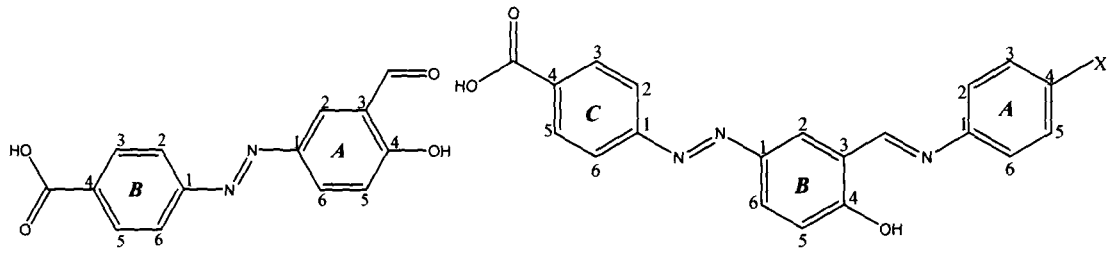

(a) (b)

Fig. 4.1 Generic structure of the ligand. Abbreviations: (a) LHH' (pre-ligand) (b) L^1HH': X = -CH_3; L^2HH': X = -Br, L^3HH': X = -Cl, L^4HH': X = -OCH_3 (condensed ligands), where H and H' represent hydroxy and carboxylic acid H atoms, respectively.

APPENDIX
Reply to the queries and specific comments